Charles University
Faculty of Science
Department of Analytical Chemistry
Ph.D. study program: Analytical Chemistry

Ph.D. Thesis

Mgr. Milan Libánský

Testing of new electrode arrangements for monitoring of electrochemically oxidisable biologically active organic compounds

Testování nových elektrodových uspořádání pro monitorování elektrochemicky oxidovatelných biologicky aktivních organických látek

Supervisor: Prof. RNDr. Jiří Zima, CSc.
Supervisors-consultants: Prof. RNDr. Jiří Barek, CSc.
RNDr. Hana Dejmková, Ph.D.

I declare that all the results which are used and published in this Ph.D. Thesis have been obtained by my own experimental work and that all the ideas taken from work of others are properly referred to in the text and the literature survey. I am conscious that the prospective use of the results, published in this Ph.D. Thesis, outside the Charles University in Prague is possible only with a written agreement of this university.

I also declare that neither this Ph.D. Thesis nor its significant part has been submitted in any form for another degree or diploma at any university or other institution of tertiary education.

Prague 28.02.2017 Mgr. Milan Libánský

.....

This Ph.D. Thesis was experimentally carried out in the period from 2013 till 2017 at the Charles University, Faculty of Science, Department of Analytical Chemistry, UNESCO Laboratory of Environmental Electrochemistry. Some experiments were carried out in cooperation with Ing. Alena Řezníčková, Ph.D. and Mgr. Oleksiy Lyutakov, Ph.D., from the University of Chemistry and Technology in Prague, Department of Solid State Engineering.

Acknowledgement

I would like to express acknowledgements to all who have supported my research efforts during this time. Especially, I thank to my supervisor **prof. RNDr. Jiří Zima, CSc.**, Faculty of Science, Charles University; to **Prof. RNDr. Jiří Barek, CSc.**, the head of the UNESCO Laboratory of Environmental Electrochemistry at the Department of Analytical Chemistry, Charles University, my consultant who supported me by fantastic usable ideas for my research and to **RNDr. Hana Dejmková, Ph.D.**, my second consultant who provided me with theoretical and practical face-to-face support in the laboratory; to all colleagues from our research group and from Department of Analytical chemistry for their extensive help and support. Further, I acknowledge the cooperation with **Ing. Alena Řezníčková, Ph.D.** and **Mgr. Oleksiy Lyutakov, Ph.D.**, from the University of Chemistry and Technology in Prague, Department of Solid State Engineering, for providing gold nanostructured film electrodes with various substrates.

Last but not least I thank to my **mother Dagmar Čejková**, to my **father Milan Libánský**, to my wife **Ing. Lucie Libánská**, and to all my friends for their support during my graduate studies.

Financial support of my research was ensured by: the Specific University Research (SVV), the Ministry of Education, Youth and Sports of the Czech Republic (Project MSM0021620857), and the Grant Agency of the Czech Republic (P206/12/G151, Centre of new approaches to bioanalysis and molecular diagnosis).

Abstract

Submitted Ph.D. Thesis is focused on the electrochemical characterization and testing of recently developed working electrodes made from pure gold or graphitic carbon particles and electrochemical arrangements. These electrodes are suitable for large screening measurements of various organic compounds. The development of new sensitive voltammetric methods for determination of oxidisable biologically active organic compounds is another aim of this work.

To verify its applicability, the array of carbon composite film electrodes integrated in measuring cell system was selected for the development of voltammetric methods for determination of homovanillic acid, vanillylmandelic acid, and indoxyl sulphate. These analytes, which belong to the group of biomarkers of human diseases, were selected for increasing interest in their determination in medical laboratories. Moreover, determination of indoxyl sulphate was coupled to its solid phase extraction from human urine prior to voltammetric determination. Obtained results were compared with measurements of standards with well-established carbon paste electrode.

Sputtered (physical vapour deposition method) gold nanostructured film electrodes on treated PTFE substrates and gold nanostructured film electrodes modified with various functional groups on the surface were selected for testing and electrochemical characterization as an interesting analytical tool with promising use as disposable sensors for *in-situ* measurements with microvolumes of the sample. Electrochemical characterization was carried out by examination of the electrode reaction (reversibility, repeatability) of standard redox probes (ferrocyanide/ferricyanide, hydroquinone/benzoquinone) in different types of supporting electrolytes, by evaluation of the parameters of calibration curves of probes, by calculations of their real surface areas from Randles-Sevcik equation, and by observation of blocking of modified electrode surfaces by grafted functional groups. The whole study was complemented by critical evaluation and suggestion of possibilities for improvements of tested electrodes and arrangements. Obtained results were again compared to measurements with conventional bulk gold electrode or pristine gold nanostructured electrode sputtered on glass substrate.

Abstrakt

Předložená disertační práce je zaměřena na elektrochemickou charakterizaci a testování nově vyvinutých pracovních elektrod a jejich uspořádání. Tyto elektrody byly vyrobené z čistého atomárního zlata nebo z mikročástic grafitického uhlíku a jsou vhodné pro velkoplošné monitorování různých organických látek; dalším, ale neméně důležitým cílem práce je vývoj nových citlivých voltametrických metod pro stanovení oxidovatelných biologicky aktivních organických látek.

Měřící systém cel s integrovanými uhlíkovými kompozitními elektrodami byl vybrán pro vývoj voltametrické metody vhodné ke stanovení homovanilové kyseliny, vanilylmandlové kyseliny a indoxylsulfátu. Tyto biomarkery různých onemocnění lidského těla byly vybrány z důvodu neustálého nárůstu zájmu lékařských laboratoří o jejich stanovování. Navíc, před samotným stanovením indoxylsulfátu byla provedena jeho extrakce na tuhé fázi z matrice lidské moči. Všechny naměřené výsledky byly porovnány s výsledky měření s již standardně používanou uhlíkovou pastovou elektrodou.

Zlaté naprašované (metoda fyzikální parní depozice) nanostrukturované filmové elektrody s povrchem modifikovaným různými funkčními skupinami a substráty a zlaté nanostrukturované filmové elektrody naprášené na upraveném PTFE byly vybrány pro testování a elektrochemickou charakterizaci. Tyto elektrody představují zajímavý analytický nástroj vhodný pro použití jako jednorázový senzor pro měření v terénu v mikrolitrových objemech. Elektrochemická charakterizace zahrnovala: sledování parametrů elektrochemické reakce (opakovatelnost, reverzibilita) různých standardních analytů (ferrokyanid, hydrochinon) v rozdílných základních elektrolytech, vyhodnocení parametrů naměřených kalibračních křivek zmíněných analytů, výpočet reálných aktivních ploch elektrod pomocí Randlesovy-Ševčíkovy rovnice a sledování, zda není povrch modifikovaných elektrod blokován naroubovanými funkčními skupinami. Vše bylo následně kriticky zhodnoceno a byla navržena možná vylepšení. Získané výsledky byly opět porovnány s měřením na klasické zlaté elektrodě (bulk electrode) nebo na zlaté nemodifikované nanostrukturované elektrodě naprášené na skleněném substrátu.

Keywords:

Carbon composite film electrodes

Carbon paste electrode

Electrochemical characterization

Environmental pollutants

pNIPAAM (poly(n-isopropylacrylamide))

Gold nanostructured film electrodes

Gold sputtering

Grafting

Tumor biomarkers

Klíčová slova:

Uhlíkové kompozitní filmové elektrody

Uhlíková pastová elektroda

Elektrochemická charakterizace

Látky znečišťující životní prostředí

pNIPAAM (poly (n-isopropylakrylamid))

Zlaté nanostrukturované filmové elektrody

Naprašování zlata

Roubování

Biomarkery nádorových onemocnění

List of symbols and abbreviations:

α	significance level (95%)
AuNPs	gold nanoparticles
BPD	biphenyldithiol
BR	Britton-Robinson
c	molar concentration (mol L^{-1})
CFE	carbon film electrode
CPE	carbon paste electrode
CV	cyclic voltammetry
DPV	differential pulse voltammetry
E	potential
E_p	peak potential
HQ	hydroquinone
HVA	homovanillic acid
GNFE	gold nanostructured film electrode
I_a	anodic peak current
I_c	cathodic peak current
I_p	peak current
LOD	limit of detection
LOQ	limit of quantification
n	number of measurements
pNIPAAM	poly (n-isopropylacrylamide)
PTFE	polytetrafluoroethylen
R^2	coefficient of determination
SERS	surface enhanced Raman scattering
SPE	solid phase extraction
υ	scan rate
VMA	vanillylmandelic acid

Contents

1. Introduction

This Ph.D. Thesis was worked out at the Department of Analytical chemistry, Faculty of Science at Charles University. Its scientific aims are focused on a long-term research in the theoretical and practical field of intensive **testing** of new electrode materials and arrangements for electroanalytical applications, especially in the field of miniaturized film arrangements with working electrodes made from gold or various form of carbon. These developed electrodes and arrangements were tested and characterized in many possible ways and all obtained results were compared with results of commonly used **carbon** and **gold electrodes**.

The Ph.D. Thesis presents results obtained in the last four years and it is based on following six scientific publications [1-6] which are attached as Appendix parts I – VI (chapters 7-12). To distinguish the references to these publications in entire text of this Ph.D. Thesis, corresponding numbers in square brackets are in bold and underlined.

[1] **Libansky M.**, Zima J., Barek J., Dejmkova H., Voltammetric Determination of Homovanillic Acid and Vanillylmandelic Acid on a Disposable Electrochemical Measuring Cell System with Integrated Carbon Composite Film Electrodes, *Monatshefte Fur Chemie*, 147 (2016) 89-96.

[2] Bergerova M., **Libansky M.**, Dejmkova H., Determination of Urinary Indican on Carbon Film Composite Electrode and Carbon Paste Electrode *Current Analytical Chemistry*, *Submitted* (2017).

[3] **Libansky M.**, Zima J., Barek J., Reznickova A., Svorcik V., Dejmkova H., Basic Electrochemical Properties of Sputtered Nanostructured Gold Film Electrodes, *Electrochimica acta*, *Submitted* (2017).

[4] Guselnikova O., Postnikov P., Kalachyova Y., **Libansky M.**, Zima J., Kolska Z., Svorcik V., Lyutakov O., Large-scale Ultrasensetive, Highly Reproducible and Regenerative Smart SERS Platform Based on pNIPAm Grafted Gold Grating, *ChemNanoMat*, 3 (2016) 135-144.

[5] Guselnikova O., Postnikov P., Elashnikov R., Trusova M., Kalachyova Y., **Libansky M.**, Barek J., Kolska Z., Svorcik V., Lyutakov O., Surface Modification of Au and Ag Plasmonic Thin Films via Diazonium Chemistry: Evaluation of Structure and Properties, *Colloids and Surfaces A Physicochemical Engineering Aspects*, *In Press* (2016).

[6] Guselnikova O., Kalachyova Y., Faragova K., **Libansky M.**, Dejmkova H., Svorcik V., Sajdl P., Lyutakov O., Functional SPP-based SERS Sensor Platform for Lipoproteins Detection, *Talanta*, *Prepared for submission* (2017).

This **Ph.D. thesis** has been submitted as a contribution to the never ending effort of characterizing and testing of new electroanalytical arrangements indented for large scale monitoring of electrochemically oxidisable organic compounds.

Every developed working electrode has to be tested in various possible ways. It is important to explore electrochemical behaviour during measurement with different supporting electrolytes and common as well as non-traditional analytes to assess whether the electrode is suitable for given purpose. Important tested parameters are sensitivity and selectivity of the measurement, user friendliness, easy way of fabrication of the electrode, environmental friendliness, and the possibility of chemical and/or chemical modification to increase the selectivity or the sensitivity of the determination.

These requirements are satisfied by carbon composite working electrodes and working electrodes made from pure gold. These types of electrodes are suitable as an instrument for large scale monitoring of wide spectrum of organic compounds, because they have merits of simplicity of construction, good compatibility with biological samples, and they are inexpensive from the point of view of both investment and running costs in the comparison to modern spectral instruments [7]. The use of electroanalytical devices (electrochemical sensors) is particularly beneficial in the case of monitoring of environmental pollutants and markers of various diseases, where large numbers of samples are assumed and simple and inexpensive sensors are needed. Voltammetric methods are also faster than modern separation and spectrometric methods while sufficiently sensitive and selective [8].

Urine is the most frequently used body fluid for voltammetric detection and determination of toxic compounds and their metabolites in human body; because most of biomarkers of exposure, illness, or treatment are excreted via urine. Therefore, the determination of concentration of the biomarkers in urine is fundamental for determining the stage of disease, monitoring of response of human organism to treatment and for an early diagnosis of tumours and other diseases [9, 10]. Examples of the most frequently monitored biomarkers might be metabolites of catecholamines [11] or specific indole metabolites [12], which are important indicators of neurological and metabolic disorders.

With respect to all information mentioned in this chapter, the first aim of this **Ph.D. Thesis** was the development of sensitive electrochemical method for the determination

of important disease biomarkers, namely **homovanillic acid** (HVA), **vanillylmandelic acid** (VMA) **[1]** and **indoxyl sulphate** (urinary indican) **[2]** at disposable measuring cell system with integrated carbon composite film electrodes [13]. This system was developed in my Master Thesis and three standards of biomarkers were selected for this **Ph.D. Thesis** as optimal probes for the proof of practical applicability of the arrangement. The determination of indoxyl sulphate was complemented by its solid phase extraction (SPE) from human urine and results were compared with the determination on well-known carbon paste electrode **[2]**.

The second aim of this **Ph.D. thesis** was to employ sophisticated electrochemical procedures for electrochemical characterization of **gold nanostructured film electrodes** (GNFE) **[3]**, which were made by physical vapour deposition (**sputtering method**). Currently, the use of this method for fabrication of working electrodes for analytical chemistry is less common, despite the fact that it is pollution free method which has the potential to provide reliable electrochemical sensors. For this reason, other types of sputtered transparent gold electrodes/nanolayers with modified surfaces by various grafted functional groups were tested and characterized **[4-6]**.

2. Working electrodes

2.1. Carbon composite electrodes

In modern electroanalytical chemistry the development of new modern electrode materials for electrochemical sensors with favourable analytical and electrochemical properties is of a paramount importance, especially, in the field of so-called "green" materials which are not burdening the environment. This assumption is surely satisfied by bulk electrodes made from various types of carbon; however, in the last two decades researches have turned their attention to the solid composite electrodes for their outstanding electrochemical, mechanical and physical properties, which cannot be satisfied by classical carbon bulk electrodes [14].

Composite electrode surface can be arranged either as ensemble arrangement as a single large surface or as an array of microelectrodes, which are separated from each other by an insulator [15]. This is one of old definitions of composite electrodes; modern definition classifies composite electrodes as electrodes made of two or more distributed chemical components, where at least one of these components (compounds) behaves as an electric current conductor and at least one as a non-conductive phase [16]. Since their introduction, composite electrodes have gone through an extensive development and there exists many types of them sorted by their composition [16, 17]. In this **Ph.D. Thesis**, attention was paid to solid **carbon composite electrodes**, which exhibit solid consistency after mixing of all components. Conductive phase is realized by carbon particles and the electrodes fall within the category of random ensembles-dispersed-solid electrodes [17].

Conductive phase of carbon composite electrodes can be realized by many various carbon materials such as graphite [13, 18], glassy carbon [13, 19], carbon nanotubes [20, 21], graphene [22], fullerenes [23] or their combination [24]. As an insulator phase many kinds of compounds such as polymethylmethacrylate [25], polyurethane [26] polystyrene [13], polyvinylchloride [27], polyester [28] or epoxy resin [21], cellulose acetate gel [29], ionic liquids [30] or methyltrimethoxysilane [31] can be used. Electrochemical properties and especially physical properties of composite electrodes

are strongly influenced by the used combination of conductive phase, insulator phase and their ratio.

Solid carbon composite electrodes offer unique properties such as strong hydrophilicity, high mesoporosity, excellent capacitor characteristics, high current density, and many others which ensure wide range of applications from energy storage engineering [32] to analytical chemistry [33]. The attractiveness of carbon composite electrodes consists principally in environmental friendliness, easy miniaturization, easy chemical modification, low fabrication and running costs (they can be used as a disposable sensors), easy electrochemical (or mechanical) pretreatment to avoid problems with the history of the measurement with the electrode [17, 34]. These benefits were main reason why carbon composite electrodes were selected as working electrodes for a new small sized mobile electrode system (array) suitable for laboratory as well as *in-situ* measurements. The array of solid **carbon composite film electrodes** (CFE) integrated in a 96-well microtitration plate (**Fig. 2-1**) was development during **Milan Libansky** Master studies (Master Thesis) [13] and it forms certain introduction to this this **Ph.D. Thesis,** because in the presented **Ph.D. Thesis,** developed array of **CFE**s was used for the determination of standards of tested analytes to verify its practical usability **[1, 2]**.

For the fabrication of CFEs used in the system, the combination of graphitic carbon with polystyrene (9:1, *w/w*) was selected as a suitable combination of electrode materials providing the best electrochemical performance from all tested material combinations [13]. Graphitic carbon with polystyrene were intensively dispersed in toluene (volatile solvent) by stirring; polystyrene was dissolved and thus formed carbon ink was applied into the cell; after the solvent evaporation, the solid electrode was ready for the measurement. Complete preparation of the electrochemical cell system is described in the papers [**1, 2,** 13].

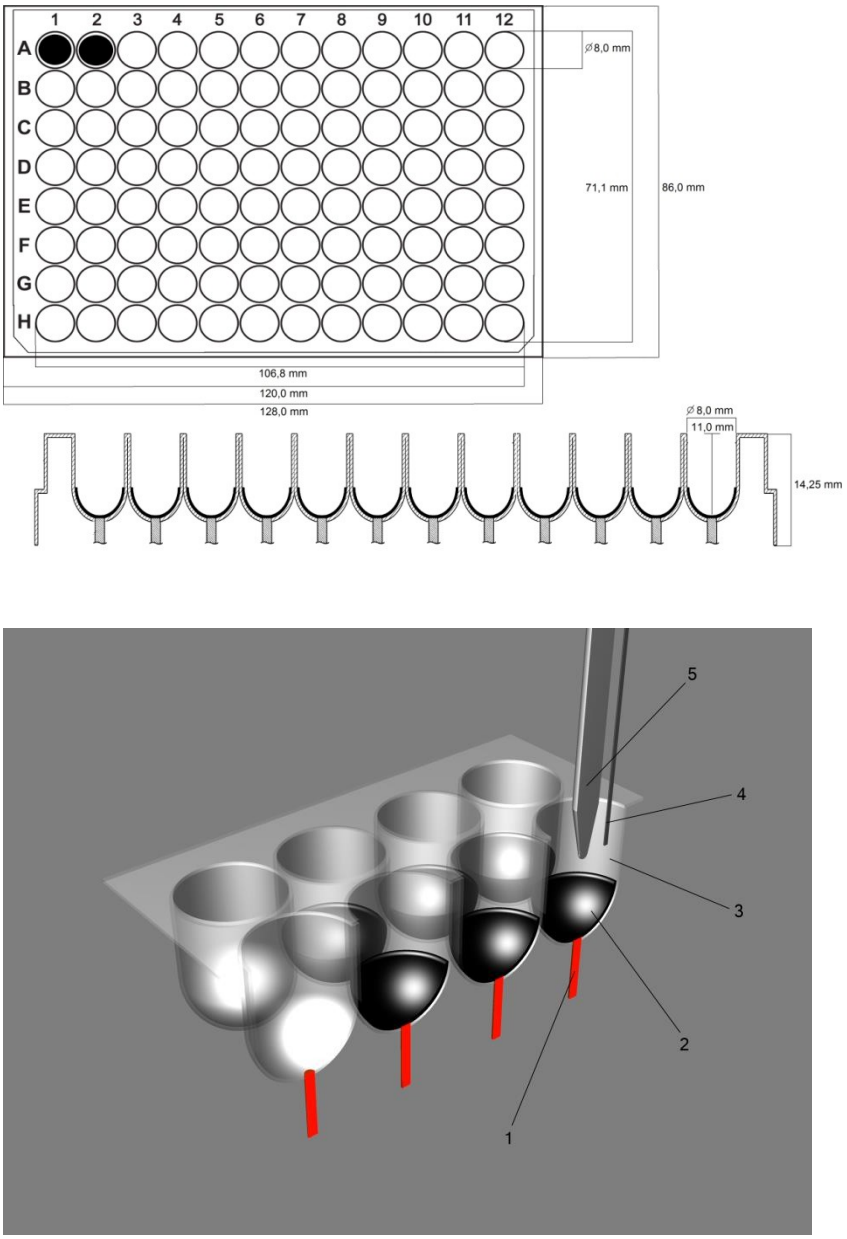

Fig. 2-1 Scheme of array of CFE integrated in a 96-well microtitration plate. (1) Inserted metal contact, (2) CFE, (3) plastic cell, (4) auxiliary electrode, (5) Reference electrode [13].

Generally, mentioned fabrication process is commonly utilized nowadays and it is frequently used during the preparation of many carbon film electrodes, such as screen-printed electrodes, where the electrode ink is printed on a suitable substrate mostly

made of plastics or ceramics [35, 36]. Electrode ink can be also applied on the common bulk electrode which serves as a conductor [18]. Another possible approach to fabrication of solid carbon composite electrodes is homogenization of carbon particles with monomer instead of polymer, subsequently; electrode material is filled into an electrode body and polymerization is initiated. After polymerization and surface polishing the electrode is prepared for the measurement [37]. Of course, many other fabrication processes were developed, because preparation process mainly depends on the type of used non-conductive phase and if the electrode would be chemically modified. Sometimes it is necessary to dissolve polymer at a higher temperature and afterwards the carbon particles are added [38]. A sol gel technique [39] or precipitation and drying technique [40] may be also used. Many fabrication processes of modified electrodes were developed, too. These electrodes can be modified in many possible ways by adding another chemical compound into electrode mixture during fabrication process or surface of the electrode may be doped by deposition of metals and metalloids [41, 42]. As an example of chemical modification it might be mentioned the addition of dispersed epinephrine in ionic liquid to the electrode forming mixture, which exhibited an obvious electrocatalytic activity towards the oxidation and determination of glutathione [43]. Another example of modification of carbon composite electrode is voltammetric determination of catechin in samples of teas, where the copper phosphate is added to increase the signal and the modified electrode allows the determination of catechin at lower potential than that observed at an unmodified electrode [38]. Interesting chemical modification of carbon composite electrode can be the functionalization of electrode by 5-amino-2-mercapto-1,3,4-thiadiazole to enhance the determination of L-tryptophan in the presence of ascorbic acid and paracetamol at physiological pH. Many other compounds can be used as modifiers for achieving desired properties, e.g., enzymes [44, 45], synthetic polymers [46], or gold nanoparticles with DNA probes [47].

Carbon composite electrodes have been applied as voltammetric sensors in a wide variety of areas of determination, including determination of anticancer drugs [26], active compounds in medicaments [48], environmental pollutants [24, 49], vitamins [50], trace amount of heavy metals in food analysis [51], toxins of bacteria [52], inorganic analytes [53] as well as organic analytes [13]. It is clear from these findings that carbon

composite electrodes are useful in a wide range of analytical flow methods as an electrochemical detector for capillary electrophoresis [31], flow injection analysis [54], high performance liquid chromatography [55], or microchip electrophoresis [56].

In **this Ph.D. Thesis**, **differential pulse voltammetry** (DPV) and **cyclic voltammetry** (CV) have been used as main voltammetric techniques for testing the proposed arrangements. These voltammetric techniques possess high sensitivity with a very large useful linear concentration range from mmol to pmol L^{-1}. DPV can reach limits of detection from $1 \cdot 10^{-5}$ mol L^{-1} to $1 \cdot 10^{-10}$ mol L^{-1} [8, 57].

2.2. Carbon paste electrodes

First attempt to establish **carbon paste electrode** (CPE) as a new electroanalytical instrument, was recorded by Adams and his student Kuwana at the University of Kansas in the year 1958. The inventors itself defined carbon paste as a mixture of conductive carbon particles with organic liquid; binding carbon particles into compact mixture, forming a typical consistency of peanut butter [58]. Carbon paste electrodes can be also defined as composite electrodes (random ensembles-dispersed), because the liquid binder mostly serves as an insulator phase and carbon as a conductive phase [17].

Since their introduction almost sixty years ago, composition of carbon pastes have gone through an extensive development and there exists many types of them. Requirements for carbon material are low adsorptive capabilities, high purity, and defined and constant size of particles. The most frequently used carbon particles are graphitic carbon particles [59]. Nevertheless, carbon pastes can be prepared from glassy carbon powder [60], graphene [61], or carbon nanotubes [62] and many other forms of carbon.

Selection of binding liquid is not a minor matter, because obvious function of binder is accompanied by many side effects, which makes binding liquid important part of the electrode. Thus, analyst should pay attention to the choice of both main parts of CPE. In the case of binding liquid; chemical inertness, zero electrochemical activity, high viscosity, low volatility, and minimal solubility in water is required [63]. Typical pasting liquids are minerals oil like Nujol and Uvasol [64]; ionic liquids can replace classic binder or act like a modificator and special matrix for enzymes [65, 66].

In this **Ph.D. thesis, CPE** was used for determination of indoxyl sulphate for the sake of comparison to results obtained with **CFE [2]**. The same type of graphitic carbon was used for the preparation of CPE and CFE; thus differences attributed to the difference in the shape of the electrodes or in the role of the insulator component in the electrode can be evaluated. Moreover, similarity to used CFE can be seen in the disposable method of use, because, easy recovery of CPE surface by wiping with wet filtration paper allows measurements always on the new surface (carbon paste was packed in the Teflon piston-driven holder).

Easy renewability is among of the most advantages of CPE. Besides easy renewability CPEs offer many other advantages such as high conductivity and low background current, easy miniaturization, compliance with green chemistry concept, and modification in many possible ways. Of course, CPE exhibits some disadvantages mostly linked with aging of carbon paste; therefore, analytical performance is changed with time. The most stable signal should be obtained during time period from 1 day to 1 month after fresh preparation of the paste due to self-homogenization process [67]. Thus, it is necessary to keep some basic rules during storage of CPEs. CPE should not be stored basically on air due to drying and subsequent cracking of the paste. Storing of CPE in distilled water avoid this problem [63]. Another major disadvantage is the tendency to disintegration of carbon paste mixture in the contact (or during measurement) with organic solvents or supporting electrolytes. This problem can be avoided by the stabilization of the paste by addition of some solid surfactant [68]. The last of main pitfalls of CPE are complications connected with the presence of oxygen in carbon paste. Reduction of oxygen during measurement in cathodic potential windows presents rather difficult problem [67].

As mentioned above, properties of CPE can be changed by the modification of carbon paste according to the desired application. The electrode can be chemically modified with various chemical compounds (CMCPE) [69], biologically modified with enzymes (CP-biosensor) [70], and chemically modified by a strong electrolyte (electroactive electrodes, CPEE) [71] or electrodes with plated surface by metallic films and metallic nanoparticles [72]. In the world of electroanalytical analysis are many others specific CPEs. All are mentioned in excellent review by the research group of Svancara and Vytras [73].

Carbon paste electrodes have been applied as voltammetric sensors in a wide variety of areas of determination from food analysis to drugs [60, 74, 75].

2.3. Gold nanostructured electrodes

According to IUPAC nomenclature, nanostructured arrangements/structures are classified as structures in which at least one dimension has in order of nanometers and morphology consisting of phase nanodomains [76]. Nanostructured arrangements have received considerable attention and extensive development over the last decade in a broad variety of application including electroanalytical chemistry, physical chemistry etc., where the interfacial nature of measurements favours the fabrication of miniaturized analytical devices. In this context, nano-thin-film technology is of great utility [77].

The unique chemical and electrical properties of nanostructured layers (films/electrodes) are usually influenced by their fabrication process, by the size of nanoparticles and their density, more than by the nature of the used material (type of particles) [78].

In the case of **nanostructured gold electrodes** (electrodes from AuNPs), many different manufacturing processes were developed. The gold nanostructured electrodes made from gold nanoparticles (AuNPs) and atomic gold can be prepared by utilizing self-assembly of AuNPs at the surface covered by a thiol spacer which is self-assembled at common bulk electrode serving as a conductor [79]. Other possible approaches to the fabrication of gold nanostructured electrode are *in-situ* or *ex-situ* plating of gold particles from the solution of $HAuCl_4$ onto selected substrate under certain potential. This method is called electrografting [80, 81]. However, these procedures are very time consuming especially as far as the finding of optimal condition for deposition of gold is concerned, they require large amounts of chemicals, and a lot of user experience. The deposition of gold can be followed by deposition of mercury on the surface of substrate bulk electrode; deposition of gold from the concentrated solution of $HAuCl_4$ can be followed by subsequent deposition of mercury from the concentrated solution of $Hg(NO_3)_2$ resulting in the gold nanostructured amalgam film electrode. It is called hybrid nanostructure [82]. In the case of nanostructured gold film electrodes made by electrografting or by deposition from solution, it is difficult to ensure that the thickness and shape of the gold layer is completely identical for each thus prepared electrode, especially in nanoscale. To avoid this problem, gold screen-printed electrodes can be

used. During the preparation of screen-printed electrodes, the electrode ink is instrumentally applied on a suitable substrate and it is easier to ensure the same thickness in nanoscale for all electrodes. Moreover, traditional three-electrode configuration printed on the same strip is also pronounced advantage of any screen-printed electrodes [83]. Modern approach to fabrication of gold nanostructured film electrodes is **physical vapour deposition** of Au atoms using **sputtering** method. This fabrication process can be used in the case of the necessity to use a non-conventional reference electrode or different electrode arrangement, shape and size, which cannot be satisfied by using screen printed electrodes.

Advantage of sputtering lies in simplicity, reproducibility, and low price of final products. Moreover, it is considered as pollution free ("green") method. Disadvantage of gold sputtering is that gold is one of the most inert metals and the adhesion between AuNPs and a polymeric substrate is poor. Film adhesion and electrical contact properties are strongly influenced by the interface structure. Also, film adhesion may become worse when electrodes are exposed to some types of organic solvents or concentrated acids. For this reason, several modification techniques (physical, chemical or their combination) have been suggested for enhancing metal to polymer adhesion, for example treatment by plasma [84, 85] or fixing of AuNPs by thiol groups containing spacer [79, 84, 86].

Gold nanolayers made by **physical vapour deposition** are well known and commonly used for many biophysical and material applications. However, their use for fabrication of working electrodes for electroanalytical purposes is less common, so the aim of this Thesis was to test them properly in the field of analytical electrochemistry. In **this Ph.D. Thesis** a few types of gold nanostructured film electrodes made by **sputtering** method were characterized and tested. All used types of electrodes were developed and supplied by University of Chemistry and Technology in Prague, Department of Solid State Engineering.

The first category of tested **gold nanostructured film electrodes** (GNFE) comprised 80 nm thin gold nanolayers **sputtered** on 50 μm thick foil of polytetrafluoroethylene (non-conductive substrate) with 3 different degrees of treatment: pristine PTFE (**GNFE-Pristine**), plasma treated (**GNFE-Plasma**) and plasma treated and subsequently grafted (spontaneous grafting) with biphenyl-4,4′-dithiol (**GNFE-BPD**). Scheme of fabrication

of all GNFE is shown in Fig. 2-2. Sputtering of gold from Au target was realized through contact mask to ensure identical shape of electrodes with parameters: round shape head with 3 mm in diameter with connected tail 15 mm long and 1 mm thick; the tail was used for connection to potentiostat. The round shape head was isolated from the tail by non-conductive lacquer to ensure uniform electrode area (**Fig. 2-3**). The set of disposable GNFEs is displayed in **Fig. 2-4**.

It is envisaged that these electrodes could be used for the determination of oxidisable biomarkers in urine and of environmental pollutants in water. In this **Ph.D. thesis**, among the other tests; the applicability of the electrodes was verified by differential pulse voltammetric determination of hydroquinone (HQ) as a one of the most commonly used probes of organic environmental pollutants **[3]**. All results were compared to commercial bulk gold electrode supplied by Metrohm.

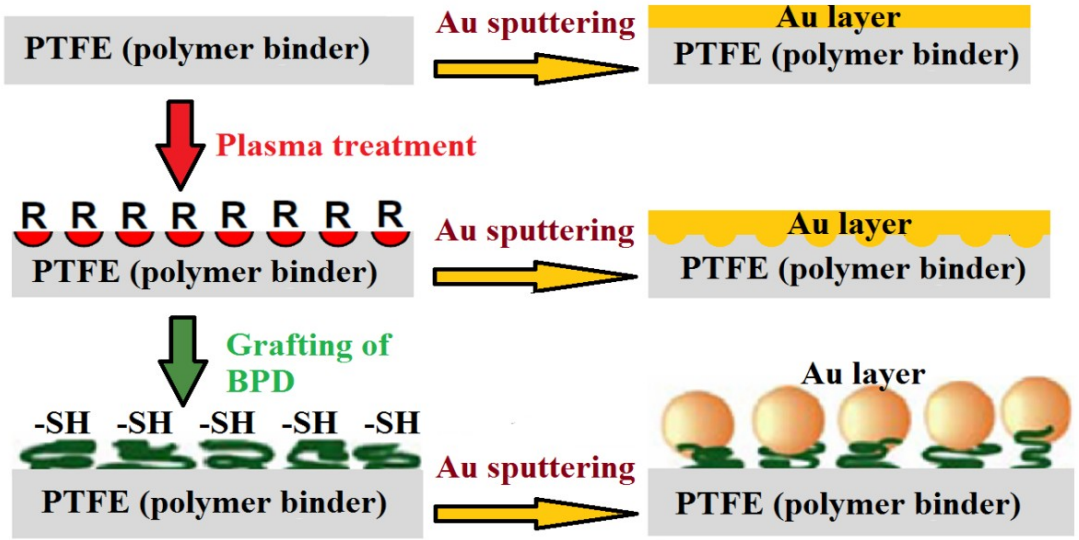

Fig. 2-2 Scheme of fabrication of all types of GNFEs (Author: Milan Libansky).

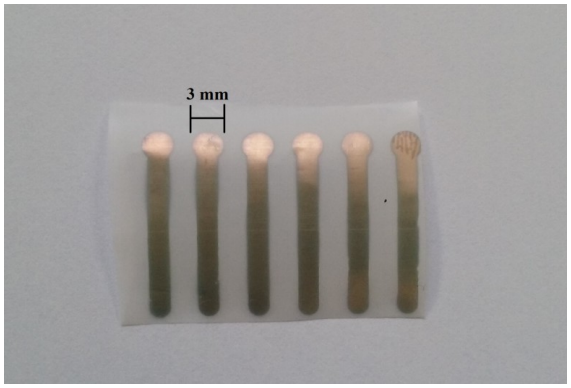

Fig. 2-3 Disposable GNFEs before isolation by non-conductive lacquer.

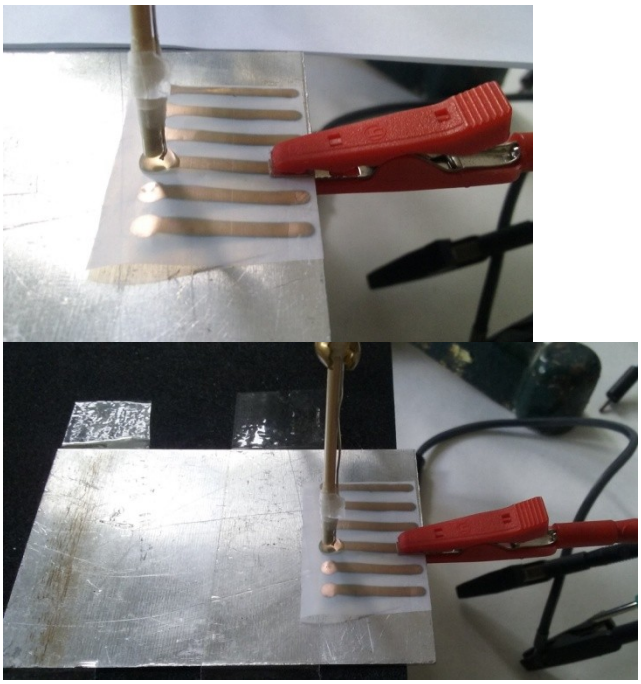

Fig. 2-4 GNFEs connected to the potentiostat during measurement with reference gel leakless Ag/AgCl electrode and platinum wire as an auxiliary electrode.

The second type of tested **gold nanostructured film electrodes** comprised of 10 nm thin transparent gold nanolayers **sputtered** on the surface of Su-8 polymer patterned by laser. Various substrates (functional groups) were grafted on the surface of GNFEs. Used substrates were poly n-isopropylacrylamide (pNIPAAM) **[4]**, -NO_2, -C_8F_{17} **[5]**, -C_1H_3, -C_4H_9, -$C_{10}H_{21}$, and -$C_{16}H_{33}$ **[6]**. Complete fabrication processes are mentioned in publications **[4-6]**. GNFE with **pNIPAAM** substrate is shown in **Fig. 2-5** (before isolation of electroactive area by non-conductive lacquer).

These electrodes could be used for the determination of environmental pollutants e.g. azodyes (crystal violet, metanil yellow, etc.) in extremely low concentration. Especially, GNFE with pNIPAAM substrate is promising from the point of view of the use in electroanalytical chemistry due to its phase transition from swollen to collapsed state, because it can be used for entrapping of the analyte molecules [87]. In this **Ph.D. thesis**, basic **CV** measurements with inorganic probes were done.

Fig. 2-5 GNFE with pNIPAAM substrate connected to the potentiostat with reference gel leakless Ag/AgCl electrode and platinum wire as an auxiliary electrode.

Aim of this **Ph.D. Thesis** was the electrochemical characterization of selected GNFEs made by sputtering method and the attempt to utilize the unique properties of gold nanomaterials for electroanalytical purposes.

Generally speaking, electrodes made of gold nanoparticles offer unique physicochemical properties and advantages such as high surface-to-volume ratio, surface charge, possible change of the hydrophobicity or hydrophilicity, easy miniaturization and change of shape; they can be chemically modified and mechanically or electrochemically pre-treated to further improve their native properties [88]. The electrode material can be physically modified by addition of other nanoparticles (carbon or metal particles). Combination of two nanomaterials with different properties can provide a unique hybrid nanoparticle electrode with new properties [89]. In addition, it is possible to combine the electrode material with various chemical compounds as a certain type of chemical modification. Mixture of thio compounds [90], nucleobases [91], organic acids [92], etc. can be used for modification, if any special application is required. A specific example of chemical modification might be modification based on combination of L-cysteine and gold nanoparticles to increase the rate of electron transfer during determination of dopamine hydrochloride [93]. Another example of modification of nanostructured gold electrodes is electrochemical impedance

spectroscopic determination of human immunoglobulin G, where polymeric pyrrole is linked with gold nanoparticles to form a permeable immunosensor [94].

Nanostructured gold electrodes made by various techniques have been used as voltammetric sensors for the determination of inorganic [95] and organic analytes [96], as well as metabolites of human body processes [97-99], pharmaceuticals [81] and for voltammetric studies of DNA [100]. Nanostructured gold electrodes are usable in a wide range of chemical disciplines such as impedance spectroscopy and chronopotentiometry in analytical chemistry [101], as an electrocatalytic mediator of luminescence in spectroscopy [102] or as biosensors in biochemistry [103, 104]. It is necessary to mention special usability of these electrodes in supercapacitors, in microelectronics and photovoltaics [105, 106].

3. Probes and analytes

3.1. Homovanillic acid and vanillylmandelic acid

Homovanillic acid (HVA) and **vanillylmandelic acid** (VMA) are final products of metabolism of catecholamines in human body [11]. Main endogenous catecholamines (epinephrine and norepinephrine) are formed in the adrenal medulla and in the brain. These catecholamines are subsequently metabolized in human body to major metabolites, HVA and VMA (Fig 3-1) [107]. Monitoring of concentration of these two acids represents a useful tool for early diagnosis of large number of metabolic and neurological disorders. Both acids can be found and determined in various human fluids such as urine, blood plasma, serum [108], cerebrospinal fluid [109], and brain fluid [110].

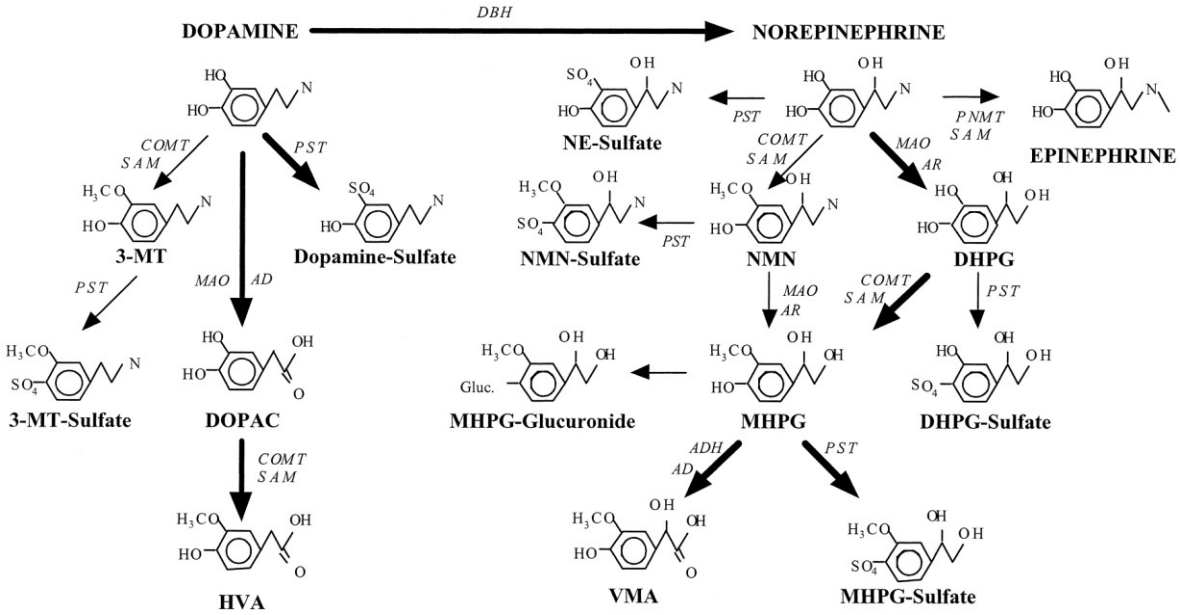

Fig 3-1 Scheme of dopamine metabolism (source www.researchgate.net).

Non-physiologically high values of concentration of these biomarkers are linked with tumours in the adrenal medulla [111], neuroblastomas [112] and pheochromocytomas [113]. Neuroblastoma is the most common cancer in babies and the third most common cancer in children age; about 90% of cases occur in children less than 5 years old and it is rare in adults. On the other hand, pheochromocytoma is only a matter of adults

between 40 and 50 years of life [114]. These tumours cause overproduction of catecholamines, then excessive production and release of catecholamine metabolites to blood, which leads to subsequent excessive release of HVA and VMA to urine [115]; thus, monitoring excretion of HVA and VMA to urine is fundamental for determining the stage of disease and for an early diagnosis of tumours mentioned above [107]. Other scientific studies revealed relationship between increased concentration of HVA in cerebrospinal fluid [116] and suicide attempts [117], post-traumatic stress disorders [118], chronical schizophrenia [119], Parkinson's disorder and bulimia [120]. It is necessary to mention that not only absolute concentration of acids can be used as a diagnostic marker; determination of ratio HVA/VMA (concentration) is important screening method for early detection of Menkes disease influencing the level of copper in human organism [121, 122].

Reference intervals of concentration of HVA and VMA in human urine are from 7 μmol L^{-1} to 40 μmol L^{-1} [123, 124]. In the case of blood plasma, values are about 400 times lower. For this reason, urine is the most common matrix for determination of these acids. Determination of HVA and VMA in other human fluids is uncommon and complicated from the point of view of reliable sampling [125].

Besides the low concentration in human urine, during determination of HVA and VMA attention must be paid to the almost similar structures of acids (**Fig. 3-2**). Therefore sensitive methods, separation techniques and extraction techniques are required. Theirs phenolic structure suggests their oxidisability under relatively low potentials accessible for various types of electrodes, which can be used for determination. Therefore HVA and VMA were chosen as optimal probes/analytes for testing and verification of usability of array of solid **carbon composite film electrodes** integrated in a 96-well microtitration plate **[1]**.

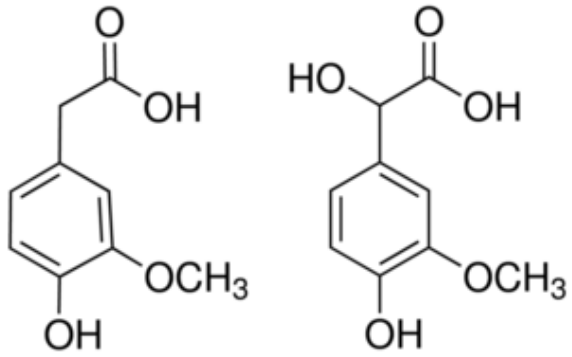

Fig 3-2 Chemical structure of HVA and VMA.

For the determination and separation of HVA and VMA, many sensitive analytical methods have been developed. Techniques such as GC-MS [126], UHPLC-MS/MS [127], HPLC-DAD [128], HPLC with fluorescence detection [129], HPLC-ED [130], CZE-ED [131] and voltammetric determination [118, 121, 132-134] are the most commonly used. Of course, the lowest limits of quantification and determination were obtained by modern HPLC methods with MS detection (pmol L^{-1}) [135, 136]. In comparison with HPLC, modern electrochemical arrangements and methods offer fast, simple and user-friendly ways of determination of biomarkers.

3.2. Indoxyl sulphate

In the last decade, **indoxyl sulphate** (urinary indican) became one of the most determined and studied compound in human plasma and urine. This toxic compound accumulates in plasma of patients with renal failure and kidney diseases [137]. Occurrence of high concentration of urinary indican in human body is also associated with cardiovascular problems during kidney dialysis and after transplantation, problems of colon microbial metabolism or increase of glomerular sclerosis and oxidative stress [138].

Urinary indican is relatively small molecule (**Fig. 3-3**) soluble in water and in living organisms it is 90 % bound with plasma proteins, especially with albumin and only 10 % is "free form" as a standalone molecule [139]. Indoxyl sulphate is a product of "intestinal putrefaction of dietary proteins", which is origin of the protein bonding. Tryptophan absorbed from food is converted to indole in colon by intestinal microflora; then indole is metabolized to indoxyl sulphate by liver after transfer to systematic circulation. Subsequently, indoxyl sulphate is secreted by the kidneys through tubular secretion to urine (**Fig. 3-4**). When kidney disease occurs, kidney clearance decreased and indoxyl sulphate accumulates in plasma and urine of organism which can lead to cardiovascular problems [140]. However, final concentration of indican in human plasma and urine is also based on liver condition and can be influenced by intake of antibiotics which suppress colon intestinal microflora or by high (or low) protein diet [141]. On the other hand, indoxyl sulphate's toxicity was proven in cultured human cells and animals and its toxicity in humans has not yet been conclusively established and it is in the interest of many clinical laboratories, because monitoring of excretion of urinary indican to urine could be fundamental for determining the first stages of kidney diseases and for the preventing of unwanted heart problems [142]. So that modern techniques for extraction and determination of indican are required.

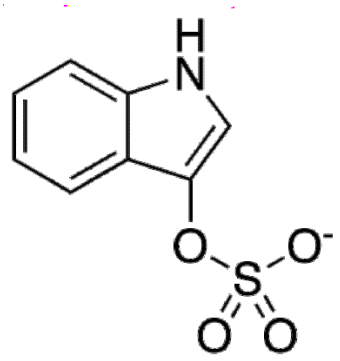

Fig 3-3 Chemical structure of indoxyl sulphate (urinary indican).

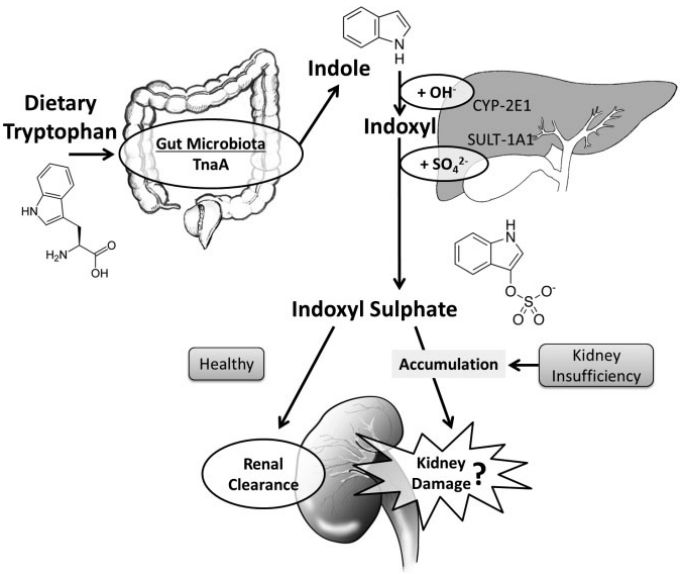

Fig 3-4 Scheme of tryptophan metabolism [143].

Reference intervals of concentration of indican in human urine of healthy patients are from 1.1 to 3.9 µmol L^{-1}. Patients with kidney diseases like a uremia demonstrate the values from 100 to 170 µmol L^{-1} due to accumulation effect [144]. Concentration of indoxyl sulphate in human plasma is in one order difference of urine levels, depends on the weight of body, urination level and clearance [143, 145]. These relatively high and accessible concentration intervals together with the promise of usability of developed methods for determination of urinary indican in the future were the main reasons for selection of urinary indican as an ideal probe/analyte for testing and verification of usability of array of solid **carbon composite film electrodes** integrated in a 96-well microtitration plate (in this **Ph.D. Thesis**) **[2]**. In addition to that, it was attempted to extract the indoxyl sulphate by solid phase extraction as an inexpensive substitution for

modern separation techniques. In this paper **[2]**, all obtained results were compared to results of measurement on graphitic carbon paste electrode.

Despite the many medical studies and well investigated mechanism of electrochemical oxidation of indican, where the oxidation of pyrrole ring is followed by the hydroxylation of the benzene moiety and subsequent oxidation of hydroxyl group (**Fig 3-4**) [146], not many electrochemical method were developed for the determination of indican. As one of the few we can mention determination of indican on disposable screen-printed graphene electrode by square-wave voltammetry [147]. Nevertheless, determination of indican by HPLC-MS is very common [148-150].

4. Results and discussion

4.1. Carbon composite electrode

4.1.1. Homovanillic acid and vanillylmandelic acid

In the framework of my Master Thesis, an array of solid **carbon composite film electrodes** (CFE) integrated in plastic cells was developed and patented. This electrode arrangement was tested from the point of view of composition of electrode material, electrochemical behaviour during CV measurements of oxidation of ferrocyanide, and widths of potential window in BR buffer of various pH. Finally, voltammetric method for determination of environmental pollutant 5-chloro-2-(2,4-dichlorophenoxy)-phenol named triclosan was developed to verify practical applicability. At the CFE, differential pulse voltammetry (DPV) was used with the limit of quantification 0.25 μmol L^{-1} for electrode made from graphitic carbon with polystyrene as a matrix and 0.50 μmol L^{-1} for electrode made from graphitic carbon with polycarbonate matrix. The method was successfully applied for practical samples of river water and toothpaste. From the comparison of obtained results using both graphitic electrodes it was obvious that for the measurement of real samples it is preferable to use carbon composite film electrode based on polystyrene, because it exhibited higher precision and accuracy [13]. In this **Ph.D. Thesis**, this type of electrode was selected for further testing and application.

For next verification of practical applicability of CFE, the array was applied to DPV determination of standards of oxidisable tumour biomarkers 2-(4-hydroxy-3-methoxy-phenyl)acetic acid (homovanillic acid, **HVA**) and (*RS*)-hydroxy(4-hydroxy-3-methoxy-phenyl)acetic acid (vanillylmandelic acid, **VMA**) **[1] (Appendix I)**. Phenolic structure of these acids suggests their oxidisability under potentials accessible for CFE, which was advantageously used for the investigation of the electrochemical behaviour and determination using DPV.

The influence of the pH on the DPV voltammograms was investigated in separate solutions of 100 μmol L^{-1} standards of HVA and VMA in BR buffer in the pH range from 2 to 12. Parameters of the DPV potential program were not optimized (0.1 s pulse width, 50 mV pulse height, 20 mV s^{-1} scan rate, sampling time 20 ms). In the case of

HVA, one well-shaped anodic voltammetric peak was observed in the whole pH range. In the case of VMA, two anodic peaks were observed up to pH 11. At pH 12, conjunction of two peaks occurred. Oxidation peaks correspond to the oxidation of hydroxyl group at aromatic system, however for HVA and VMA, two different oxidation mechanism are presumed [151]. The peak potential (E_p) was shifted to less positive anodic potentials linearly with increasing pH. It is necessary to mention that the potential of the peak potential of HVA is similar to the first peak of VMA; the potential difference between the peaks increases with decreasing pH and in acidic pH, the peaks are independently evaluable, which is promising for simultaneous determination of both analytes in one solution. Moreover, the highest and best-developed voltammetric peaks were observed in acidic media and thus BR buffer of pH 2 was selected as an optimum medium.

In the next step, adsorptive accumulation of both analytes was tested in the BR buffer of pH 2 for the verification, whether it is possible to use adsorptive stripping voltammetry. Undeniable advantages of this voltammetric technique lie in the possibility to increase the sensitivity of the measurement associated with lower quantification limits [8]. The measurements were carried out in non-stirred separate solutions of standards of HVA and VMA at two concentration levels: 100 μmol L^{-1} and 10 μmol L^{-1} within accumulation time 1, 5, and 10 minutes. But even after 10 minutes of accumulation time, current response did not show any increase and values of peak current became stable for both analytes; values of *RSD* of the peak current of all measurements were approximately 3.5 % for both concentration levels and both analytes. It is clear that the adsorptive step could not be utilized.

Under optimum conditions, the calibration curves were measured in the concentration range from 100 to 0.8 μmol L^{-1} for HVA and from 100 to 1 μmol L^{-1} for VMA. Achieved limits of quantification were 0.3 μmol L^{-1} for HVA and 1.0 μmol L^{-1} for VMA. The concentration dependences were linear within the whole concentration range for both analytes, so that least square linear regression method was used for calculation of quantification limits as the concentration of the analyte which gave a signal ten times higher than the standard deviation of the lowest evaluable concentration [152]. *RSD* of the lowest evaluable concentration (0.8 μmol L^{-1}, n = 10) were 6.6 % for HVA and 11 % (1 μmol L^{-1}) for both peaks of VMA. This explained higher *LOQ* in the case of

VMA. In comparison with other DPV determinations of standards of acids on various carbon electrodes [121, 134], developed method on CFE offers comparable results.

Both analytes are usually determined side by side in one solution, because of their origin in similar human body fluids. As mentioned above, E_p of HVA is close to E_p of the first peak of VMA. Second peak of VMA is well separated, thus it is possible to determine the concentration of VMA and then calculate the concentration of HVA from the first peak corresponding to the sum of both compounds. This was confirmed by measuring four calibration sets of mixed solutions of standards of analytes, where each calibration set was prepared from standard of HVA or VMA in the concentration range from 10 to 1 μmol L^{-1} with constant addition of the second analyte at concentration 10 or 5 μmol L^{-1}. Then calibration curves were evaluated; the values of slopes of first peak should correspond to the slopes of standards and the intercepts should correlate with the current increase caused by the addition of the second biomarker. The good agreement with standard values of calibration curves was obtained; the results of HVA show higher consistency than those of VMA, which differ from the standard of approximately 20 %. This inconsistence was caused by the change of the baseline in the mixture of analytes and also by lower repeatability of the measurements of VMA standards. Obtained result from the measurement of calibration curves of mixture of acids was verified also by calculation method (described in **[1]**) **(Appendix I)**. The calculated average recovery of the spiked concentrations was almost 90 % for both analytes.

It can be concluded, that electrode system tested in this Ph.D. Thesis can be successfully used for determination of oxidisable biologically active organic compounds. However, obtained limits of quantification of developed method are deficient in comparison to modern spectrometric techniques. This problem can be overcome by the use of more sensitive voltammetric method (SWV) and SPE can be also used for preliminary separation and preconcentration of the tested analytes form urine, but this this the aim of the future research and it was not investigated in this **Ph.D. Thesis**. Nevertheless, it can be concluded that the recently developed CFEs combined with modern voltammetric method offer ssufficient sensitivity and accuracy required in screening measurements.

4.1.2. Indoxyl sulphate

In this **Ph.D. Thesis**, a previously mentioned array of CFEs integrated in microtitration plate was used for determination of oxidisable biomarker of kidney diseases **indoxyl sulphate** (**urinary indican**) to verify practical applicability of the arrangement **[2] (Appendix II)**. This determination was combined with a preliminary separation and preconcentration of indoxyl sulphate from human urine using solid phase extraction. Moreover, all obtained results from measurement with CFE were compared to measurement with well-known carbon paste electrode (CPE) made from the same type of carbon material like CFE **[2]**. DPV was used in both cases **(Appendix II)**.

Firstly, the pH dependences were measured. Electrochemical oxidation of indoxyl sulphate provided two well-shaped and well-separated voltammetric peaks from the two step electron exchange mechanism (described in [146]). The pH dependences were measured in the range from pH 2 to 12 in the 50 μmol L^{-1} solution of standard of indoxyl sulphate in BR buffer. Parameters of the DPV potential program were not optimized (0.1 s pulse width, 50 mV pulse height, 20 mV s^{-1} scan rate, sampling time 20 ms). The peak potentials (E_p) of both peaks were shifted to less positive anodic potentials linearly with increasing pH on both electrodes with the same vigour. The highest and best-developed voltammetric peaks were observed in acidic media, current response was decreasing linearly with increasing pH; in the strong alkaline medium, the first peak was still evaluable and the height of second peak dropped to zero. For CFE and for CPE, pH 2 and pH 3 were selected as optimum media, and only the first peak of indoxyl sulphate was used for evaluation of results, because second peak of indoxyl sulphate was lower than first and more difficult to evaluate due to coincidence with the end of potential window.

Under optimal condition, the repeatability of height of the peak was carried out in the solution of 50 μmol L^{-1} indoxyl sulphate in BR buffer. During measurement (n = 10) with the new electrode (CFE) or on renewed surface of the electrode (CPE), repeatability of height of the first peak was 4.2 % for CFE and 3.4 % for CPE. The results are appropriate for voltammetric determinations at solid electrodes made of graphitic carbon [13]. On the other hand, the CFE and CPE surfaces after repeated measurements were passivated by oxidation electrode reaction products; therefore, the

peak current decreased for almost 60 %. Moreover, in the case of CFE, decrease of peak current was magnified by increase of background current in each subsequent scan. Thus, these results pointed to the fact; that it is necessary to use each measuring cell with integrated CFE only once as a disposable sensor and that CPE surface have to be renewed after each single measurement.

Adsorptive accumulation of indoxyl sulphate was tested in the BR buffer of pH 2 (CFE) and pH 3 (CPE) for the verification, whether it is possible to use adsorptive stripping voltammetry. The measurements were carried out in the solution of 5 μmol L^{-1} standard of urinary indican in BR buffer of pH 2, 6 and 9 within 5 minutes of accumulation time period, in the case of CPE under the stirring of the solution. After prolonged time, the increase of current response was negligible (ca 30 %). Therefore, the adsorptive step was not further utilized.

Under optimum conditions, the calibration curves were measured in the concentration range from 50 to 1 μmol L^{-1} for both electrodes. Achieved limits of quantification were 0.7 μmol L^{-1} for CFE and 1.7 μmol L^{-1} for CPE, respectively. The concentration dependences were linear within the whole concentration range for both analytes, so that least square linear regression method was used for calculation of quantification limits, which were calculated as the concentration of the analyte which gave a signal ten times higher than the standard deviation of the lowest evaluable concentration [152]. *RSD* of the lowest evaluable concentration (1 μmol L^{-1}, n = 10) were 7 % for CFE and 15 % for CPE. This explained higher calculated *LOQ* in the case of CPE. The small differences in the electrochemical behaviour attributed to the difference in shape or in the role of the insulator component in the electrode were observed **[2]** (**Appendix II**).

For the verification of practical applicability of CFE with combination of newly developed voltammetric method, solid phase extraction was employed for the preliminary separation and preconcentration of indoxyl sulphate in fortified urine samples. SPE was performed prior to the voltammetric determination to remove part of the matrix oxidisable compounds and urine interferents. All obtained results from SPE were compared to measurement of solutions of standard of indoxyl sulphate without SPE. The entire conditions of SPE are described in **[2]** (**Appendix II**).

As a feed solution for SPE, a solution of the 10 mL of 10 μmol L^{-1} indoxyl sulphate in BR buffer of pH 3 was selected for the measurements. Urine samples were adjusted

to pH 3 with phosphoric acid and 1 mL of BR buffer of the same pH was used as the washing step between the sorption and the elution. Analyte was eluted by 2 mL of methanol for the first choice. Sorption and elution of indoxyl sulphate under these conditions occurred on EN extraction columns with concentration recovery from 95 to 100 %. However, this procedure was not satisfactory during the measurement with human urine, as the analyte peaks were coupled with the major interferents which were eluted from the column. The fact, that the common concentration of indoxyl sulphate in human urine of healthy subject is negligible in comparison with other oxidisable compounds, also contributes to the difficulty of the task.

In the next step washing step was altered, the volume of washing solution was increased to 5 mL and pH was changed to pH 8. Under these conditions, some impurity from human urine were washed away and background current decreased; however major interfering compounds still remained in the measured fraction after elution and extraction was not successful.

Last logic step was the change of the eluent strength to elute only the analyte instead of other compounds/interferents in human urine. 5 % methanol and 10 % methanol were tested as a series of standalone eluents. In 5 % methanol, the recovery was in the range from 91 to 100 % and in the case of 10 % methanol the recovery was from 90 to 100 %. Nevertheless, not all interferents from human urine were eliminated again, during the measuring of fortified sample. The SPE was not successful at all and methanol was not suitable eluent for indoxyl sulphate separation. On the other hand, selection of BR buffer (5 ml) as an optimal washing solution was successful, because it decreased background current caused by urine impurities.

It can be concluded from obtained results in this **Ph.D. Thesis** that it is possible to use an array of carbon composite electrodes for determination of oxidisable biologically active organic compound, indoxyl sulphate with sufficient sensitivity and accuracy required in screening measurements. Otherwise, an array of integrated CFEs achieved slightly better results during determination of standard of the indoxyl sulphate with developed voltammetric method in comparison to well-known CPE **[2]** (**Appendix II**). Nevertheless, for determination of indoxyl sulphate in human urine matrix in the future, it is priority to develop a suitable technique for its preliminary separation and preconcentration from urine samples. With a successful extraction comes the possibility

of using this electrode arrangement as cheap disposable sensors for large-scale screening of proposed analyte in human urine.

4.2. Gold nanostructured electrodes

4.2.1. Gold nanostructured film electrodes on PTFE substrate

The method of easy fabrication of thin gold nanolayers by sputtering of gold atoms (group of physical vapour deposition method) was developed by Department of Solid State Engineering at the University of Chemistry and Technology in Prague. This type of fabrication of gold layers is predominantly used for many biophysical and material applications, but its use for fabrication of working electrodes intended for electroanalytical applications is less common despite the fact that sputtering of gold layers for fabrication of **nanostructured gold film electrodes, GNFE** is considered as pollution free ("green") and very user friendly method.

In this **Ph.D. Thesis**, 80 nm thin gold nanolayers sputtered on **PTFE** with 3 different degrees of treatment were used: i) pristine PTFE (**GNFE-Pristine**), ii) plasma treated (**GNFE-Plasma**), and iii) plasma treated and subsequently grafted (spontaneous grafting) with biphenyl-4,4´-dithiol (**GNFE-BPD**). These gold nanolayers were provided by Department of Solid State Engineering at the University of Chemistry and Technology in Prague and they were applied as disposable nanostructured gold film electrodes. All types of GNFEs were electrochemically and physically characterized and its applicability as a disposable electrochemical sensor was verified **[3]**.

Electrochemical arrangement consists of GNFE, a gel leakless Ag/AgCl reference electrode, and platinum wire used as an auxiliary electrode and it is depicted in **Fig 2-4**. Complete fabrication procedure and conditions are described in paper **[3]** **(Appendix III)**. The GNFEs were designed to be stable and mechanically resistant sensors for long-term use. On the other hand, if any changes in its electrochemical performance occur with prolonged time (*e.g.*, increasing background current/noise or changing shape of voltammograms), a relatively low fabrication cost does not prevent the production of new sensors. This is another advantage of these nanostructured sensors made by sputtering method. The other main benefits of these sputtered electrodes are the easy portability, easy miniaturization, and the ability to measure in microliter volumes.

Before electrochemical characterization itself, the surface analysis was performed in cooperation with co-author of the paper **[3]**, **Ing. Alena Řezníčková, Ph.D.**, from the

University of Chemistry and Technology in Prague, Department of Solid State Engineering. Chemical composition of the surface of GNFEs was examined by scanning electron microscopy (SEM) combined with energy dispersive spectroscopy (EDS). Roughness and morphology was examined by atomic force microscopy and wettability was examined by drop shape analyzer. All obtained results are discussed in detail in the paper **[3] (Appendix III)**. From the surface analysis it can be concluded, that all types of GNFEs exhibited homogeneous gold layer with small differences in coverage of the PTFE. The weakest adhesion of gold layer was observed in the case of GNFE-Pristine. GNFE-Plasma exhibited the strongest adhesion of gold layer and the highest levels of surface concentration of Au from all GNFEs. GNFE-BPD exhibited a maximum surface roughness (26.5 nm) caused by the plasma treatment and by grafting of BPD on the surface of PTFE. Differences in values of water contact angles were not statistically significant **(Appendix III)**.

Electrochemical behaviour of potassium chloride, potassium nitrate, sulphuric acid and BR buffers pH 2, 7 and 12 was examined by DVP under following conditions: 0.1 s pulse width, 20 ms sampling time, 50 mV pulse height, 20 mV s^{-1} scan rate. Maximum accessible potentials for oxidation were reached in electrolytes of neutral pH. In the case of measurement in acidic pH, potential window was limited by peaks of alpha and beta gold oxides which appeared at potentials around 0.7 V. Acidic environment disrupted thin nanolayer of gold nanostructured electrode resulting early formation of the gold oxides [153, 154]. It was also observable that acidic medium coupled with high inserted oxidation potential results in the decrease of the adhesion of thin nanolayer and in fissures leading to the exposure of the surface of PTFE. In alkaline medium, conjunction of two peaks of alpha and beta gold oxides were observable with shift of the peak potential to 0.5 V. In the neutral media, peaks of gold oxides coincide with the end of potential window and potential windows were wider (0.9 V); thus they were selected as optimal media. In general, in comparison to gold bulk electrode, susceptibility to oxidation of the surface is generally higher in the case of GNFEs.

After the measurement, only gold bulk electrode was mechanically renewed, which was easy. GNFEs were not renewed due to low mechanical robustness during polishing of the surface and the electrodes were used as disposable sensors. If it is necessary to renew GNFEs, it might be possible to use chemical cleaning with concentrated ethanol.

Next study of electrochemical behaviour of GNFEs was performed by CV at scan rates from 10 to 500 mV s^{-1} in 1 mmol L^{-1} potassium hexacyanoferrate in 0.1 mol L^{-1} potassium nitrate. Potassium hexacyanoferrate was chosen; because it is the most commonly used probe for the characterization of electrochemical behaviour of electrodes in aqueous solutions and its electrochemical behaviour is well-known. Repeatability of measurements, reversibility of one electron reaction and the dependence of electrode response on scan rate was evaluated and complemented by calculations of real surface areas of electrodes from Randles-Sevcik equation [155].

The linear relation between the anodic peak current values and the square root of scan rate was obtained (R^2>0.993) for all used electrodes in measured range of scan rates. For all types of GNFEs, slopes of these dependences were 2 times higher than for gold bulk electrode which can be explained by higher active area of GNFEs. It was expected, that only amount of electroactive gold material on the electrode surface influenced the resulting values of the slopes. Then the trend of values should be: Plasma>BFD>Pristine. This assumption has not been fulfilled and order of values of slopes was: Plasma>Pristine>BFD. Difference in the slope values are probably also caused by the different kinetics of electrochemical reaction on the surface of different electrode. Full explanation is unclear yet and it would require further research.

Obtained values for ΔE_p were higher (70<ΔE_p<100 mV) than predicted for typical Nernstian reversible one electron reaction (59 mV), but the values did not exceed commonly obtained values on gold electrodes (70 mV for gold bulk) [156]. Average repeatability of all types of GNFEs was from 1.1 % to 8.5 % for the height of forward anodic peak as well as backward cathodic peak of 1 mmol L^{-1} potassium hexacyanoferrate in 0.1 mol L^{-1} potassium nitrate. At GNFE-Plasma the obtained repeatability was better than for other two GNFE, which should correspond with the highest amount of electroactive material, and the most homogenous Au layer. Calculated average values for the ratio I_A/I_C for all measurements at 50 mV s^{-1} scan rate were nearly 1.0, which pointed to reversible kinetics of the electrode reaction.

Active areas of all types of GNFE were calculated by the Randles–Sevcik equation from 10 CV measurements at scan rate 50 mV s^{-1}. As mentioned above, the diameter of all used electrodes was 3 mm; therefore, their geometric area was 7.1 mm^2. Active areas 7.5 ± 0.5 mm^2, 8.4 ± 0.2 mm^2, and 7.3 ± 0.5 mm^2 (active area ± confidence intervals)

were calculated for GNFE-Pristine, GNFE-Plasma, and GNFE-BPD, respectively. The increase of active area by plasma treatment was observed in the case of GNFE-Plasma. Calculated active areas of other two GNFEs were statistically comparable, but with higher values of confidence intervals caused by deviations from the ideal behaviour (mentioned in [156]). Nevertheless, all obtained results demonstrated higher active areas and acceptable usability of sputtered GNFEs in comparison with gold bulk electrode **(Appendix III)**.

Afterwards, the inorganic probe mentioned above was replaced by hydroquinone (HQ) as an organic probe to see a difference in the electrochemical behaviour. Hydroquinone was chosen as an organic compound representing well-known researched oxidisable environmental pollutant. As a supporting electrolyte buffer of pH 7 was selected. Experimental conditions became the same ($c_{\text{hydroquinone}}$ = 1 mmol L^{-1}, scan rates from 10 to 500 mV s^{-1}, repeatability of 10 CV measurements at 50 mV s^{-1} scan rate). The linear relation between the anodic peak current values and the square root of scan rate was obtained (R^2>0.995) for all used electrodes. The relationships of log I_p vs log v were constructed; the slope values about 0.45 for all electrodes were close to the theoretical value of 0.5 and proved diffusion behaviour. The oxidation of hydroquinone is a quasireversible process at most solid electrodes [156], thus the achieved peak-to-peak separation values with GNFEs (ΔE_p) were higher than predicted for Nernstian reversible simultaneous two electron reaction (30 mV) and it was necessary to impose relatively large overpotential of the GNFE to provide sufficient energy for the redox reaction [157]. Bulk electrode exhibited smaller peak-to-peak separation, which can be attributed to the most compact gold material of bulk electrode without disruptions with lower values of electric resistance [156].

For all types of GNFEs, slopes of these dependences were again 2 times higher than for gold bulk electrode and higher active area of GNFEs (roughness caused by plasma treatment of PTFE) was confirmed. The order of values of slopes was: Pristine>BFD>Plasma, which differ from the trend obtained in the measurement of ferrocyanide/ferricyanide redox system (mentioned above) and it indicates diversity of behaviour of organic vs. inorganic probes and that molecular size of probes with chosen electrolyte can influence electrochemical behaviour of the system on the electrode

surface. Therefore, such an electrochemical calibration of "behaviour" for each probe is desirable.

The involvement of electrochemical side reactions where different product is formed [157] was observed, because backward reduction peak was minimally 10 % lower than oxidation peak (I_A/I_C = 1.1 – 1.2), but the effect of passivation during repeated measurements was not observed. Repeatability of the height of forward anodic peak and backward cathodic peak of 1 mmol L^{-1} HQ in BR buffer pH 7 was from 3.8 % to 7.3 %; these results were comparable to the performance of gold bulk electrode.

To explore the possible practical application of GNFEs, DPV concentration dependences of HQ were investigated in the concentration range from 10 to 100 µmol L^{-1} in BR buffer pH 7. The oxidation peak currents of HQ increased linearly with the concentration on all types of GNFEs (R^2>0.990). *RSD* of the lowest evaluable concentration (10 µmol L^{-1}, n = 10) was 9 % for GNFE-Pristine, 7 % for GNFE-Plasma and 11 % for GNFE-BPD. Achieved limits of quantification of hydroquinone were 4.3 µmol L^{-1} for GNFE-Pristine, 4.2 µmol L^{-1} for GNFE-Plasma, and 9.0 µmol L^{-1} for GNFE-BPD, respectively. Low value of calibration straight-line slope and high value of repeatability explains higher *LOQ* in the case of GNFE-BPD. In comparison with other DPV determinations on various nanostructured gold electrodes and bulk electrodes [158, 159], developed GNFE offer higher *LOQ* and it is necessary to improve structure and fabrication process to obtain more compact gold layers on plasma treated PTFE surface resulting in improved *S*/*N* ratio.

It can be concluded that all GNFEs showed acceptable electrochemical parameters, which are comparable to parameters of gold bulk electrode. The increase of current response due to the increase of surface area by plasma treatment of PTFE and by sputtering of Au atoms (resulting in nanolayer) was observed and confirmed the fact, that sputtering method can be useful for fabrication of disposable working electrodes for electroanalytical chemistry. On the other hand, not all acquired parameters and the results of measurements were fully satisfactory. For example high *LOQ* cannot yet compete with low *LOQ* of modern nanostructured gold electrodes or of factory-made gold electrodes. But, here is a possibility to improve GNFEs via improvement of their fabrication process to obtain better performance. For example, the improvement of fabrication process is possible by extension of the deposition time and changes in the

conditions of deposition of Au atoms, which can lead to more compact gold layers without disruptions and with a higher content of Au or change of the substrate (ex. glass) with better adhesion is also possible. Nevertheless, gold electrodes made by sputtering offer certain advantages like small volume of used sample, easy miniaturization, possibility of recycling of gold from used electrodes, and also "green" method of fabrication, which is promising for the future use of these electrodes for determination of oxidisable electroactive organic compounds.

4.2.2. GNFE with pNIPAAM substrate

As was mentioned in **Section 2.3**., gold nanostructured electrodes/layers can be modified by many possible ways, for example, on the surface of the electrode can be deposited "intelligent molecule", commonly polymer. One of the most applicable intelligent polymer is poly(n-isopropylacrylamide) (**pNIPAAM**). This polymer with its temperature-dependent variation of thermodynamic state has been extensively used as a key component in smart materials field, especially in dynamic SERS substrates [160]. Phase transition influenced by temperature of pNIPAAM from swollen hydrated state (T<32°C) to collapsed dehydrated state (T>32°C) can be used for entrapping of analyte molecules and subsequent Raman scattering determination. Typical model probes for entrapping and subsequent spectrometric determination are dyes [161]; however, in this **Ph.D. Thesis [4]**, ferrocyanide was used for its well-known electrochemical behaviour. The main tasks were to find out, whether GNFE with grafted pNIPAAM substrate on the surface would be electric conductor, if electrochemical reaction of ferrocyanide/ferricyanide redox system would be fast enough and if would be possible to entrap analyte/probe on the surface by the change of the temperature.

Electrodes with grafted pNIPAAM substrate were provided by Department of Solid State Engineering at the University of Chemistry and Technology in Prague. This type of electrode was recently developed and material analysis was performed by Mgr. Oleksiy Lyutakov, Ph.D. and his research team. From theirs obtained results was obvious, that the main attractiveness of these sputtered gold layers/electrodes with pNIPAAM substrate lies again in their easy portability, the ability to measure in microliter volumes, and possibility of determination of submicromolar concentrations of active organic compounds **[4]**.

Gold nanostructured film electrode with deposited pNIPAAM substrate on the surface was applied as disposable electrochemical sensor. Electrochemical arrangement consists of GNFE with pNIPAAM substrate, a gel leakless Ag/AgCl reference electrode and platinum wire auxiliary electrode and it is depicted in **Fig 2-5**. Entire fabrication procedure and conditions are described in the paper **[4] (Appendix IV)** and simplified scheme of deposition of pNIPAAM follows in **Fig. 4-1**.

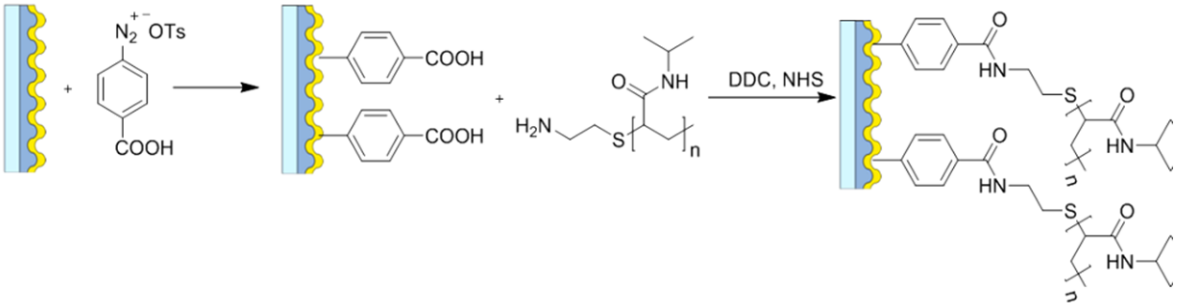

Fig. 4-1 Scheme of deposition of pNIPAAM substrate of the surface of gold nanostructured electrode **[4]**.

The electrochemical characterization was performed by CV measurement (scan rate 0.05 V s^{-1}) of 1 mmol L^{-1} ferrocyanide diluted in 0.1 mol L^{-1} potassium nitrate in the potential range from -0.1 V to 0.6 V, where the measurement is not affected by formation of gold oxides on gold surfaces. For each measurement the new electrode was used and volume of the solution used for the measurement was 10 µL. All measurements were carried out at two temperatures (25°C and 45°C), which represent two physical states of pNIPAAM. All results were compared to measurement with pristine gold nanostructured electrode without grafted pNIPAAM substrate on the surface. It was revealed, that surface of the electrode is not blocked by pNIPAAM substrate. Electrochemical reaction demonstrates sufficient repeatability of the height of forward anodic and backward cathodic peak of 1 mmol L^{-1} ferrocyanide (under 5 %) and reversibility (ΔE_p = 95 mV, I_{anod}/I_{cathod} = 1.1) of one electron reaction. These results were comparable to measurement with pristine electrode. Moreover, the electrochemical behaviour did not change even after the increase of the temperature from 25°C to 45°C.

On the other hand, a significant change of the electrochemical behaviour was observed during the measurement of repeated scans at 45°C on one single electrode. Each subsequent scan resulted in increase of the height of the anodic oxidation peak as

well as cathodic reduction peak (limiting scan was not found). The slight shift (10 mV) of the E_p was observed in each subsequent scan. These phenomena can be explained by pNIPAAM collapsing at the electrode surface, resulted in the deviation of the classic process from a diffusion-controlled mechanism; thus, molecules of ferrocyanide were entrapped and accumulated in the pNIPAAM layer on the electrode surface and increase of the signal was observed.

In general, observed CV results demonstrate that the grafting of pNIPAAM substrate does not lead to blocking of gold layer surface, which remains electrochemically available. Positive entrapping and accumulation of the molecules of inorganic probe was observed and laid the groundwork for further research. In this Ph.D. Thesis, the possibility of applicability of GNFE-pNIPAAM in electroanalytical chemistry was proved **(Appendix IV)**.

4.2.3. GNFEs with alkyl and other various organic functional groups

This chapter of Ph.D. Thesis builds on testing of GNFEs made by sputtering method with a substrate grafted on the gold surfaces. In this case, pNIPAAM was replaced by various more common substrates/functional groups. Again was necessary to verify electric conductivity of substrates and electrochemical behaviour during measurement with inorganic probe.

Electrodes with grafted substrates were provided by Department of Solid State Engineering at the University of Chemistry and Technology in Prague. Gold nanostructured film electrodes with deposited various substrates/functional groups on the surface were applied as disposable electrochemical sensors. Proposed functional groups were: $-NO_2$, $-C_8F_{17}$ (spontaneously grafted and electrografted) **[5]**, $-C_1H_3$, $-C_4H_9$, $-C_{10}H_{21}$, and $-C_{16}H_{33}$ (electrografted) **[6]**. Entire fabrication procedure, fabrication conditions and described arrangements are mentioned in the papers **[5, 6]**, **Appendixes V** and **VI** and are similar for all GNFEs. All obtained results dealing with $-NO_2$, $-C_8F_{17}$ functional groups are discussed in detail in the paper **[5]** and experimental results dealing with $-CH_3$, $-C_4H_9$, $-C_{10}H_{21}$, $-C_{16}H_{33}$ groups are discussed in detail in the **Appendix VI [6]**.

The electrochemical characterization was performed by CV investigation (scan rate 0.05 V s^{-1}) of 1 mmol L^{-1} ferrocyanide in the potential range from -0.1 V to 0.6 V,

where the measurement is not affected by the formation of gold oxides on gold surfaces. For each measurement the new electrode was used and volume of the solution used for the measurement was 10 μL. All results were compared to measurement with pristine gold nanostructured electrode without grafted substrate on the surface.

In the case of GNFEs with grafted **alkyl groups** (-C_1H_3, -C_4H_9, -$C_{10}H_{21}$, and -$C_{16}H_{33}$), the cyclic voltammetry was performed in two solutions of ferrocyanide (1 mmol L^{-1}) either dissolved in 0.1 mol L^{-1} potassium nitrate as an aqueous medium or dissolved in 0.1 mol L^{-1} potassium nitrate with 50 % content of methanol (*v/v*) as a mixed water-methanol medium. The mixed water-methanol medium was chosen for the purpose of evaluation of hydrophobicity of the surface, which should be dependent on the length of the alkyl chain of the substrate. On the electrode without surface modification, typical reduction and oxidation behaviour of a diffusion controlled redox couple changing one electron was observed (ΔE_p = 100 mV, I_{anod}/I_{cathod} = 1.1, I_{anod} = 9.5 μA, repeatability heights of peaks = 5 %). Behaviour changed when -C_xH_n groups were grafted onto the surface of the electrode. The peaks become less pronounced and the electron transfer kinetics significantly slowed down due to partial surface blocking. When –C_1H_3 substrate was grafted, negligible blocking of ferrocyanide molecules with lower rate of reversibility of the electrochemical reaction was observed (ΔE_p = 200 mV, I_{anod}/I_{cathod} = 1.4, I_{anod} = 8.9 μA). In the case of -C_4H_9 and -$C_{10}H_{21}$ trend continued; evaluable height of the peaks decreased down to I_{anod} < 2.0 μA. After -$C_{16}H_{33}$ functional group grafting, forward as well as backward peak fully disappeared, it is indicating the full blocking of surface so that the probe molecules cannot reach the metal surface. Slight differences in electrochemical behaviour were observed during the measurements in the mixed aqueous-methanol medium (50 % *v/v*). Pristine electrode and electrodes with grafted -C_1H_3 and -C_4H_9 groups exhibited oxidation peak at the same potential with the shift of the potential of reduction peak, but grafting of functional group (-$C_{10}H_{21}$) with increasing carbon chain length did not lead to full peak suppression. Despite the fact that grafted -$C_{16}H_{33}$ group should fully blocked the electrode surface, small oxidation peak around the potential of 350 mV was observed, which indicated the influence of the used mixed solvent. Methanol pushed inorganic probe through the substrate to the surface of gold electrode and the electron transfer controlled by

diffusion could be completed; however, the electrochemical reaction is not reversible at all.

It was confirmed, that used alkyl substrates can block the entire surface of the gold layer. Nevertheless, electron reaction can be promoted by the change of the solvent or co-solvent (to mixed aqueous-methanolic medium) which leads to revelation of defects where molecular layer of organic groups is not sufficiently bent and unevenly arranged to block electron transfer and the gold surface is electrochemically available. So that these electrodes can be used in analytical chemistry for the determination oxidisable compounds in mixed aqueous-methanolic medium without problems with disrupting of gold layer by organic solvent like in the case of some carbon electrodes.

In the case of GNFEs with **-NO_2, -C_8F_{17}** functional groups, the process of grafting was carried out in two mechanisms (spontaneous grafting and electrografting under certain potential, **Fig 4-2**), and compared to each other to observe changes in electrochemical behaviour.

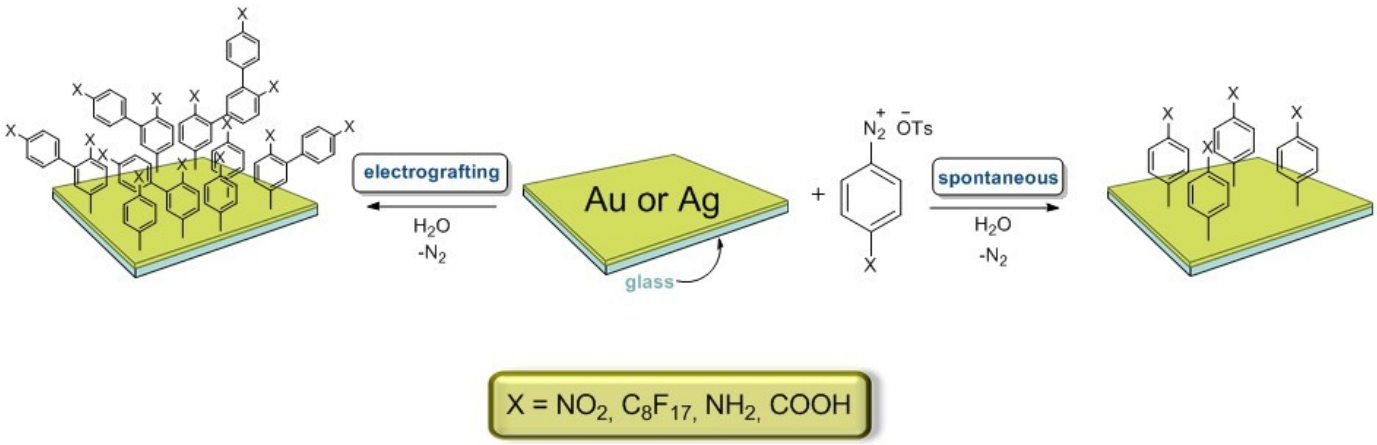

Fig 4-2 Universal scheme of deposition of various substrates of the surface of gold nanostructured electrode/layer **[5]**.

The cyclic voltammetry was performed in 1 mmol L^{-1} solution of potassium ferrocyanide dissolved in 0.1 mol L^{-1} potassium nitrate. Cyclic voltammograms recorded on pristine GNFE showed typical reduction and oxidation behaviour with the apparent positive and negative peaks located around 0.33 V. After the spontaneous mechanism of grafting, the peaks become less pronounced, due to partial surface blocking by substrates. When the electrochemically induced modification was applied,

the ferrocyanide/ferricyanide probe-related peaks fully disappeared, indicating the full blocking of the gold surface, thus the probe cannot reach the metal surface.

It can be concluded, the modification of sputtered gold nanostructured film electrodes by grafting of various active substrates is a new interesting field of application of new electrode materials in electroanalytical chemistry. Obtained results pointed to the fact, that not all used functional groups are useful for electroanalytical purposes and more testing and research in this field.

5. Conclusion

The submitted Ph.D. Thesis represents a contribution to the effort to find and test new interesting electrode materials and arrangements as electroanalytical sensors indented for large scale monitoring of electrochemically oxidisable organic compounds. Every new arrangement has to be tested from the point of view of user friendliness; easy way of fabrication of the working electrode, good compatibility with biological samples, and environmental friendliness is insurmountable advantage. Furthermore, it is essential whether the voltammetric measurement with the working electrode provides a high level of precision and selectivity of the measurement for given purposes [7].

In this Ph.D. Thesis, a several types of miniaturized film arrangements based on working electrodes made from graphitic carbon or pure gold were tested, characterized in many possible ways and compared with commonly used carbon and gold electrodes. Namely, an array of carbon composite film electrodes integrated in microtitration plate as a disposable measuring cell system, gold nanostructured film electrodes/layers sputtered on treated PTFE substrates and gold nanostructured film electrodes modified by grafted functional group/substrate onto electrode surface were proposed and tested and their applicability for electroanalytical purposes was evaluated.

Moreover, their practical applicability was verified by the development of voltammetric methods for the determination of metabolites of catecholamines: homovanillic acid, vanillylmandelic acid [11]; and indole metabolite, indoxyl sulphate [12]. The determination of these biomarkers is fundamental for determining the stage of disease, monitoring of response of human organism to treatment and for an early diagnosis of tumours and other diseases [9].

The obtained results can be summarized as follows:

- An array of carbon composite film electrodes (CFE) integrated in microtitration plate (measuring cell system) proved sufficient applicability for determination of mixture of homovanillic acid and vanillylmandelic acid in concentration range from 100 to 0.8 μmol L^{-1}. The lowest limit of quantification (*LOQ*) was 0.3 μmol L^{-1}, which was reached using differential

pulse voltammetry. Method for the determination of homovanillic acid and vanillylmandelic acid in their mixture was evaluated as well.

- Array of integrated CFEs was used for the study of electrochemical behavior and for sensitive determination of indoxylsulphateprobe in the concentration range from 50 to 1 μmol L^{-1}. Achieved *LOQ* was 0.7 μmol L^{-1}. For comparison, *LOQ* achieved with CPE was 1.7 μmol L^{-1}.
- For the verification of practical applicability of the array of integrated CFEs with newly developed voltammetric method, solid phase extraction was employed for extraction of indoxyl sulphate from human urine. However, SPE was not fully successful. A few urine interferents remained in solution with the analyte.
- This disposable array of integrated CFEs intended for screening measurements offers an inexpensive, independent, and reliable alternative to more frequently used spectrometric methods. This array offers easy portability and possibility of simple *in-situ* measurements in small sample volumes.
- Gold nanostructured film electrodes (GNFEs, 80 nm thin) sputtered on three types of treated PTFE were electrochemically characterized and its applicability as disposable electrochemical sensors was verified.
- All GNFEs showed acceptable electrochemical parameters, which are comparable to parameters of gold bulk electrode. The increase of current response due to the increase of active surface area by sputtering of Au atoms (resulting in roughened nanolayer) was observed.
- GNFEs on PTFE substrate were used for the study of electrochemical behavior and for determination of hydroquinone in concentration range from 100 to 10 μmol L^{-1}. Achieved *LOQ* were 4.3 μmol L^{-1} for GNFE-Pristine, 4.2 μmol L^{-1} for GNFE-Plasma, and 9.0 μmol L^{-1} for GNFE-BPD, respectively.
- GNFEs on PTFE substrate made by sputtering offer certain advantages e.g. small volume of used sample, easy miniaturization, possibility of recycling of gold from used electrodes, and also “green” method of fabrication.

- Basic electrochemical parameters of gold nanostructured film electrode (10 nm thin) modified by grafting of thermosensitive polymer pNIPAAM on the surface (GNFE-pNIPAAM) were evaluated.
- Positive entrapping and accumulation of the molecules of ferrocyanide on the surface of GNFE-pNIPAAM was observed. It resulted in the increase of the sensitivity of the measurement.
- Basic electrochemical parameters of gold nanostructured film electrode (10 nm thin) modified by grafting of $-NO_2$, $-C_8F_{17}$ substrates on the surface were evaluated. It was found out that forced electrografting under certain potential caused a complete blockage of the electrode surface; afterwards it is not possible to measure with the electrode.
- In the case of GNFEs-C_xH_n, it was confirmed, that long alkyl substrates can block the entire surface of the gold layer, depends on the length of carbon chain.

6. References

[1] Libansky M., Zima J., Barek J., Dejmkova H., Voltammetric Determination of Homovanillic Acid and Vanillylmandelic Acid on a Disposable Electrochemical Measuring Cell System with Integrated Carbon Composite Film Electrodes, *Monatshefte Fur Chemie*, 147 (2016) 89-96.
[2] Bergerova M., Libansky M., Dejmkova H., Determination of Urinary Indican on Carbon Film Composite Electrode and Carbon Paste Electrode *Current Analytical Chemistry*, *Submitted* (2017).
[3] Libansky M., Zima J., Barek J., Reznickova A., Svorcik V., Dejmkova H., Basic Electrochemical Properties of Sputtered Nanostructured Gold Film Electrodes, *Electrochimica acta*, *Submitted* (2017).
[4] Guselnikova O., Postnikov P., Kalachyova Y., Libansky M., Zima J., Kolska Z., Svorcik V., Lyutakov O., Large-Scale Ultrasensetive, Highly Reproducible and Regenerative Smart Sers Platform Based on Pnipam Grafted Gold Grating, *ChemNanoMat*, 3 (2016) 135-144.
[5] Guselnikova O., Postnikov P., Elashnikov R., M. T., Kalachyova Y., Libansky M., Barek J., Kolska Z., Svorcik V., Lyutakov O., Surface Modification of Au and Ag Plasmonic Thin Films Via Diazonium Chemistry: Evaluation of Structure and Properties, *Colloids and Surfaces A Physicochemical Engineering Aspects*, *In Press* (2016).
[6] Guselnikova O., Kalachyova Y., Faragova K., Libansky M., Dejmkova H., Svorcik V., Sajdl P., Lyutakov O., Functional Spp-Based Sers Sensor Platform for Lipoproteins Detection, *Talanta*, *Prepared for submission* (2017).
[7] Barek J., Fischer J., Navratil T., Peckova K., Yosypchuk B., Zima J., Nontraditional Electrode Materials in Environmental Analysis of Biologically Active Organic Compounds, *Electroanalysis*, 19 (2007) 2003-2014.
[8] Wang J., Analytical Electrochemistry, 3rd ed., John Wiley & Sons, Hoboken, New Jersey, 2006.
[9] Daniel D., Lalitha R.M., Tumor Markers - a Bird's Eye View, *Journal of Oral and Maxillofacial Surgery Medicine and Pathology*, 28 (2016) 475-480.
[10] Basuyau J.P., Leroy M., Brunelle P., Determination of Tumor Markers in Serum. Pitfalls and Good Practice, *Clinical Chemistry and Laboratory Medicine*, 39 (2001) 1227-1233.
[11] Eisenhofer G., Kopin I.J., Goldstein D.S., Catecholamine Metabolism: A Contemporary View with Implications for Physiology and Medicine, *Pharmacological Reviews*, 56 (2004) 331-349.
[12] Cassani E., Barichella M., Cancello R., Cavanna F., Iorio L., Cereda E., Bolliri C., Maria P.Z., Bianchi F., Cestaro B., Pezzoli G., Increased Urinary Indoxyl Sulfate (Indican): New Insights into Gut Dysbiosis in Parkinson's Disease, *Parkinsonism & Related Disorders*, 21 (2015) 389-393.
[13] Libansky M., Zima J., Barek J., Dejmkova H., Construction of an Electrochemical Cell System Based on Carbon Composite Film Electrodes and Its Application for Voltammetric Determination of Triclosan, *Electroanalysis*, 26 (2014) 1920-1927.
[14] Ramirez- Garcia S., Alegret S., Cespedes F., Forster R.J., Carbon Composite Electrodes: Surface and Electrochemical Properties, *Analyst*, 127 (2002) 1512-1519.

[15] Petersen S.L., Tallman D.E., Silver Composite Electrode for Voltammetry, *Analytical Chemistry*, 60 (1988) 82-86.
[16] Tallman D.E., Petersen S.L., Composite Electrodes for Electroanalysis: Principles and Applications, *Electroanalysis (N. Y.)*, 2 (1990) 499-510.
[17] Navratil T., Composite Solid Electrodes - Tool for Organic Electrochemistry, *Current Organic Chemistry*, 15 (2011) 2996-3013.
[18] Yosypchuk B., Barek J., Fojta M., Carbon Powder Based Films on Traditional Solid Electrodes as an Alternative to Disposable Electrodes, *Electroanalysis*, 18 (2006) 1126-1130.
[19] Sun D.Z., Zhu L.D., Zhu G.Y., Glassy Carbon Ceramic Composite Electrodes, *Analytica Chimica Acta*, 564 (2006) 243-247.
[20] dos Santos S.X., Cavalheiro E.T.G., Evaluation of the Potentialities of a Carbon Nanotubes/Silicone Rubber Composite Electrode in the Determination of Hydrochlorothiazide, *Analytical Letters*, 45 (2012) 1454-1466.
[21] Pumera M., Merkoci A., Alegret S., Carbon Nanotube-Epoxy Composites for Electrochemical Sensing, *Sensors and Actuators B-Chemical*, 113 (2006) 617-622.
[22] Chakrabarti M.H., Low C.T.J., Brandon N.P., Yufit V., Hashim M.A., Irfan M.F., Akhtar J., Ruiz-Trejo E., Hussain M.A., Progress in the Electrochemical Modification of Graphene-Based Materials and Their Applications, *Electrochimica Acta*, 107 (2013) 425-440.
[23] Noked M., Soffer A., Aurbach D., The Electrochemistry of Activated Carbonaceous Materials: Past, Present, and Future, *Journal of Solid State Electrochemistry*, 15 (2011) 1563-1578.
[24] dos Santos S.X., Cavalheiro E.T.G., Determination of Hydroquinone with a Carbon Nanotube/Polyurethane Resin Composite Electrode, *Analytical Letters*, 49 (2016) 1513-1525.
[25] Regel A., Lunte S., Integration of a Graphite/Poly(Methylmethacrylate) Composite Electrode into a Poly(Methylmethacrylate) Substrate for Electrochemical Detection in Microchips, *Electrophoresis*, 34 (2013) 2101-2106.
[26] Chiorcea-Paquim A.M., Diculescu V.C., Cervini P., Cavalheiro E.T.G., Brett A.M.O., Graphite-Castor Oil Polyurethane Composite Electrode Surfaces - Afm Morphological and Electrochemical Characterisation, *Journal of Electroanalytical Chemistry*, 731 (2014) 172-178.
[27] Zhu J.W., Li X., Qin Y., Zhang Y.H., Single-Piece Solid-Contact Ion-Selective Electrodes with Polymer-Carbon Nanotube Composites, *Sensors and Actuators B-Chemical*, 148 (2010) 166-172.
[28] Freitas K.H.G., Fatibello O., de Mattos I.L., Square-Wave Voltammetric Determination of Rutin in Pharmaceutical Formulations Using a Carbon Composite Electrode Modified with Copper (Ii) Phosphate Immobilized in Polyester Resin, *Brazilian Journal of Pharmaceutical Sciences*, 48 (2012) 639-649.
[29] Barsan M.M., Brett C.M.A., A New Modified Conducting Carbon Composite Electrode as Sensor for Ascorbate and Biosensor for Glucose, *Bioelectrochemistry*, 76 (2009) 135-140.
[30] Ping J., Wang Y., Wu J., Ying Y., Ji F., Determination of Ascorbic Acid Levels in Food Samples by Using an Ionic Liquid-Carbon Nanotube Composite Electrode, *Food Chemistry*, 135 (2012) 362-367.
[31] Hua L., Tan S.N., Amperometric Detection for Capillary Electrophoresis at a Sol-Gel Carbon Composite Electrode, *Analytica Chimica Acta*, 403 (2000) 179-186.

[32] Ordenana-Martinez A.S., Rincon M.E., Composite Mwcnt/Carbon Xerogel-Nafion Electrode for Energy Storage, *Journal of Solid State Electrochemistry*, 20 (2016) 1391-1396.
[33] Sharp D., Burkitt R., Carbon Materials for Analytical Electrochemistry: Printed Carbon Materials and Composites, *Materials Technology*, 30 (2015) B155-B162.
[34] Navratil T., Barek J., Analytical Applications of Composite Solid Electrodes, *Critical Reviews in Analytical Chemistry*, 39 (2009) 131-147.
[35] Metters J.P., Kadara R.O., Banks C.E., Electroanalytical Properties of Screen Printed Graphite Microband Electrodes, *Sensors and Actuators B-Chemical*, 169 (2012) 136-143.
[36] Khodari M., Bilitewski U., Basry A.A.H., Screen-Printed Electrodes for Amperometric Determination of Iodide, *Electroanalysis*, 27 (2015) 281-284.
[37] Navratil T., Barek J., Kopanica M., Anodic Stripping Voltammetry Using Graphite Composite Solid Electrode, *Collection of Czechoslovak Chemical Communications*, 74 (2009) 1807-1826.
[38] Freitas K.H.G., Fatibello-Filho O., Carbon Composite Electrode Modified with Copper(Ii) Phosphate Immobilized in a Polyester Resin for Voltammetric Determination of Catechin in Teas, *Analytical Letters*, 43 (2010) 2091-2104.
[39] Rasines G., Lavela P., Macias C., Zafra M.C., Tirado J.L., Ania C.O., Mesoporous Carbon Black-Aerogel Composites with Optimized Properties for the Electro-Assisted Removal of Sodium Chloride from Brackish Water, *Journal of Electroanalytical Chemistry*, 741 (2015) 42-50.
[40] Albertus F., Llerena A., Alpizar J., Cerda V., Luque M., Rios A., Valcarcel M., A Pvc-Graphite Composite Electrode for Electroanalytical Use. Preparation and Some Applications, *Analytica Chimica Acta*, 355 (1997) 23-32.
[41] Cesarino I., Gouveia-Caridade C., Pauliukaite R., Cavalheiro E.T.G., Brett C.M.A., Characterization and Application of Bismuth-Film Modified Graphite-Polyurethane Composite Electrodes, *Electroanalysis*, 22 (2010) 1437-1445.
[42] Cesarino I., Cesarino V., Lanza M.R.V., Carbon Nanotubes Modified with Antimony Nanoparticles in a Paraffin Composite Electrode: Simultaneous Determination of Sulfamethoxazole and Trimethoprim, *Sensors and Actuators B-Chemical*, 188 (2013) 1293-1299.
[43] Liu B.Z., Wang M., Xiao B., Application of Carbon Nanotube-Ionic Liquid-Epinephrine Composite Gel Modified Electrode as a Sensor for Glutathione, *Journal of Electroanalytical Chemistry*, 757 (2015) 198-202.
[44] Min K., Yoo Y.J., Amperometric Detection of Dopamine Based on Tyrosinase-Swnts-Ppy Composite Electrode, *Talanta*, 80 (2009) 1007-1011.
[45] Renedo O.D., Alonso-Lomillo M.A., Martinez M.J.A., Recent Developments in the Field of Screen-Printed Electrodes and Their Related Applications, *Talanta*, 73 (2007) 202-219.
[46] Sanghavi B.J., Kalambate P.K., Karna S.P., Srivastava A.K., Voltammetric Determination of Sumatriptan Based on a Graphene/Gold Nanoparticles/Nafion Composite Modified Glassy Carbon Electrode, *Talanta*, 120 (2014) 1-9.
[47] Liu X., Shuai H.L., Liu Y.J., Huang K.J., An Electrochemical Biosensor for DNA Detection Based on Tungsten Disulfide/Multi-Walled Carbon Nanotube Composites and Hybridization Chain Reaction Amplification, *Sensors and Actuators B-Chemical*, 235 (2016) 603-613.

[48] Yigit A., Yardim Y., Celebi M., Levent A., Senturk Z., Graphene/Nafion Composite Film Modified Glassy Carbon Electrode for Simultaneous Determination of Paracetamol, Aspirin and Caffeine in Pharmaceutical Formulations, *Talanta*, 158 (2016) 21-29.
[49] Zhang J., Niu Y., Li S., Luo R., Wang C., A Molecularly Imprinted Electrochemical Sensor Based on Sol-Gel Technology and Multiwalled Carbon Nanotubes-Nafion Functional Layer for Determination of 2-Nonylphenol in Environmental Samples, *Sensors and Actuators, B: Chemical*, 193 (2014) 844-850.
[50] Jirimali H.D., Nagarale R.K., Saravanakumar D., Lee J.M., Shin W., Hydroquinone Modified Chitosan/Carbon Film Electrode for the Selective Detection of Ascorbic Acid, *Carbohydrate Polymers*, 92 (2013) 641-644.
[51] Ping J.F., Wu J., Ying Y.B., Wang M.H., Liu G., Zhang M., Development of a Novel Carbon Composite Electrode for Trace Determination of Heavy Metals in Milk, *Trans. ASABE*, 54 (2011) 1829-1835.
[52] Zhang X.A., Shen J.Z., Zhang F., Ma H.L., Han E., Dong X.Y., Electrochemical Immunosensor for Determination of Microcystins Based on Carbon Nanotubes/Au Nanoparticles Composite Film, *Chinese Journal of Analytical Chemistry*, 42 (2014) 1301-1306.
[53] Rajalakshmi K., John S.A., Highly Sensitive Determination of Nitrite Using Fmwcnts-Conducting Polymer Composite Modified Electrode, *Sensors and Actuators B-Chemical*, 215 (2015) 119-124.
[54] Manikandan P.N., Imran H., Dharuman V., Direct Glucose Sensing and Biocompatible Properties of a Zinc Oxide - Multiwalled Carbon Nanotube-Poly(Vinyl Chloride) Ternary Composite, *Analytical Methods*, 8 (2016) 2691-2697.
[55] Xu X., Weber S.G., Carbon Fiber/Epoxy Composite Ring-Disk Electrode: Fabrication, Characterization and Application to Electrochemical Detection in Capillary High Performance Liquid Chromatography, *Journal of Electroanalytical Chemistry*, 630 (2009) 75-80.
[56] Li X.C., Chen Z.G., Zhong Y.W., Yang F., Pan J.B., Liang Y.J., Cobalt Hexacyanoferrate Modified Multi-Walled Carbon Nanotubes/Graphite Composite Electrode as Electrochemical Sensor on Microfluidic Chip, *Analytica Chimica Acta*, 710 (2012) 118-124.
[57] Chillawar R.R., Tadi K.K., Motghare R.V., Voltammetric Techniques at Chemically Modified Electrodes, *Journal of Analytical Chemistry*, 70 (2015) 399-418.
[58] Adams R.N., Carbon Paste Elctrode, *Analytical Chemistry*, 30 (1958) 1576-1576.
[59] de Araujo E.G., Fernandes N.S., Solon L.G.D., Aragao C.F.S., Martinez-Huitle C.A., Voltammetric Determination of Folic Acid Using a Graphite Paste Electrode, *Electroanalysis*, 27 (2015) 398-405.
[60] Bavol D., Zima J., Barek J., Dejmkova H., Voltammetric Determination of Cymoxanil and Famoxadone at Different Types of Carbon Electrodes, *Electroanalysis*, 28 (2016) 1029-1034.
[61] Parvin M.H., Simultaneous Determination of Ascorbic Acid, Dopamine and Uric Acid, at a Graphene Paste Electrode Modified with Functionalized Graphene Sheets, *Electroanalysis*, 27 (2015) 1394-1402.
[62] Mohamadi M., Mostafavi A., Torkzadeh-Mahani M., Voltammetric Behavior of Uric Acid on Carbon Paste Electrode Modified with Salmon Sperm Dsdna and Its Application as Label-Free Electrochemical Sensor, *Biosensors & Bioelectronics*, 54 (2014) 211-216.

[63] Svancara I., Vytras K., Barek J., Zima J., Carbon Paste Electrodes in Modern Electroanalysis, *Crit. Rev. Anal. Chem.* , 31 (2001) 311-345.
[64] Lowinsohn D., Gan P., Tschulik K., Foord J.S., Compton R.G., Nanocarbon Paste Electrodes, *Electroanalysis*, 25 (2013) 2435-2444.
[65] Ensafi A.A., Izadi M., Karimi-Maleh H., Sensitive Voltammetric Determination of Diclofenac Using Room-Temperature Ionic Liquid-Modified Carbon Nanotubes Paste Electrode, *Ionics*, 19 (2013) 137-144.
[66] Zhang Y., Zheng J.B., Comparative Investigation on Electrochemical Behavior of Hydroquinone at Carbon Ionic Liquid Electrode, Ionic Liquid Modified Carbon Paste Electrode and Carbon Paste Electrode, *Electrochimica Acta*, 52 (2007) 7210-7216.
[67] Svancara I., Walcarius A., Kalcher K., Vytras K., Carbon Paste Electrodes in the New Millennium, *Central European Journal of Chemistry*, 7 (2009) 598-656.
[68] Marcoux L.S., Prater K.B., Prater B.G., Adams R.N., A Nonaqueous Carbon Paste Electrode, *Analytical Chemistry*, 37 (1965) 1446-&.
[69] Sobhanmanesh B., Najafi M., Selective Determination of Unsymmetrical Dimethylhydrazine on a Prussian Blue Modified Carbon Paste Electrode, *Journal of the Brazilian Chemical Society*, 26 (2015) 451-457.
[70] Oliveira T., Barroso M.F., Morais S., de Lima-Neto P., Correia A.N., Oliveira M., Delerue-Matos C., Biosensor Based on Multi-Walled Carbon Nanotubes Paste Electrode Modified with Laccase for Pirimicarb Pesticide Quantification, *Talanta*, 106 (2013) 137-143.
[71] Bauer D., Gaillochet M.P., Study of Relation of Carbon Paste to Incorporated Electroactive Compound, *Electrochimica Acta*, 19 (1974) 597-606.
[72] Zhang F.F., Gu S.Q., Ding Y.P., Zhou L.X., Zhang Z., Li L., Electrooxidation and Determination of Cefotaxime on Au Nanoparticles/Poly (L-Arginine) Modified Carbon Paste Electrode, *Journal of Electroanalytical Chemistry*, 698 (2013) 25-30.
[73] Svancara I., Vytras K., Kalcher K., Walcarius A., Wang J., Carbon Paste Electrodes in Facts, Numbers, and Notes: A Review on the Occasion of the 50-Years Jubilee of Carbon Paste in Electrochemistry and Electroanalysis, *Electroanalysis*, 21 (2009) 7-28.
[74] Youssef A.F.A., Issa Y.M., Shehab O.R., Sherief H., Determination of Microgram Amounts of Copper in Real Samples Using New Modified Carbon Paste Electrode, *International Journal of Electrochemical Science*, 10 (2015) 4752-4769.
[75] Atta N.F., Galal A., Abdel-Gawad F.M., Mohamed E.F., Electrochemical Morphine Sensor Based on Gold Nanoparticles Metalphthalocyanine Modified Carbon Paste Electrode, *Electroanalysis*, 27 (2015) 415-428.
[76] McNaught A.D., Wilkinson A., Pure I.U.o., Chemistry A., Compendium of Chemical Terminology: Iupac Recommendations, Blackwell Science1997.
[77] Lopez-Lorente A.I., Valcarcel M., The Third Way in Analytical Nanoscience and Nanotechnology: Involvement of Nanotools and Nanoanalytes in the Same Analytical Process, *Trac-Trends in Analytical Chemistry*, 75 (2016) 1-9.
[78] Diao P., Guo M., Zhang Q., How Does the Particle Density Affect the Electrochemical Behavior of Gold Nanoparticle Assembly?, *Journal of Physical Chemistry C*, 112 (2008) 7036-7046.
[79] Raoof J.B., Kiani A., Ojani R., Valiollahi R., Rashid-Nadimi S., Simultaneous Voltammetric Determination of Ascorbic Acid and Dopamine at the Surface of Electrodes Modified with Self-Assembled Gold Nanoparticle Films, *Journal of Solid State Electrochemistry*, 14 (2010) 1171-1176.

[80] Svancara I., Matousek M., Sikora E., Schachl K., Kalcher K., Vytras K., Carbon Paste Electrodes Plated with a Gold Film for the Voltammetric Determination of Mercury(Ii), *Electroanalysis*, 9 (1997) 827-833.
[81] Aflhami A., Bahiraei A., Madrakian T., Gold Nanoparticle/Multi-Walled Carbon Nanotube Modified Glassy Carbon Electrode as a Sensitive Voltammetric Sensor for the Determination of Diclofenac Sodium, *Materials Science & Engineering C-Materials for Biological Applications*, 59 (2016) 168-176.
[82] Welch C.M., Nekrassova O., Dai X., Hyde M.E., Compton R.G., Fabrication, Characterisation and Voltammetric Studies of Gold Amalgam Nanoparticle Modified Electrodes, *Chemphyschem*, 5 (2004) 1405-1410.
[83] Garcia-Gonzalez R., Fernandez-Abedul M.T., Pernia A., Costa-Garcia A., Electrochemical Characterization of Different Screen-Printed Gold Electrodes, *Electrochimica Acta*, 53 (2008) 3242-3249.
[84] Reznickova A., Kolska Z., Hnatowicz V., Svorcik V., Nano-Structuring of Ptfe Surface by Plasma Treatment, Etching, and Sputtering with Gold, *Journal of Nanoparticle Research*, 13 (2011) 2929-2938.
[85] Wilson D.J., Williams R.L., Pond R.C., Plasma Modification of Ptfe Surfaces Part I: Surfaces Immediately Following Plasma Treatment, *Surface and Interface Analysis*, 31 (2001) 385-396.
[86] Siegel J., Lyutakov O., Rybka V., Kolska Z., Svorcik V., Properties of Gold Nanostructures Sputtered on Glass, *Nanoscale Research Letters*, 6 (2011).
[87] Mias S., Sudor J., Camon H., Pnipam: A Thermo-Activated Nano-Material for Use in Optical Devices, *Microsystem Technologies-Micro-and Nanosystems-Information Storage and Processing Systems*, 14 (2008) 691-695.
[88] Passos M.L.C., Pinto P., Santos J.L.M., Saraiva M., Araujo A., Nanoparticle-Based Assays in Automated Flow Systems: A Review, *Analytica Chimica Acta*, 889 (2015) 22-34.
[89] Lopez-Lorente A.I., Simonet B.M., Valcarcel M., Analytical Potential of Hybrid Nanoparticles, *Analytical and Bioanalytical Chemistry*, 399 (2011) 43-54.
[90] Luczak T., Beltowska-Brzezinska M., Gold Electrodes Modified with Gold Nanoparticles and Thio Compounds for Electrochemical Sensing of Dopamine Alone and in Presence of Potential Interferents. A Comparative Study, *Microchimica Acta*, 174 (2011) 19-30.
[91] Vulcu A., Grosan C., Muresan L.M., Pruneanu S., Olenic L., Modified Gold Electrodes Based on Thiocytosine/Guanine-Gold Nanoparticles for Uric and Ascorbic Acid Determination, *Electrochimica Acta*, 88 (2013) 839-846.
[92] Li T.B., Xu J., Zhao L., Shen S.F., Yuan M.S., Liu W.M., Tu Q., Yu R.J., Wang J.Y., Au Nanoparticles/Poly(Caffeic Acid) Composite Modified Glassy Carbon Electrode for Voltammetric Determination of Acetaminophen, *Talanta*, 159 (2016) 356-364.
[93] Song Y.Z., Zhu F.X., Song Y., Zhou J.F., Chu X.Z., Wu F.Y., Zhu A.F., Wei C.M., Song J., Li X., Xu J., Gold-Nanoparticle on the Surface of L-Cysteine Modified Gold Electrode and Its Application, *Russian Journal of Physical Chemistry A*, 87 (2013) 80-83.
[94] Tabrizi M.A., Shamsipur M., Mostafaie A., A High Sensitive Label-Free Immunosensor for the Determination of Human Serum Igg Using Overoxidized Polypyrrole Decorated with Gold Nanoparticle Modified Electrode, *Materials Science & Engineering C-Materials for Biological Applications*, 59 (2016) 965-969.

[95] Dai X., Compton R.G., Gold Nanoparticle Modified Electrodes Show a Reduced Interference by Cu(Ii) in the Detection of as(Iii) Using Anodic Stripping Voltammetry, *Electroanalysis*, 17 (2005) 1325-1330.
[96] Tominaga M., Shimazoe T., Nagashima M., Taniguchi I., Electrocatalytic Oxidation of Glucose at Gold Nanoparticle-Modified Carbon Electrodes in Alkaline and Neutral Solutions, *Electrochemistry Communications*, 7 (2005) 189-193.
[97] Raj C.R., Okajima T., Ohsaka T., Gold Nanoparticle Arrays for the Voltammetric Sensing of Dopamine, *Journal of Electroanalytical Chemistry*, 543 (2003) 127-133.
[98] Wang L., Bai J.Y., Huang P.F., Wang H.J., Zhang L.Y., Zhao Y.Q., Self-Assembly of Gold Nanoparticles for the Voltammetric Sensing of Epinephrine, *Electrochemistry Communications*, 8 (2006) 1035-1040.
[99] Agui L., Pena-Farfal C., Yanez-Sedeno P., Pingarron J.M., Electrochemical Determination of Homocysteine at a Gold Nanoparticle-Modified Electrode, *Talanta*, 74 (2007) 412-420.
[100] Tsai C.Y., Chang T.L., Chen C.C., Ko F.H., Chen P.H., An Ultra Sensitive DNA Detection by Using Gold Nanoparticle Multilayer in Nano-Gap Electrodes, *Microelectronic Engineering*, 78-79 (2005) 546-555.
[101] Ding X.Q., Yang M., Hu J.B., Li Q.L., McDougall A., Study of the Adsorption of Cytochrome C on a Gold Nanoparticle - Modified Gold Electrode by Using Cyclic Voltammetry, Electrochemical Impedance Spectroscopy and Chronopotentiometry, *Microchimica Acta*, 158 (2007) 65-71.
[102] Cui H., Xu Y., Zhang Z.F., Multichannel Electrochemiluminescence of Luminol in Neutral and Alkaline Aqueous Solutions on a Gold Nanoparticle Self-Assembled Electrode, *Analytical Chemistry*, 76 (2004) 4002-4010.
[103] Pingarron J.M., Yanez-Sedeno P., Gonzalez-Cortes A., Gold Nanoparticle-Based Electrochemical Biosensors, *Electrochimica Acta*, 53 (2008) 5848-5866.
[104] Zhang F.H., Cho S.S., Yang S.H., Seo S.S., Cha G.S., Nam H., Gold Nanoparticle-Based Mediatorless Biosensor Prepared on Microporous Electrode, *Electroanalysis*, 18 (2006) 217-222.
[105] Mandal S., Pal A., Arun R.K., Chanda N., Gold Nanoparticle Embedded Paper with Mechanically Exfoliated Graphite as Flexible Supercapacitor Electrodes, *Journal of Electroanalytical Chemistry*, 755 (2015) 22-26.
[106] Ankamwar B., Das P., Sur U.K., Graphene-Gold Nanoparticle-Based Nanocomposites as an Electrode Material in Supercapacitors, *Indian Journal of Physics*, 90 (2016) 391-397.
[107] Fitzgibbon M.C., Tormey W.P., Pediatric Reference Ranges for Urinary Catecholamines Metabolites and Their Relevance in Neuroblastoma Diagnosis, *Annals of Clinical Biochemistry*, 31 (1994) 1-11.
[108] Sadilkova K., Dugaw K., Benjamin D., Jack R.M., Analysis of Vanillylmandelic Acid and Homovanillic Acid by Uplc-Ms/Ms in Serum for Diagnostic Testing for Neuroblastoma, *Clinica Chimica Acta*, 424 (2013) 253-257.
[109] Zhang W., Xie Y.F., Ai S.Y., Wan F.L., Wang J., Jin L.T., Jin J.Y., Liquid Chromatography with Amperometric Detection Using Functionalized Multi-Wall Carbon Nanotube Modified Electrode for the Determination of Monoamine Neurotransmitters and Their Metabolites, *Journal of Chromatography B-Analytical Technologies in the Biomedical and Life Sciences*, 791 (2003) 217-225.
[110] Vaarmann A., Kask A., Maeorg U., Novel and Sensitive High-Performance Liquid Chromatographic Method Based on Electrochemical Coulometric Array

Detection for Simultaneous Determination of Catecholamines, Kynurenine and Indole Derivatives of Tryptophan, *Journal of Chromatography B-Analytical Technologies in the Biomedical and Life Sciences*, 769 (2002) 145-153.
[111] Lu Y., Li P., Gan W., Zhao X., Shen S., Feng W., Xu Q., Bi Y., Guo H., Zhu D., Clinical and Pathological Characteristics of Hypertensive and Normotensive Adrenal Pheochromocytomas, *Experimental and Clinical Endocrinology & Diabetes*, 124 (2016) 372-379.
[112] Barco S., Gennai I., Reggiardo G., Galleni B., Barbagallo L., Maffia A., Viscardi E., De Leonardis F., Cecinati V., Sorrentino S., Garaventa A., Conte M., Cangemi G., Urinary Homovanillic and Vanillylmandelic Acid in the Diagnosis of Neuroblastoma: Report from the Italian Cooperative Group for Neuroblastoma, *Clinical Biochemistry*, 47 (2014) 848-852.
[113] Kiernan C.M., Solorzano C.C., Pheochromocytoma and Paraganglioma Diagnosis, Genetics, and Treatment, *Surgical Oncology Clinics of North America*, 25 (2016) 119-125.
[114] organization W.h., World Cancer Report, International Agency for Research on Cancer, Lyon, France, 2014.
[115] Flottmann D., Hins J., Rettenmaier C., Schnell N., Kuci Z., Merkel G., Seitz G., Bruchelt G., Two-Dimensional Isotachophoresis for the Analysis of Homovanillic Acid and Vanillylmandelic Acid in Urine for Cancer Therapy Monitoring, *Microchimica Acta*, 154 (2006) 49-53.
[116] Marin-Valencia I., Serrano M., Ormazabal A., Perez-Duenas B., Garcia-Cazorla A., Campistol J., Artuch R., Biochemical Diagnosis of Dopaminergic Disturbances in Paediatric Patients: Analysis of Cerebrospinal Fluid Homovanillic Acid and Other Biogenic Amines, *Clinical Biochemistry*, 41 (2008) 1306-1315.
[117] Sher L., Mann J.J., Traskman-Bendz L., Winchel R., Huang Y.Y., Fertuck E., Stanley B.H., Lower Cerebrospinal Fluid Homovanillic Acid Levels in Depressed Suicide Attempters, *Journal of Affective Disorders*, 90 (2006) 83-89.
[118] Revin S.B., John S.A., Simultaneous Determination of Two Important Dopamine Metabolites at Physiological Ph by Voltammetry, *Analytical Methods*, 4 (2012) 348-352.
[119] Suzuki E., Kanba S., Nibuya M., Adachi S., Sekiya U., Shintani F., Kinoshita N., Yagi G., Asai M., Longitudial Changes in Symptoms and Plasma Homovanillic Acid Levels in Chronically Medicated Schizophrenic Patients, *Biological Psychiatry*, 36 (1994) 654-661.
[120] LeWitt P., Schultz L., Auinger P., Lu M., Parkinson Study Grp D., Csf Xanthine, Homovanillic Acid, and Their Ratio as Biomarkers of Parkinson's Disease, *Brain Research*, 1408 (2011) 88-97.
[121] Li Q.A., Batchelor-McAuley C., Compton R.G., Electrooxidative Decarboxylation of Vanillylmandelic Acid: Voltammetric Differentiation between the Structurally Related Compounds Homovanillic Acid and Vanillylmandelic Acid, *Journal of Physical Chemistry B*, 114 (2010) 9713-9719.
[122] Matsuo M., Tasaki R., Kodama H., Hamasaki Y., Screening for Menkes Disease Using the Urine Hva/Vma Ratio, *Journal of Inherited Metabolic Disease*, 28 (2005) 89-93.
[123] Siren H., Mielonen M., Herlevi M., Capillary Electrophoresis in the Determination of Anionic Catecholamine Metabolites from Patients' Urine, *Journal of Chromatography A*, 1032 (2004) 289-297.

[124] Garcia A., Heinanen M., Jimenez L.M., Barbas C., Direct Measurement of Homovanillic, Vanillylmandelic and 5-Hydroxyindoleacetic Acids in Urine by Capillary Electrophoresis, *Journal of Chromatography A*, 871 (2000) 341-350.
[125] Unceta N., Rodriguez E., de Balugera Z.G., Sampedro C., Goicolea M.A., Barrondo S., Salles J., Barrio R.J., Determination of Catecholamines and Their Metabolites in Human Plasma Using Liquid Chromatography with Coulometric Multi-Electrode Cell-Design Detection, *Analytica Chimica Acta*, 444 (2001) 211-221.
[126] Monteleone M., Naccarato A., Sindona G., Tagarelli A., A Reliable and Simple Method for the Assay of Neuroendocrine Tumor Markers in Human Urine by Solid-Phase Microextraction-Gas Chromatography-Triple Quadrupole Mass Spectrometry, *Analytica Chimica Acta*, 759 (2013) 66-73.
[127] Bergh M.S.S., Bogen I.L., Lundanes E., Oiestad A.M.L., Validated Methods for Determination of Neurotransmitters and Metabolites in Rodent Brain Tissue and Extracellular Fluid by Reversed Phase Uhplc-Ms/Ms, *Journal of Chromatography B-Analytical Technologies in the Biomedical and Life Sciences*, 1028 (2016) 120-129.
[128] Remane D., Grunwald S., Hoeke H., Mueller A., Roeder S., von Bergen M., Wissenbach D.K., Validation of a Multi-Analyte Hplc-Dad Method for Determination of Uric Acid, Creatinine, Homovanillic Acid, Niacinamide, Hippuric Acid, Indole-3-Acetic Acid and 2-Methylhippuric Acid in Human Urine, *Journal of Chromatography B-Analytical Technologies in the Biomedical and Life Sciences*, 998 (2015) 40-44.
[129] Tsunoda M., Mitsuhashi K., Masuda M., Imai K., Simultaneous Determination of 3,4-Dihydroxyphenylacetic Acid and Homovanillic Acid Using High Performance Liquid Chromatography-Fluorescence Detection and Application to Rat Kidney Microdialysate, *Analytical Biochemistry*, 307 (2002) 153-158.
[130] Zydron M., Baranowski J., Bialkowski J., Baranowska I., Hplc-Fl/Ed in the Analysis of Biogenic Amines and Their Metabolites in Urine, *Separation Science and Technology*, 40 (2005) 3137-3148.
[131] Zhang H.T., Li Z., Zhang J.B., Zhang Y., Ye J.N., Chu Q.C., Zhang M.J., Simultaneous Determination of Catecholamines and Related Metabolites by Capillary Electrophoresis with Amperometric Detection, *Chemical Research in Chinese Universities*, 29 (2013) 850-853.
[132] Selvaraju T., Ramaraj R., Simultaneous Detection of Ascorbic Acid, Uric Acid and Homovanillic Acid at Copper Modified Electrode, *Electrochimica Acta*, 52 (2007) 2998-3005.
[133] Hatefi-Mehrjardi A., Ghaemi N., Karimi M.A., Ghasemi M., Islami-Ramchahi S., Poly-(Alizarin Red S)-Modified Glassy Carbon Electrode for Simultaneous Electrochemical Determination of Levodopa, Homovanillic Acid and Ascorbic Acid, *Electroanalysis*, 26 (2014) 2491-2500.
[134] Dineiro Y., Menendez M.I., Blanco-Lopez M.C., Lobo-Castanon M.J., Miranda-Ordieres A.J., Tunon-Blanco P., Computational Approach to the Rational Design of Molecularly Imprinted Polymers for Voltammetric Sensing of Homovanillic Acid, *Analytical Chemistry*, 77 (2005) 6741-6746.
[135] Zhang L.H., Cai H.L., Jiang P., Li H.D., Cao L.J., Dang R.L., Zhu W.Y., Deng Y., Simultaneous Determination of Multiple Neurotransmitters and Their Metabolites in Rat Brain Homogenates and Microdialysates by Lc-Ms/Ms, *Analytical Methods*, 7 (2015) 3929-3938.

[136] Mamedov I.S., Zolkina I.V., Glagovsky P.B., Sukhorukov V.S., Comparison of Chromatographic Methods for Determination of the Major Metabolites of Catecholamines and Serotonin, *International Journal of Biomedicine*, 5 (2015) 87-90.
[137] Agatsuma S., Sekino H., Watanabe H., Indoxyl-Beta-D-Glucuronide and 3-Indoxyl Sulfate in Plasma of Hemodialysis Patients, *Clinical Nephrology*, 45 (1996) 250-256.
[138] Cao X.S., Chen J., Zou J.Z., Zhong Y.H., Teng J., Ji J., Chen Z.W., Liu Z.H., Shen B., Nie Y.X., Lv W.L., Xiang F.F., Tan X., Ding X.Q., Association of Indoxyl Sulfate with Heart Failure among Patients on Hemodialysis, *Clinical Journal of the American Society of Nephrology*, 10 (2015) 111-119.
[139] Niwa T., Takeda N., Tatematsu A., Maeda K., Accumulation of Indoxyl Sulfate, an Inhibitor of Drug-Binding, in Uremic Serum as Demostrated by Internal-Surface Reversed-Phase Liquid-Chromatography, *Clinical Chemistry*, 34 (1988) 2264-2267.
[140] Lin C.J., Liou T.C., Pan C.F., Wu P.C., Sun F.J., Liu H.L., Chen H.H., Wu C.J., The Role of Liver in Determining Serum Colon-Derived Uremic Solutes, *Plos One*, 10 (2015).
[141] Patel K.P., Luo F.J.G., Plummer N.S., Hostetter T.H., Meyer T.W., The Production of P-Cresol Sulfate and Indoxyl Sulfate in Vegetarians Versus Omnivores, *Clinical Journal of the American Society of Nephrology*, 7 (2012) 982-988.
[142] Vanholder R., Schepers E., Pletinck A., Nagler E.V., Glorieux G., The Uremic Toxicity of Indoxyl Sulfate and P-Cresyl Sulfate: A Systematic Review, *Journal of the American Society of Nephrology*, 25 (2014) 1897-1907.
[143] Ellis R.J., Small D.M., Vesey D.A., Johnson D.W., Francis R., Vitetta L., Gobe G.C., Morais C., Indoxyl Sulphate and Kidney Disease: Causes, Consequences and Interventions, *Nephrology*, 21 (2016) 170-177.
[144] Duranton F., Cohen G., De Smet R., Rodriguez M., Jankowski J., Vanholder R., Argiles A., European Uremic Toxin Work G., Normal and Pathologic Concentrations of Uremic Toxins, *Journal of the American Society of Nephrology*, 23 (2012) 1258-1270.
[145] Liabeuf S., Desjardins L., Massy Z.A., Brazier F., Westeel P.F., Mazouz H., Titeca-Beauport D., Diouf M., Glorieux G., Vanholder R., Jaureguy M., Choukroun G., Levels of Indoxyl Sulfate in Kidney Transplant Patients, and the Relationship with Hard Outcomes, *Circulation Journal*, 80 (2016) 722-730.
[146] Enache T.A., Oliveira-Brett A.M., Pathways of Electrochemical Oxidation of Indolic Compounds, *Electroanalysis*, 23 (2011) 1337-1344.
[147] Filik H., Avan A.A., Aydar S., Voltammetric Sensing of Uremic Toxin Indoxyl Sulfate Using High Performance Disposable Screen-Printed Graphene Electrode, *Current Pharmaceutical Analysis*, 12 (2016) 36-42.
[148] Shu C., Chen X.J., Xia T.Y., Zhang F., Gao S.H., Chen W.S., Lc-Ms/Ms Method for Simultaneous Determination of Serum P-Cresyl Sulfate and Indoxyl Sulfate in Patients Undergoing Peritoneal Dialysis, *Biomedical Chromatography*, 30 (2016) 1782-1788.
[149] Giebultowicz J., Korytowska N., Sankowski B., Wroczynski P., Development and Validation of a Lc-Ms/Ms Method for Quantitative Analysis of Uraemic Toxins P-Cresol Sulphate and Indoxyl Sulphate in Saliva, *Talanta*, 150 (2016) 593-598.
[150] Gu L.Q., Wang X.F., Zhang Y.Y., Jiang Y., Lu H., Bi K.S., Chen X.H., Determination of 12 Potential Nephrotoxicity Biomarkers in Rat Serum and Urine by Liquid Chromatography with Mass Spectrometry and Its Application to Renal Failure Induced by Semen Strychni, *Journal of Separation Science*, 37 (2014) 1058-1066.

[151] Blanco-Lopez M.C., Lobo-Castanon M.J., Ordieres A.J.M., Tunon-Blanco P., Electrochemical Behavior of Catecholamines and Related Compounds at in Situ Surfactant Modified Carbon Paste Electrodes, *Electroanalysis*, 19 (2007) 207-213.
[152] Inczedy J., Compendium of Analytical Nomenclature (Definitive Rules 1997), Blackwell Science, Santa Fe, 1998.
[153] Oesch U., Janata J., Electrochemical Study of Gold Electrodes with Anodic Oxide-Films 1. Formation on Reduction Behavior of Anodic Oxides on Gold, *Electrochimica Acta*, 28 (1983) 1237-1246.
[154] Oesch U., Janata J., Electrochemical Study of Gold Electrodes with Anodic Oxide-Films 2. Inhibiton of Electrochemical Redox Reactions by Monolayers of Surface Oxides, *Electrochimica Acta*, 28 (1983) 1247-1253.
[155] Randles J.E.B., A Cathode Ray Polarograph 2. The Current-Voltage Curves, *Transactions of the Faraday Society*, 44 (1948) 327-&.
[156] Adams R.N., Electrochemistry at Solid Electrodes, Marcel Dekker Inc., New York, 1969.
[157] Compton R.G., Banks C.E., Understanding Voltammetry 2nd Edition, Imperial College Press, London, 2011.
[158] Hu S., Wang Y.H., Wang X.Z., Xu L., Xiang J., Sun W., Electrochemical Detection of Hydroquinone with a Gold Nanoparticle and Graphene Modified Carbon Ionic Liquid Electrode, *Sensors and Actuators B-Chemical*, 168 (2012) 27-33.
[159] Ma X.M., Liu Z.N., Qiu C.C., Chen T., Ma H.Y., Simultaneous Determination of Hydroquinone and Catechol Based on Glassy Carbon Electrode Modified with Gold-Graphene Nanocomposite, *Microchimica Acta*, 180 (2013) 461-468.
[160] Zheng Y.H., Soeriyadi A.H., Rosa L., Ng S.H., Bach U., Gooding J.J., Reversible Gating of Smart Plasmonic Molecular Traps Using Thermoresponsive Polymers for Single-Molecule Detection, *Nature Communications*, 6 (2015).
[161] Nguyen M., Kanaev A., Sun X.N., Lacaze E., Lau-Truong S., Lamouri A., Aubard J., Felidj N., Mangeney C., Tunable Electromagnetic Coupling in Plasmonic Nanostructures Mediated by Thermoresponsive Polymer Brushes, *Langmuir*, 31 (2015) 12830-12837.

7. Appendix I

Voltammetric Determination of Homovanillic Acid and Vanillylmandelic Acid on a Disposable Electrochemical Measuring Cell System with Integrated Carbon Composite Film Electrodes

Libánský Milan, Zima Jiří, Barek Jiří, Dejmková Hana

Monatshefte Fur Chemie

Volume 147, Pages 89-96, Year 2016

Monatsh Chem (2016) 147:89–96
DOI 10.1007/s00706-015-1583-8

ORIGINAL PAPER

Voltammetric determination of homovanillic acid and vanillylmandelic acid on a disposable electrochemical measuring cell system with integrated carbon composite film electrodes

Milan Libansky[1] · Jiri Zima[1] · Jiri Barek[1] · Hana Dejmkova[1]

Received: 1 September 2015 / Accepted: 12 October 2015 / Published online: 3 November 2015

Abstract An array of carbon composite electrodes embedded in a 96-well microtitration plate was applied to differential pulse voltammetry determination of standards of tumor biomarkers 2-(4-hydroxy-3-methoxy-phenyl) acetic acid (homovanillic acid, HVA) and (*RS*)-hydroxy (4-hydroxy-3-methoxy-phenyl) acetic acid (vanillylmandelic acid, VMA). For the preparation of composite electrodes, graphitic conductive microparticles and nonconductive polystyrene binder were used. For the measurement, a buffer of pH 2 was selected as the optimum medium for both analytes. In this medium, concentration dependences of stand-alone standards were measured; calculated quantification limits were 0.3 μmol dm^{-3} for HVA and 0.8 μmol dm^{-3} for VMA. Sorption of analytes on employed working electrode was examined in order to verify, whether the current is influenced by the time period between cell filling and measurement. The sorption was not observed and the current was stable even after 10 min. Developed method was verified by the determination of a mixture of standards of both analytes. Mixtures of analytes of various proportions were measured and the obtained calibration curves showed good agreement with standard values. Furthermore, the results showed that the behavior of the mixture of analytes is not different from the behavior of the actual standards, so that it is possible to calculate the concentration of both analytes side by side.

Graphical abstract

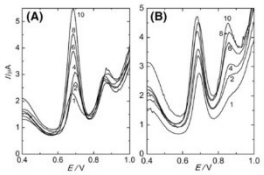

Keywords Array of electrodes · Electrochemistry · Microtitration plate · Oxidations · Tumor biomarkers · Voltammetry

✉ Hana Dejmkova
dejmkova@natur.cuni.cz

Milan Libansky
libanskm@natur.cuni.cz

[1] Department of Analytical Chemistry, Faculty of Science, University Research Centre UNCE "Supramolecular Chemistry", UNESCO Laboratory of Environmental Electrochemistry, Charles University in Prague, Albertov 6, 12843 Prague 2, Czech Republic

Introduction

Homovanillic acid (HVA) and vanillylmandelic acid (VMA) are important and well-known products of catecholamine metabolism in human body [1, 2]. The determination of these biomarkers in human fluids is important especially for diagnosis of metabolic [3] and neurological [4, 5] disorders.

High concentration of these acids in human blood, plasma, and urine indicates a large number of various diseases. The tumors of adrenal medulla [6], neuroblastoms [4, 7, 8], and feochromocytoms [5, 9] cause excessive production of catecholamines, which leads to subsequent excessive release of HVA and VMA to blood and urine [10]. Further scientific studies found that concentration of HVA and VMA is also related to Parkinson disease [11],

schizophrenia [12], suicide attempts [13, 14], and to post-traumatic stress disorder [14].

Monitoring of increasing renal excretion of HVA and VMA is fundamental for determining the stage of disease, monitoring of response of human organism to treatment and for an early diagnosis of tumors mentioned above [1].

Levels of HVA and VMA are mostly determined in urine samples as a concentration of each acid, as a ratio HVA:VMA [15] or with a correction to amount of excreted creatinine from human kidneys [16].

For the determination and separation of HVA and VMA, many sensitive analytical methods have been developed. Techniques such as GC–MS [17, 18], HPLC–MS [7, 19], HPLC with fluorescence detection [20], HPLC-ED [21], CZE-ED [22], and voltammetric determination [14, 15, 23–25] are most commonly used.

Phenolic structure of catecholamine metabolites suggests their oxidizability under potentials accessible for carbon electrodes, which can be used for their determination.

Properties of the solid carbon composite electrodes are comparable with properties of common carbon electrodes. Carbon composites electrodes offer certain advantages such as low cost, relatively broad potential window (dependent on pH of the measured solution), high signal-to-noise ratio, and easy miniaturization. They can be easily chemically modified and mechanically or electrochemically pretreated to decrease problems with their passivation [26, 27]. Last but not least, these electrodes are usually made from non-toxic components and thus they are environment-friendly [28]. The working carbon electrodes based on composite materials can be used as voltammetric sensors for the determination of inorganic analytes [29], as well as of organic compounds [30].

The main aim of this study is focused on the development of a reliable electrochemical determination of HVA and VMA standards at array of carbon composite film electrodes embedded in 96-well microtitration plate as a basis for the further research of real samples determination.

Results and discussion

Dependence on pH

At first, the dependence of voltammetric behavior of HVA and VMA on pH was investigated using differential pulse voltammetry (DPV). Behavior of HVA and VMA was investigated in separate solutions of standards in media of pH range from 2 to 12. The measured concentration of both acids was 100 μmol dm^{-3}.

HVA provides one voltammetric peak in anodic potential range, corresponding to the oxidation of hydroxyl group at aromatic system, with the peak potential

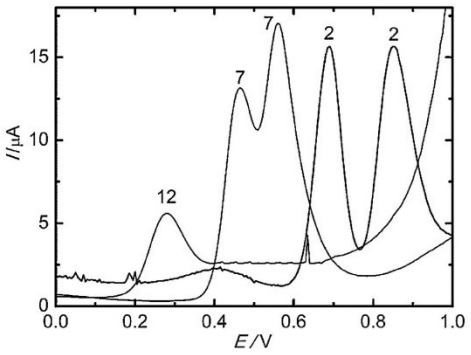

Fig. 1 DP voltammograms of 100 μmol dm^{-3} VMA in BR buffer pH 2, 7, and 12 at carbon composite film electrode. Corresponding pH is marked near the *curves*

decreasing linearly with increasing pH according to Eq. (1).

$$E_p/V = -0.0496\,\mathrm{pH} + 0.782 \quad (R^2 = 0.989) \tag{1}$$

On the other hand, VMA provides two voltammetric peaks up to pH 11, where conjunction of peaks is observed (Fig. 1). This fact is caused by the different mechanism of oxidation of hydroxyl group of VMA compared to the mechanism of HVA oxidation [31]. The potential of the first peak of VMA is similar to the peak potential of HVA; the potential difference between the peaks increases with decreasing pH and in acidic pH, the peaks are independently evaluable.

The peak potential of both peaks of VMA is decreasing linearly with increasing pH according to Eq. (2) for the first peak and to Eq. (3) for the second peak.

$$E_{p1}/V = -0.040\ \mathrm{pH} + 0.753 \ (R^2 = 0.992) \tag{2}$$

$$E_{p2}/V = -0.057\,\mathrm{pH} + 0.962 \ (R^2 = 0.985) \tag{3}$$

The current response is highest and most reproducible in the acidic media. For further measurements, pH 2 was selected as an optimum medium for both analytes.

Invariance of behavior of analytes on the working electrode

Sorption of both analytes on the employed composite electrodes was examined in order to verify, whether the peak height is influenced by the time period between cell filling and actual measurement or whether we are able to use adsorptive stripping voltammetry to increase sensitivity of the measurement. The measurements were carried out in separate solutions of 100 and 10 μmol dm^{-3} HVA, and

100 and 10 μmol dm^{-3} VMA in BR buffer of pH 2. Current responses were measured in non-stirred solutions after time period of 0, 1, 5 and 10 min.

The electrode response did not show any trend even after 10 min of accumulation time for both analytes. In the case of HVA, value of RSD of the peak current of all measurements (n = 5, all times included) was 1.3 % for the higher measured concentration and 3.8 % for the lower measured concentration. In the case of VMA, values of RSD of the first and second peak current were 5.0 and 5.8 % for the higher measured concentration and 3.5 and 3.1 % for the lower measured concentration, respectively. It follows from the obtained results that it is not necessary to perform the determination immediately after dispensing the sample; however, the adsorptive step could not be utilized.

Concentration dependences

Concentration dependences were measured under the optimal conditions (pH 2, without sorption) in the concentration range from 100 to 0.8 μmol dm^{-3} for HVA and from 100 to 1 μmol dm^{-3} for VMA (Table 1). The concentration dependences were linear within the whole concentration range for both analytes. Measured DP voltammograms are shown in Fig. 2 for HVA and in Fig. 3 for VMA.

Repeatability of the measurement of HVA was 6.6 % (n = 10) and repeatability of the measurement of VMA was 11 % (n = 10, both peaks) for the lowest measured concentration, which explains higher LOQ in the case of VMA. Achieved limits of quantification of both analytes are shown in Table 1.

Low value of all intercepts refers to the absence of side reactions at the electrode and of the impurities in the solutions. In comparison with other DPV determinations on various carbon electrodes [15, 25], developed method on carbon composite film electrodes offers similar results.

Determination of standards of acids in the mixture

Whereas the analytes are often determined side by side, it was necessary to analyze how the electrochemical behavior of standards is influenced by the simultaneous presence of both analytes.

As mentioned previously, the potential of the first peak of VMA is similar to the peak potential of HVA and the sum of the first peak current in the mixture is equal to sum of peak currents of separate standards. The second VMA peak is separated from the other peaks well enough to enable VMA determination. The combination of these facts can be used for the determination of both analytes in the mixture—determination of VMA can be based on the second peak and with its known concentration, HVA can be determined from the first summary peak.

The first condition for the applicability of this procedure is that the sum of the first peak current in the mixture equals to the sum of corresponding peak currents of separate standards. For the confirmation, four calibration sets of mixed solutions of analytes were prepared and measured. Each calibration set was prepared from standard of VMA or HVA in the concentration range from 10 to 1 μmol dm^{-3} with constant addition of the second analyte of concentration 10 or 5 μmol dm^{-3} (Table 2). Selected DP voltammograms are shown in Fig. 4.

Slopes and intercepts for the first peak of all calibration curves were evaluated and compared to values obtained from the measurements of stand-alone standards (concentration range from 10 to 1 μmol dm^{-3}). For the good agreement of results, the values of slopes of first peak should correspond with the slopes of standards and the intercepts should match with the current increase caused by addition of second acid (Table 2).

Obtained calibration curves showed good agreement with standard values and linear growth of intercept (Figs. 5, 6); the results of HVA show higher consistency than those of VMA, which differ from the standard of approximately 20 %. This inconsistence was probably caused by change of the baseline in the mixture of analytes and also by lower repeatability of the measurements of VMA standards. Low correlation of the intercepts of the VMA second peak dependence is acceptable, considering that all the intercepts for this set of dependences are statistically insignificant ($\alpha = 0.05$); influence of the small signal in supporting electrolyte, visible in Fig. 2, is negligible.

Table 1 Parameters of HVA and VMA concentration dependences measured by DVP at carbon composite film electrode in buffer of pH 2

Analyte/peak	Slope/μA dm^{-3} mol^{-1}	Intercept/μA[a]	SD[b]/μA	R^2	LOQ/μmol dm^{-3}
HVA/1	0.31	0.05	0.17	0.999	0.3
VMA/1	0.19	−0.08	0.38	0.997	0.8
VMA/2	0.17	0.04	0.47	0.995	1.4

[a] Intercept is not significantly different from zero ($\alpha = 0.05$)

[b] The standard deviation of the regression line

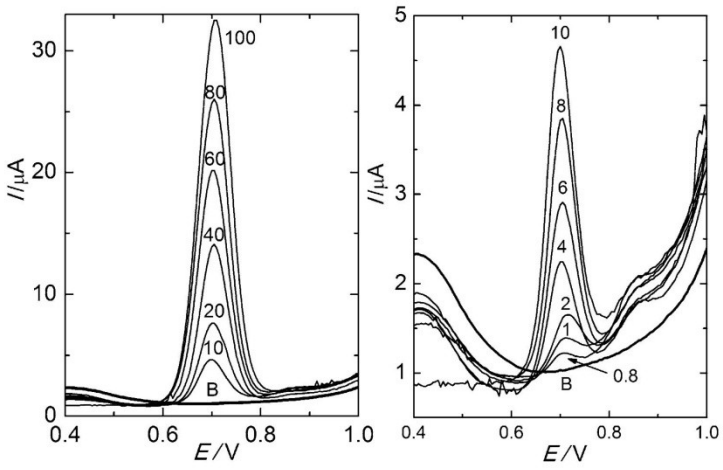

Fig. 2 DP voltammograms of HVA in BR buffer pH 2 at carbon composite film electrode. Corresponding concentration in μmol dm^{-3} is displayed near the *curves*

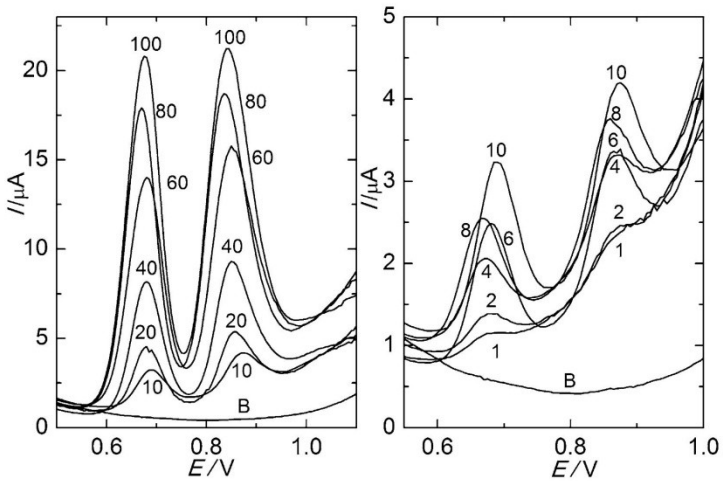

Fig. 3 DP voltammograms of VMA in BR buffer pH 2 at carbon composite film electrode. Corresponding concentration in μmol dm^{-3} is displayed near the *curves*

For further verification of the proposed method, the known concentrations of the analytes in the mixtures were compared with the concentrations calculated by the described procedure (Table 3). Equation (4) was used for HVA determination and Eqs. (5) and (6) for VMA determination.

$$c_{HVA} = \frac{(I_{SUM} - I_{VMA/1}) + 0.16}{0.35} \quad (4)$$

$$I_{VMA/1} = 0.19\, c_{VMA} - 0.03 \quad (5)$$

$$c_{VMA} = \frac{I_{VMA/2} - 0.06}{0.17} \quad (6)$$

(I_{Sum} = sum of the current of the first peaks, $I_{VMA/1}$ = current of the first peak of VMA).

The obtained results correspond to the known values with the exception of mixtures, where concentration of one of the analytes is markedly lower in comparison with the other one. In this case, the general tendency to provide lower results is pronounced and yields lower than 50 % are sometimes reached.

Table 2 Parameters of mixture of HVA and VMA concentration dependences measured by DPV at carbon composite film electrode in buffer of pH 2

Calibration curve/peak	Addition/μmol dm^{-3}	Slope[c]/μA dm^{-3} mol^{-1} Intercept/μA	Slope[d]/μA dm^{-3} mol^{-1} Intercept/μA	Agreement slope Intercept (%)
HVA	10[b]	0.36	0.35	104
		1.61	1.58	102
HVA	5[b]	0.36	0.35	102
		0.70	0.82	85
VMA/1	10[a]	0.23	0.19	123
		3.31	3.30	99
VMA/1	5[a]	0.16	0.19	84
		1.70	1.52	111
VMA/2	10[a]	0.22	0.17	127
		−0.12	−0.061	200
VMA/2	5[a]	0.17	0.17	100
		−0.023	−0.061	38

[a] Addition of HVA

[b] Addition of VMA

[c] Slopes and intercepts obtained from measurement of mixture of analytes

[d] Expected values of slopes and intercepts from measurement of standards of analytes

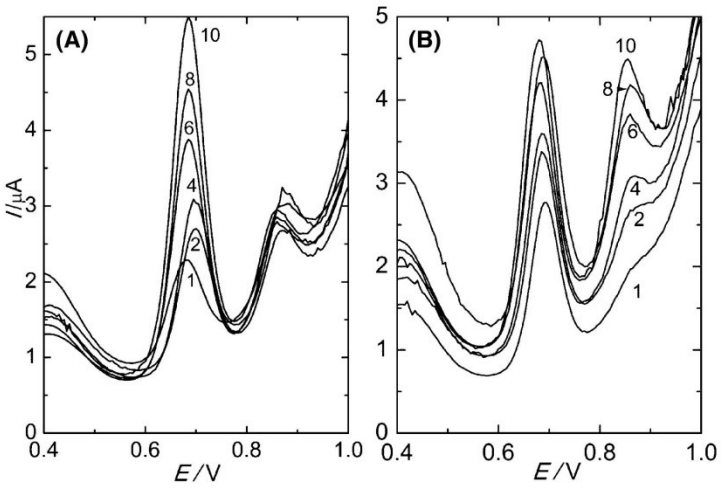

Fig. 4 DP voltammograms of **a** HVA with addition of 5 μmol dm^{-3} VMA and **b** VMA with addition of 5 μmol dm^{-3} HVA in BR buffer pH 2 at carbon composite film electrode. Corresponding concentration of analytes in μmol dm^{-3} is displayed near the *curves*

From the calculated results using standards and mixtures of analytes it is obvious that using the developed method, it is possible to determine HVA and VMA in the mixture with precision sufficient for the screening measurements, provided that the concentrations of both compounds are comparable.

Conclusion

Voltammetric method for the determination of HVA and VMA, oxidizable tumor biomarkers, was developed using electrochemical measuring system with carbon composite electrode embedded in 96-well microtitration plate.

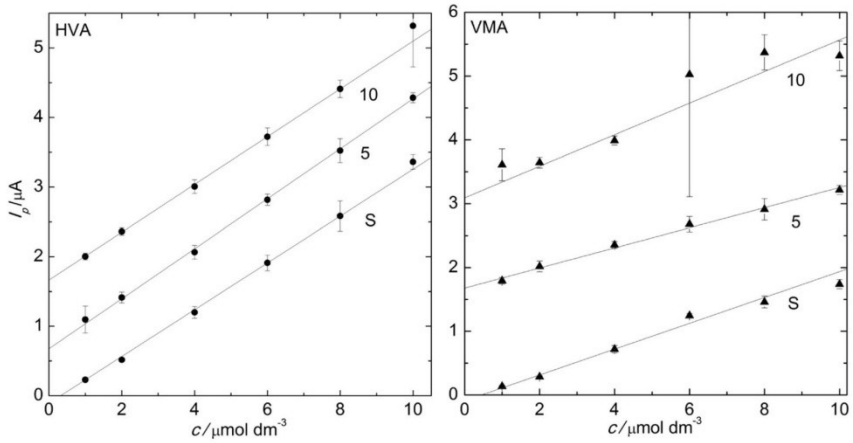

Fig. 5 The first peak current dependences on the concentration of standards of HVA or VMA with addition of second acid. Corresponding concentration of addition in μmol dm^{-3} is displayed near the *curves*

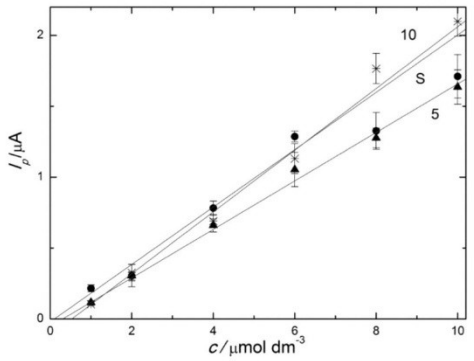

Fig. 6 The second peak current dependences on the concentration of standards of VMA (S) with addition of HVA. Corresponding concentration of addition of HVA in μmol dm^{-3} is displayed near the *curves*

From the dependence of peak heights on supporting electrolyte composition, a buffer of pH 2 was selected as the optimum medium. In this medium, concentration dependences were measured; calculated HVA determination limit was 0.3 μmol dm^{-3} and calculated VMA determination limit was 0.8 μmol dm^{-3}. The peak current was not influenced by the accumulation time even after 10 min of accumulation for both analytes.

For exploring the electrochemical behavior of mixtures of both analytes in one solution, four calibration sets of these mixtures were prepared and measured. Slopes and intercepts were compared to values obtained from the measurements of stand-alone standards. Obtained calibration curves show good agreement with standard values, particularly in case of HVA calibration. Concentrations of the respective compounds in mixtures were calculated using the concentration dependences of single standards. Also these values correspond well with the expected values, provided that the concentrations of both compounds are similar. Average recovery was 86 % for HVA and 89 % for VMA.

All the results showed that it is possible to use carbon composite film electrodes for simultaneous DPV determination of HVA and VMA with the sufficient sensitivity and accuracy required in screening measurements. Moreover, used electrochemical system offers advantages such as low purchase price and integrated working electrodes that are made from non-toxic components and thus environment-friendly.

On the other hand, limits of quantification of an analysis are deficient in comparison to modern spectrometric techniques [20] and it is necessary to overcome this problem by another improvement of the method by the further research which would include DPV and SWV determination of analytes standards in urine and determination of real samples with a pre-concentration step or with a preliminary separation step.

Table 3 Calculated values of concentration of mixture of HVA and VMA measured by DPV at carbon composite film electrode in buffer of pH 2

Concentration[a]/μmol dm^{-3} HVA/VMA	Concentration[b]/μmol dm^{-3} HVA/VMA	Recovery HVA/%	Recovery VMA/%
10/10	8.9/11.2	89	112
10/8	9.7/10.1	97	126
10/6	10.7/6.3	107	105
10/4	9.1/3.7	91	93
10/2	9.2/1.6	92	79
10/1	9.9/0.3	99	26
5/10	3.9/9.3	78	93
5/8	4.2/7.2	83	90
5/6	4.2/5.9	84	98
5/4	4.5/3.5	90	89
5/2	4.6/1.5	93	73
5/1	4.6/0.3	92	34
10/10	8.9/11.2	89	112
8/10	6.8/10.4	84	104
6/10	5.3/9.5	88	95
4/10	3.4/9.1	85	91
2/10	1.5/9.2	75	92
1/10	0.8/8.6	78	86
10/5	9.5/4.6	95	93
8/5	7.4/4.4	92	89
6/5	5.2/4.7	87	94
4/5	3.4/4.1	85	82
2/5	1.2/4.6	61	92
1/5	0.6/4.1	58	82
	Average	86	89

[a] Spiked concentrations of analytes

[b] Concentrations calculated from measurement of mixture of analytes

Experimental

Chemicals

For the fabrication of composite electrodes, graphite powder with a diameter of particles from 3.5 to 5 μm (CR-2, Grafit Tyn, Czech Republic) was used as conductive component; polystyrene (packaging EPS polystyrene) served as the nonconductive binder and toluene obtained in p.a. grade from Lachema, Czech Republic as a volatile solvent.

The stock solutions of 1 mmol dm^{-3} HVA (fluorimetric reagent, Sigma Aldrich, USA) and 1 mmol dm^{-3} VMA (≥98 %, TLC, Sigma Aldrich, USA) were prepared by dissolving the exact amount of the substances in deionized water (Milli-Q-Gradient, Millipore, USA) and they were kept in the refrigerator. Britton-Robinson buffers serving as supporting electrolyte were prepared by mixing of 0.2 mol dm^{-3} of sodium hydroxide (Penta, Czech Republic) with a solution of phosphoric acid, boric acid and acetic acid (all Lachema, Czech Republic), 0.04 mol dm^{-3} each. All chemicals used for buffers preparation were of analytical grade purity and used without further purification. The standard solutions of the mixture of analytes were prepared by mixing the exact volume of the stock solutions of both analytes with Britton-Robinson buffer.

Apparatus

Voltammetric measurements were performed with portable potentiostat PalmSens (Palm Instruments, Netherlands), controlled by PSTrace 4.0.0 software. Differential pulse voltammetry was carried out with carbon composite film electrode (described below), platinum wire auxiliary electrode and Ag/AgCl (3 mol dm^{-3} KCl) reference electrode (Eco-Trend Plus, Czech Republic), to which all potentials values are referred. The pH of the solutions was measured with a pH meter Jenway 3510 (Jenway, United Kingdom) with a combined glass electrode.

Preparation of the electrochemical cell system

The carbon ink for the fabrication of carbon composite film electrodes was prepared by thorough mixing of graphite and polystyrene in 9:1 ratio; subsequently, 0.5 cm^3 of toluene for each 0.1 g of total weight of solid particles was added and the electrode mixture was homogenized by intensive stirring. As the platform of a cell system, the 96-well microtitration plate (U96 Microwell plates natural, Schoeller Pharma Praha, Czech Republic) with round bottom was used. Metal contact was introduced through the bottom of the hole and 80 mm^3 of the carbon ink was applied into each cell. After the solvent evaporation, the cell set with integrated solid carbon composite film electrodes (hemispherical shape of diameter 8.05 mm, geometric area 1.0 cm^2) was ready for the measurement [32, 33].

Procedures

Parameters of the DPV potential program were: 0.1 s pulse width, 50 mV pulse height, 20 mV s^{-1} scan rate (parameters were not optimized) and potential range from −100 to 1000 mV. Volume of the solution used for the measurement was 370 mm^3. All measurements were repeated five times and each measurement was performed in the new cell, unless stated otherwise. Calibration dependences were evaluated by least squares linear regression method. The quantification limits were calculated as the concentration of the analyte which gave a signal ten times higher than the standard deviation of the lowest evaluable concentration [34].

Acknowledgments This research was realized in the frame of specific university research SVV. Financial support of the Grant Agency of the Czech Republic (project P206/12/G151) is gratefully acknowledged.

References

1. Fitzgibbon MC, Tormey WP (1994) Ann Clin Biochem 31:1
2. Eisenhofer G, Kopin IJ, Goldstein DS (2004) Pharmacol Rev 56:331
3. Matsuo M, Tasaki R, Kodama H, Hamasaki Y (2005) J Inherit Metab Dis 28:89
4. Barco S, Gennai I, Reggiardo G, Galleni B, Barbagallo L, Maffia A, Viscardi E, De Leonardis F, Cecinati V, Sorrentino S, Garaventa A, Conte M, Cangemi G (2014) Clin Biochem 47:848
5. Lenders JWM, Pacak K, Walther MM, Linehan WM, Mannelli M, Friberg P, Keiser HR, Goldstein DS, Eisenhofer G (2002) J Am Med Assoc 287:1427
6. Lionetto L, Lostia AM, Stigliano A, Cardelli P, Simmaco M (2008) Clin Chim Acta 398:53
7. Sadilkova K, Dugaw K, Benjamin D, Jack RM (2013) Clin Chim Acta 424:253
8. Monsaingeon M, Perel Y, Simonnet G, Corcuff JB (2003) Eur J Pediatr 162:397
9. Rosano TG, Swift TA, Hayes LW (1991) Clin Chem 37:1854
10. Flottmann D, Hins J, Rettenmaier C, Schnell N, Kuci Z, Merkel G, Seitz G, Bruchelt G (2006) Microchim Acta 154:49
11. LeWitt P, Schultz L, Auinger P, Lu M, Parkinson Study Group D (2011) Brain Res 1408:88
12. Suzuki E, Kanba S, Nibuya M, Adachi S, Sekiya U, Shintani F, Kinoshita N, Yagi G, Asai M (1994) Biol Psychiatry 36:654
13. Sher L, Mann JJ, Traskman-Bendz L, Winchel R, Huang YY, Fertuck E, Stanley BH (2006) J Affect Disord 90:83
14. Revin SB, John SA (2012) Anal Methods 4:348
15. Li QA, Batchelor-McAuley C, Compton RG (2010) J Phys Chem B 114:9713
16. Pussard E, Neveux M, Guigueno N (2009) Clin Biochem 42:536
17. Kaluzna-Czaplinska J, Socha E, Rynkowski J (2010) Med Sci Monit 16:445
18. Monteleone M, Naccarato A, Sindona G, Tagarelli A (2013) Anal Chim Acta 759:66
19. Park JY, Myung SW, Kim IS, Choi DK, Kwon SJ, Yoon SH (2013) Biol Pharm Bull 36:252
20. Tsunoda M, Mitsuhashi K, Masuda M, Imai K (2002) Anal Biochem 307:153
21. Zydron M, Baranowski J, Bialkowski J, Baranowska I (2005) Sep Sci Technol 40:3137
22. Zhang HT, Li Z, Zhang JB, Zhang Y, Ye JN, Chu QC, Zhang MJ (2013) Chem Res Chin Univ 29:850
23. Selvaraju T, Ramaraj R (2007) Electrochim Acta 52:2998
24. Hatefi-Mehrjardi A, Ghaemi N, Karimi MA, Ghasemi M, Islami-Ramchahi S (2014) Electroanalysis 26:2491
25. Dineiro Y, Menendez MI, Blanco-Lopez MC, Lobo-Castanon MJ, Miranda-Ordieres AJ, Tunon-Blanco P (2005) Anal Chem 77:6741
26. Albertus F, Llerena A, Alpizar J, Cerda V, Luque M, Rios A, Valcarcel M (1997) Anal Chim Acta 355:23
27. Navratil T (2011) Curr Org Chem 15:2996
28. Barek J, Fischer J, Navratil T, Peckova K, Yosypchuk B, Zima J (2007) Electroanalysis 19:2003
29. Noskova GN, Zakharova EA, Kolpakova NA, Kabakaev AS (2012) J Solid State Electrochem 16:2459
30. Prasek J, Huska D, Jasek O, Zajickova L, Trnkova L, Adam V, Kizek R, Hubalek J (2011) Nanoscale Res Lett 6:385
31. Blanco-Lopez MC, Lobo-Castanon MJ, Ordieres AJM, Tunon-Blanco P (2007) Electroanalysis 19:207
32. Libansky M, Zima J, Barek J, Dejmkova H (2014) Electroanalysis 26:1920
33. Dejmkova H, Milan L, Zima J, Barek J (2013) Elektrochemická měřicí cela a soustava elektrochemických měřicích cel. CZ Patent 304 176, Nov 23, 2013; (2013) Chem Abstr 1926602
34. Inczedy J (1998) Compendium of analytical nomenclature (definitive rules 1997). Blackwell, Santa Fe

8. Appendix II

Determination of Urinary Indican on Carbon Film Composite Electrode and Carbon Paste Electrode

Bergerová Michaela, **Libánský Milan**, Dejmková Hana

Current Analytical Chemistry

Submitted, Year 2017

Send Orders for Reprints to reprints@benthamscience.ae

Current Analytical Chemistry, Year, *Volume*

Determination of Urinary Indican on Carbon Film Composite Electrode and Carbon Paste Electrode

Michaela Bergerova, Milan Libansky, and Hana Dejmkova*

[a]*UNESCO Laboratory of Environmental Electrochemistry, Department of Analytical Chemistry, Faculty of Science, University Research Centre "Supramolecular chemistry", Charles University, Albertov 6, Prague, Czech Republic*

Abstract: Background: This paper is focused on application of a recently developed disposable array of carbon composite electrodes and well-known carbon paste electrode for determination of indoxyl sulphate (urinary indican) in human urine matrix.

Results: Measurement of basic electrochemical behaviour of indoxyl sulphate on working electrode resulted in selection of BR buffer pH 2 and pH 3 as the optimum medium for carbon composite film electrode and carbon paste electrode, respectively. In this medium, concentration dependences of standard of indoxyl sulphate were measured; calculated quantification limits were 0.7 μmol L^{-1} for carbon composite film electrode and 1.7 μmol L^{-1} for the carbon paste electrode. Accumulation of indican on employed working electrodes was examined in order to increase sensitivity of the measurement. However, after time period of 5 minute; observed increase of the current response was negligible and accumulation step was not inserted. Developed method was complemented by the solid phase extraction of indoxyl sulphate from spiked human urine matrix, where methanol, BR buffer, deionised water and their combination were used as elution reagents.

Conclusion: Selected graphite-based working electrodes were successfully applied for the development of suitable voltammetric method for the determination of indoxyl sulphate in BR buffer and the sufficient sensitivity and accuracy required in screening measurements was observed; however, solid phase extraction was not successful due to ineffectual removal of interferents from human urine.

Keywords: Indican, Carbon composite film electrode, Carbon paste electrode, Differential pulse voltammetry, Solid phase extraction, Oxidation

*Address correspondence to this author at the Department of Analytical Chemistry, Faculty of Science, Charles University, Albertov 6, Prague, Czech republic, CZ-128 00; Tel/Fax: +420-221951223; E-mail: dejmkova@natur.cuni.cz

1. INTRODUCTION

Indoxyl suphate is a product of tryptophan metabolism. Tryptophan absorbed from food is metabolized by colon microbes to indole and then to indoxy sulphate by the liver after transfer into systemic circulation. Subsequently, indoxyl suphate is cleared by the kidneys through tubular secretion and excreted to urine. Only 10 % of indoxyl sulphate is circulating in the metabolism as a "free" form, the remaining amount of indoxyl sulphate is present as a form bounded to plasma proteins, mostly to albumin [1, 2]. Final concentration of indoxyl sulphate in body fluids can be influenced by high (or low) protein/tryptophan diet or by intake of drug influencing liver or bowel function [3]. In the event of an actual

XXX-XXX/14 $58.00+.00

kidney disease, tubular clearance decreases and indoxyl sulphate accumulates in plasma and urine [4], which can lead to cardiovascular problems and bone diseases [5, 6]. The indoxyl sulphate toxicity was proven in cultured human cells and animals. Toxic effect in humans has not yet been conclusively established and it is in the interest of many clinical laboratories, because monitoring of excretion of indoxyl sulphate to urine could be fundamental for prediction of forthcoming kidney diseases, renal failure, unsuccessful kidney transplantation, problems with colon microbial metabolism and for the preventing of heart problems [7, 8]. Therefore, modern techniques for extraction and determination of indoxyl sulphate are required. Despite the many medical studies, only several electrochemical methods were developed for the determination of indoxyl sulphate. Among them, we can mention determination of indoxyl sulphate on disposable screen-printed graphene electrode by square-wave voltammetry [9] or determination of indoxyl sulphate by reversed-phase liquid chromatography using an electrochemical detector based on composite electrode of carbon black and polyethylene [10]. Nevertheless, determination of indoxyl sulphate by HPLC with mass spectrometry is common [11-13].

For the development of the method, two graphite-based bicomponent electrodes were used. One of them was the recently introduced carbon composite film electrode, integrating film of graphite microparticles and polystyrene in the wells of microtitration plate. In the past, this type of solid carbon composite film electrode [14] was used for the determination of environmental pollutants, e.g. triclosan in tooth paste [15], 5-nitroquinoline [16] and 4-nitrophenol in river water [17] or homovanillic acid and vanillylmandelic acid [18]. During recent researches was revealed that this type of solid composite electrode offers certain advantages such as possibility to adjust shape and sizes of the electrode according to the requirement, low purchase price, easy fabrication process, and environmental friendliness. Moreover, developed voltammetric methods on this electrode offer sufficient sensitivity and accuracy required in screening measurements. On the other hand, low robustness during measurements in media containing higher amount organic solvents (>30 %) can be considered as a main disadvantage of this type of electrode [15, 18]. The other applied electrode was carbon paste electrode (CPE), well-known electroanalytical instrument proven by years of the usage. In case of this electrode, graphite microparticles are mixed with inert, non-electroactive liquid binder [19] and filled in the electrode body usually made of polyethylene or Teflon with inner metal piston [20]. CPEs offer highly beneficial properties such as high conductivity, low background current, easy ways of miniaturization, and easy renewability. In the last years, improvement of carbon paste electrodes by the replacement of one of the basic component of the paste by different conductive particle or ionic liquid opens new ways of usability and it is on the rise [21, 22].

This paper is focused on the development of suitable electrochemical methods for the determination of indoxyl sulphate in human urine matrix at these two graphite based electrodes and comparison of the obtained results, particularly from the perspective of large-scale solid CFE applicability for determination of biomarkers.

2. MATERIALS AND METHOD

2.1. Chemicals

The stock solution of 1 mmol L^{-1} urinary indican (indoxyl sulfate potassium salt, p.a. grade, Sigma-Aldrich, USA) was prepared by dissolving the exact amount of the substance in deionized water (resistivity = 18,2 MΩ cm^2, Milli-Q-Gradient, Millipore, USA) and it was kept in the refrigerator. Britton-Robinson (BR) buffers serving as supporting electrolyte were prepared by mixing of 0.2 mol L^{-1} of sodium hydroxide (Penta, Czech Republic) with a solution of phosphoric acid, boric acid and acetic acid (all Lachema, Czech Republic), 0.04 mol L^{-1} each. All chemicals used for buffers preparation were of analytical grade purity and used without further purification. As extraction reagents, methanol (p.a., Merck, Germany), deionized water and BR buffer were used.

2.2. Apparatus

Voltammetric measurements were performed with potentiostat EcoTribo (Polaro-Sensors, Czech Republic), controlled by Polar 5.1 software. Differential pulse voltammetry (DPV) and cyclic voltammetry (CV) were carried out with carbon composite film electrode and carbon paste electrode, platinum wire auxiliary electrode, and Ag/AgCl (3 mol L^{-1} KCl) reference electrode (Eco-Trend Plus, Czech Republic), to which all potentials values are referred. Preparation of working electrodes is described in section 2.3. The pH of the solutions was measured with a pH meter Jenway 4330 (Jenway, United Kingdom) with a combined glass electrode.

2.3. Preparation of working electrodes

The carbon ink for the fabrication of carbon composite film electrodes was prepared by thorough mixing of graphite particles with diameter from 3.5 to 5 μm (Grafit Tyn, Czech Republic) and EPS polystyrene in 9:1 ratio; subsequently 0.5 mL of toluene (p.a., Lachema, Czech Republic) for each 0.1 g of total weight of solid particles was added and the electrode mixture was homogenized by intensive stirring. The 96-well microtitration plate with round bottom (Schoeller Pharma Praha, Czech Republic) was used as the platform of a cell system. Metal contact (2 mm thick) was implemented through the bottom of the hole and 80 μL of the carbon ink was applied into each cell. After evaporation of the solvent, the cell set with integrated solid carbon composite film electrodes (hemispherical shape, diameter 8.05 mm, and geometric area 100 mm^2) was ready for the measurement [15].

Carbon paste was prepared by thorough mixing of 0.25 g graphite particles with 100 μL of mineral oil Nujol (Fluka, Switzerland). Prepared carbon paste was packed in the Teflon piston-driven holder with 2 mm inner diameter (geometric area 3.1 mm^2) [23]. The surface of the electrode was renewed by pressing about 0.1 mm of the paste out of the holder by piston and wiping with wet filtration paper.

2.5. Sample treatment and extraction

Urine samples spiked with known amount of standard of urinary indican were prepared from human urine of the healthy analyst. Interferents from model sample of urine were separated by solid phase extraction (SPE), performed using poly(styren-divinylbenzene) based solid-phase extraction columns LiChrolut EN 200 mg/3 mL (Merck, Germany).

The SPE column was first conditioned by 3 mL of deionized water and 3 mL of methanol. Conditioning was carried out at atmospheric pressure; fluids were freely allowed to pass through the cartridge. The spiked urine sample (10 mL) was adjusted to pH 3 with phosphoric acid, filtered and applied on the SPE column. After that, the cartridge was dried

under vacuum for 1 minute and subsequently non-adsorbed interferents were washed away by 5 mL of BR buffer pH 8. Elution of the adsorbed analyte was carried out by 5 % methanol with a volume 3 mL, the entire process is described in Section 3.4. Prior to sampling to the voltammetric system, 2 ml of eluent was diluted by 8 ml of BR buffer of pH 2 (CFE) or pH 3 (CPE).

2.6. Procedures

Parameters of the DPV potential program were: 0.1 s pulse width, 50 mV pulse height, 20 mV s^{-1} scan rate and potential range from 0 to 1200 mV. Volume of the solution used for the measurement was 350 μL in the case of a cell with CFE and 5 ml in the case of carbon paste electrode. All measurements were repeated five times and each measurement was performed in the new cell with CFE or with freshly renewed surface of CPE, unless stated otherwise. Calibration dependences were evaluated by least squares linear regression method. The quantification limits were calculated as the concentration of the analyte which gave a signal ten times higher than the standard deviation of the lowest evaluable concentration. [24]

3. RESULTS AND DISCUSSIONS

3.1. Dependence on pH

Firstly, dependence of height of the peak on pH was investigated using differential pulse voltammetry (DPV) on both working electrodes. Electrochemical behaviour was investigated in 50 μmol L^{-1} solution of standard of urinary indican in BR buffer of pH range from 2 to 12.

At both types of electrodes, indoxyl sulphate provides two voltammetric peaks in anodic potential window until pH 11 and one voltammetric peak in pH 12. The current responses were highest and most reproducible in the acidic media. Peak heights were decreasing with increase of pH until pH 11, where the assessable height of the second peak decreased up to zero (Fig. 1.). Peak potentials were decreasing linearly with increasing pH with following equations.

CFE:

E_{p1} (V) = -0.030 pH + 0.695

E_{p2} (V) = -0.053 pH + 1.141

CPE:

E_{p1} (V) = -0.029 pH + 0.751

E_{p2} (V) = -0.053 pH + 1.168

Shift of first and second peak potential with pH is similar for both types of electrodes. Obtained values of slopes expressed the ratio between the exchanged electrons and protons during the electrochemical reaction.

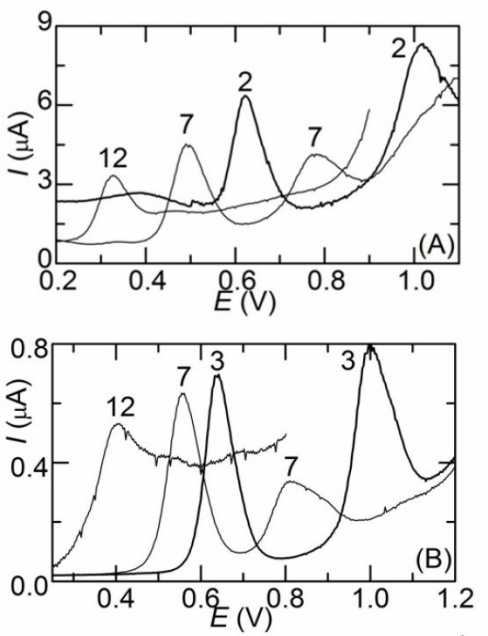

Fig. (1). DP voltammograms of 100 μmol L^{-1} indoxyl sulphate in BR buffer at (A) CFE and (B) CPE. Corresponding pH is marked near the curves.

Values for the first and second peak (0.029 V, 0.053 V) were comply with theoretical values (0.029, 0.059 V) and it indicates that during the first oxidation step, twice more electrons than protons is exchanged and in the second oxidation step, the same number of electrons and protons is exchanged. This result was compared to proposed two step mechanism of indoxyl sulphate oxidation on glassy carbon electrode [25], where the oxidation at C2 position on pyrrole ring, followed by the hydroxylation of the benzene moiety and subsequent oxidation of hydroxyl group. Agreement with proposed mechanism was observed only in the case of second peak, where two electrons and two protons are exchanged. In the case of first peak, deviation of result pointed to the difference in Nernstian electrochemical behavior on different types of carbon electrode.

For further measurements, pH 2 for CFE and pH 3 for CPE was selected as an optimum medium and only the first peak of indoxyl sulphate was used for evaluation of results, because second peak of indoxyl sulphate was lower than first and less evaluable due to overlap with end of potential window.

3.2. Repeatability and accumulation

Repeatability of the measurement both on renewed and the same surface was examined as well as the the changes of the curent response after the solution was in contact with the working electrode for a period of time. The measurement of repeatability was carried out in solution of 50 μmol L^{-1} urinary indican in BR buffer of pH 2 (CFE) and pH 3 (CPE), *i.e.* under optimum conditions. Change in the current response was tested after time period of 5 minute in the solution of 5 μmol L^{-1} urinary indican in BR buffer of pH 2, 6, and 9, in the

case of CPE under the stirring. The highest current response in DPV was obtained in pH 2 during measurement of pH dependences; however, if accumulation occurs in another pH and provides significant increase of peak current, pH might be changed for further measurements to obtain higher sensitivity.

Ten repeated scans on renewed or new surface of electrode revealed that obtained signal is stable with repeatability of the measurement 4.2 % for CFE and 3.4 % for CPE (n = 10). These values are usual for electrodes made of graphite carbon [26]. On the other hand, repeated measurement on the same surface of working electrodes resulted in decrease of peak current for almost 60 %, probably due to passivation of electrode surface by main oxidation product of electrode reaction (Fig. 2.) [9]. In the case of CFE, decrease of the peak current was magnified by increase of background current in each subsequent scan. This phenomenon can be seen in Fig. 2. These results pointed to the fact; that it is necessary to use each measuring cell with integrated CFE only once as a disposable sensor and that CPE surface have to be renewed after each single measurement.

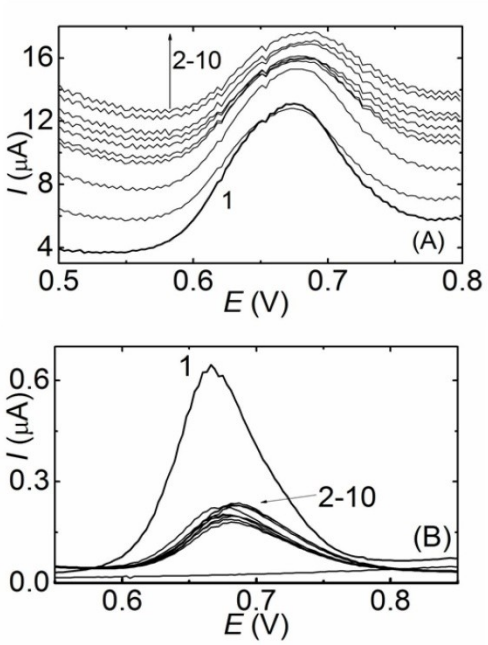

Fig. (2). DP voltammograms of 10 repeated measurements of 100 μmol L^{-1} indoxyl sulphate in BR buffer at one surface of (A) CFE and (B) CPE. Corresponding number of measurement is marked near the curves.

Measurement after prolonged time of electrode-analyte contact showed slight accumulation of indoxyl sulphate on both working electrodes, namely increase of peak current up to 30 % at pH 2 after 5 minute of accumulation time. In pH 6 and pH 9, the increase of peak current was negligible. Thus, such an increase of the current response was not satisfactory and the adsorptive step was not utilized for further measurements. On the other hand, in the case of CFE, increase of background current was observed after 5 min contact with the solution, which suggests the necessity to perform the measurement immediately after the introduction of the solution.

3.3. Concentration dependences

Concentration dependences of urinary indican were measured in acidic pH in the concentration range from 1 to 50 μmol L^{-1} for both working electrodes. The achieved results are summarized in Table **1** and selected differential pulse voltammograms are shown in Fig. 3. for CFE and Fig. 4. for CPE.

The concentration dependences were linear within the whole concentration range for both electrodes. Repeatability of measurement of peak height of urinary indican in BR buffer with CFE was 7 % (n = 5) and repeatability of measurement of urinary indican in BR buffer with CPE was 15 % (n = 5) for the lowest measured concentration (1 μmol L^{-1}). Obtained values of repeatability explain lower limit of quantification in the case of CFE. The difference in the slope value partly mirrors the difference in the electrode geometric area (3.1 mm^2 of CPE versus approx. 100 mm^2 of CFE); the remaining difference may be attributed to the difference in shape or in the role of the insulator component in the electrode. In the case of CFE, high value of intercept refers to the presence of side reaction or to the inpurities in the polystyrene binder. Intercept of the measurement with CPE was statistically insignificant.

Table 1 Parameters of urinary indican concentration dependences measured by DPV at carbon composite film electrode and carbon paste electrode in BR buffer of acidic pH.

Electrode	Slope (A L mol^{-1})	Intercept (μA)	R^2	$Sd_{x/y}$[b]	*LOQ* (μmol L^{-1})
CFE	0.151	0.24[a]	0.994	0.20	0.7
CPE	0.017	-0.01	0.999	0.02	1.7

[a]the intercept is significantly different from zero, [b]standard deviation of regression line

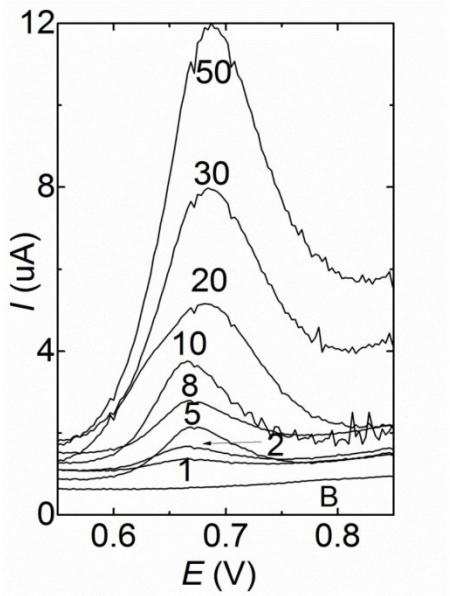

Fig. (3). DP voltammograms of urinary indican in BR buffer of pH 2 at carbon composite film electrode. Corresponding concentration in μmol L^{-1} is displayed near the curves.

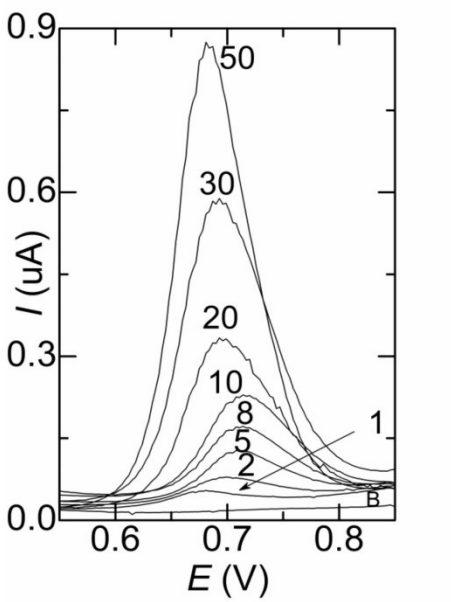

Fig. (4). DP voltammograms of urinary indican in BR buffer of pH 3 at carbon paste electrode. Corresponding concentration in μmol L^{-1} is displayed near the curves.

3.4. Determination of indican in matrix of human urine

Urine contains numerous oxidizable compounds and the application of the developed method in this matrix requires separation of the analyte, which can be most easily done by solid phase extraction (SPE). For this purpose, suitable sample treatment, washing solutions and eluent were sought. All obtained results were compared to measurement of solutions of standard of indoxyl suphate in appropriate medium.

Sorption of indoxyl sulphate from aqueous 10 μmol L^{-1} solutions occurred on EN extraction columns when the volume of 10 mL was applied; for the further measurements, urine samples were adjusted to pH 3 with phosphoric acid and 1 mL of BR buffer of the same pH was used as the washing step between the sorption and the elution. Nevertheless, the increase of the volume of the applied sample to 100 mL lead to the decrease of the adsorbed amount of the analyte, which suggests that the adsorption of indoxyl sulphate is weak and that excessive washing of the column even by aqueous solvents can partially elute the analyte.

Methanol was used as the elution solvent of the first choice. Fractional elution revealed that 2 mL of methanol elute all the analyte. Recovery of this procedure, i.e. (10 ml of indoxyl sulphate, washing solution BR buffer pH 3, elution by 2 ml MeOH) was 105±10

%. However, this procedure was not satisfactory during the measurement with human urine, as the analyte peaks were coupled with the major interferents which were eluted from the column. The fact, that the common concentration of indoxyl suphate in human urine of healthy subject (approximately 1 – 3 μmol L^{-1} [4, 27]) is negligible in comparison with other oxidizable compounds, also contributes to the difficulty of the task.

In attempted to remove the interfering matrix, the washing step was altered: the volume of washing solution was increased to 5 mL and pH was changed to pH 8. The decrease of the interfering peaks was noticeable, but not sufficient. Another option for the improved separation was the decrease of the elution strength of the elution solvent to elute only analyte. Solution containing 5 % and 10 % of methanol served as a series of standalone eluants. In 5 % methanol, the recovery reached 101±10 % and in the case of 10 % methanol the recovery reached 100±10 % .We can conclude that 5 % methanol is satisfactory for elution. Nevertheless, extraction from urine samples proved remaining high concentration of interferents, disabling the perspective of the extraction from the complex sample.

CONCLUSION

Voltammetric methods for the determination of indoxyl sulphate, biomarker of kidney diseases, was developed using an array of carbon composite electrodes and carbon paste electrode.

From the dependence of peak heights on supporting electrolyte composition, a buffer of pH 2 and pH 3 was selected as the optimum medium for CFE and CPE, respectively. The influence of the accumulation time after 5 min of accumulation for both electrodes; thus, accumulation step was not employed for further measurements. Under optimal conditions, concentration dependences were measured; found determination limits were 0.7 μmol L^{-1} for CFE and 1.7 μmol L^{-1} for CPE. The results obtained from measurements with development method were used for comparison of CFE with CPE. Selected working electrodes achieved sufficient sensitivity and accuracy required in screening measurements of indoxyl sulphate [4]. Nevertheless, CFE achieved slightly better analytical results including: lower *LOQ*, better repeatability and sensitivity, during determination of standard of the analyte in comparison to well-known carbon paste electrode. Differences between both electrodes attributed to the difference in shape or in the role of the insulator component in the electrode mixtures were observable.

Developed method was completed by solid phase extraction of indoxyl sulphate from fortified samples of human urine prior to voltammetric determination. However, the used procedures did not reached required results, because urine interferents were still present in the measured solution side by side with the analyte after extraction. Priority for further research is to overcome this problem with unsuccessful preliminary solid phase extraction and find another eluent, then it can be competitive to determination of indoxyl sulphate with aforementioned modern analytical devices methods (HPLC/MS, HPLC/ED), which achieved same or lower limits of quatification [10, 11].

CONFLICT OF INTEREST

The authors confirm that this article content has no conflict of interest.

ACKNOWLEDGEMENTS

This research was realized in the frame of specific university research SVV. Financial support of the Grant Agency of the Czech Republic (project P206/12/G151) is gratefully acknowledged.

REFERENCES

[1] Niwa, T.; Takeda, N.; Tatematsu, A.;Maeda, K. Accumulation of Indoxyl Sulfate, an Inhibitor of Drug-Binding, in Uremic Serum as Demostrated by Internal-Surface Reversed-Phase Liquid-Chromatography. *Clin. Chem.*, **1988**, *34*, 2264-2267.

[2] Agatsuma, S.; Sekino, H.;Watanabe, H. Indoxyl-beta-D-glucuronide and 3-indoxyl sulfate in plasma of hemodialysis patients. *Clin. Nephrol.*, **1996**, *45*, 250-256.

[3] Patel, K.P.; Luo, F.J.G.; Plummer, N.S.; Hostetter, T.H.;Meyer, T.W. The Production of p-Cresol Sulfate and Indoxyl Sulfate in Vegetarians Versus Omnivores. *Clin. J. Am. Soc. Nephrol.*, **2012**, *7*, 982-988.

[4] Duranton, F.; Cohen, G.; De Smet, R.; Rodriguez, M.; Jankowski, J.; Vanholder, R.; Argiles, A.;European Uremic Toxin Work, G. Normal and Pathologic Concentrations of Uremic Toxins. *J. Am. Soc. Nephrol.*, **2012**, *23*, 1258-1270.

[5] Lin, C.J.; Liou, T.C.; Pan, C.F.; Wu, P.C.; Sun, F.J.; Liu, H.L.; Chen, H.H.;Wu, C.J. The Role of Liver in Determining Serum Colon-Derived Uremic Solutes. *PLoS One*, **2015**, *10*.

[6] Leong, S.C.;Sirich, T.L. Indoxyl Sulfate-Review of Toxicity and Therapeutic Strategies. *Toxins*, **2016**, *8*.

[7] Vanholder, R.; Schepers, E.; Pletinck, A.; Nagler, E.V.;Glorieux, G. The Uremic Toxicity of Indoxyl Sulfate and p-Cresyl Sulfate: A Systematic Review. *J. Am. Soc. Nephrol.*, **2014**, *25*, 1897-1907.

[8] Cao, X.S.; Chen, J.; Zou, J.Z.; Zhong, Y.H.; Teng, J.; Ji, J.; Chen, Z.W.; Liu, Z.H.; Shen, B.; Nie, Y.X.; Lv, W.L.; Xiang, F.F.; Tan, X.;Ding, X.Q. Association of Indoxyl Sulfate with Heart Failure among Patients on Hemodialysis. *Clin. J. Am. Soc. Nephrol.*, **2015**, *10*, 111-119.

[9] Filik, H.; Avan, A.A.;Aydar, S. Voltammetric Sensing of Uremic Toxin Indoxyl Sulfate Using High Performance Disposable Screen-Printed Graphene Electrode. *Curr. Pharm. Anal.*, **2016**, *12*, 36-42.

[10] Lagana, A.; Liberti, A.; Morgia, C.;Tarola, A.M. Determination of Indican and Tryptophan in Normal and Uremic Patients by High-Performance Liquid-Chromatography With a New Electrochemical Detector. *Journal of Chromatography*, **1986**, *378*, 85-93.

[11] Shu, C.; Chen, X.J.; Xia, T.Y.; Zhang, F.; Gao, S.H.;Chen, W.S. LC-MS/MS method for simultaneous determination of serum p-cresyl sulfate and indoxyl sulfate in patients undergoing peritoneal dialysis. *Biomed. Chromatogr.*, **2016**, *30*, 1782-1788.

[12] Giebultowicz, J.; Korytowska, N.; Sankowski, B.;Wroczynski, P. Development and validation of a LC-MS/MS method for quantitative analysis of uraemic toxins p-cresol sulphate and indoxyl sulphate in saliva. *Talanta*, **2016**, *150*, 593-598.

[13] Gu, L.Q.; Wang, X.F.; Zhang, Y.Y.; Jiang, Y.; Lu, H.; Bi, K.S.;Chen, X.H. Determination of 12 potential nephrotoxicity biomarkers in rat serum and urine by liquid chromatography with mass spectrometry and its application to renal failure induced by Semen Strychni. *J. Sep. Sci.*, **2014**, *37*, 1058-1066.
[14] Yosypchuk, B.; Barek, J.;Fojta, M. Carbon powder based films on traditional solid electrodes as an alternative to disposable electrodes. *Electroanalysis*, **2006**, *18*, 1126-1130.
[15] Libansky, M.; Zima, J.; Barek, J.;Dejmkova, H. Construction of an Electrochemical Cell System Based on Carbon Composite Film Electrodes and its Application for Voltammetric Determination of Triclosan. *Electroanalysis*, **2014**, *26*, 1920-1927.
[16] Rumlova, T.; Jiranek, I.; Vyskocil, V.;Barek, J. Electrochemical study of 5-nitroquinoline using carbon film electrode and its determination in model samples of drinking and river water. *Mon. Chem.*, **2016**, *147*, 153-158.
[17] Smejkalova, H.;Vyskocil, V. Large-Surface Carbon Film Electrode - A Simple Sensor for Voltammetric Determination of Electrochemically Reducible Organic Compounds. *Chem. Listy*, **2014**, *108*, 264-270.
[18] Libansky, M.; Zima, J.; Barek, J.;Dejmkova, H. Voltammetric determination of homovanillic acid and vanillylmandelic acid on a disposable electrochemical measuring cell system with integrated carbon composite film electrodes. *Mon. Chem.*, **2016**, *147*, 89-96.
[19] Adams, R.N. Carbon paste elctrode. *Anal. Chem.*, **1958**, *30*, 1576-1576.
[20] Svancara, I.; Vytras, K.; Kalcher, K.; Walcarius, A.;Wang, J. Carbon Paste Electrodes in Facts, Numbers, and Notes: A Review on the Occasion of the 50-Years Jubilee of Carbon Paste in Electrochemistry and Electroanalysis. *Electroanalysis*, **2009**, *21*, 7-28.
[21] Parvin, M.H. Simultaneous Determination of Ascorbic Acid, Dopamine and Uric Acid, at a Graphene Paste Electrode Modified with Functionalized Graphene Sheets. *Electroanalysis*, **2015**, *27*, 1394-1402.
[22] Ensafi, A.A.; Izadi, M.;Karimi-Maleh, H. Sensitive voltammetric determination of diclofenac using room-temperature ionic liquid-modified carbon nanotubes paste electrode. *Ionics*, **2013**, *19*, 137-144.
[23] Svancara, I.; Metelka, R.;Vytras, K., Sensing in Electroanalysis, in: Vytras, K., Kalcher, K. (Eds.), Univ. Pardubice, Pardubice 2005, pp. 7-18.
[24] Inczedy, J.; Compendium of Analytical Nomenclature (Definitive Rules 1997). Blackwell Science, Santa Fe, 1998.
[25] Enache, T.A.;Oliveira-Brett, A.M. Pathways of Electrochemical Oxidation of Indolic Compounds. *Electroanalysis*, **2011**, *23*, 1337-1344.
[26] Zima, J.; Svancara, I.; Barek, J.;Vytras, K. Recent Advances in Electroanalysis of Organic Compounds at Carbon Paste Electrodes. *Critical Reviews in Analytical Chemistry*, **2009**, *39*, 204-227.
[27] Liabeuf, S.; Desjardins, L.; Massy, Z.A.; Brazier, F.; Westeel, P.F.; Mazouz, H.; Titeca-Beauport, D.; Diouf, M.; Glorieux, G.; Vanholder, R.; Jaureguy, M.;Choukroun, G. Levels of Indoxyl Sulfate in Kidney Transplant Patients, and the Relationship With Hard Outcomes. *Circ. J.*, **2016**, *80*, 722-730.

9. Appendix III

Basic Electrochemical Properties of Sputtered Nanostructured Gold Film Electrodes

Libánský Milan, Zima Jiří, Barek Jiří, Řezníčková Alena, Švorčík Václav, Dejmková Hana

Electrochimica acta

Submitted, Year 2017

Basic electrochemical properties of sputtered nanostructured gold film electrodes

Milan Libansky[a], Jiri Zima[a], Jiri Barek[a], Alena Reznickova[b], VaclavSvorcik[b], and Hana Dejmkova[a]*

[a]*Charles University, Faculty of Science, University Research Centre "Supramolecular chemistry", Department of Analytical Chemistry, UNESCO Laboratory of Environmental Electrochemistry, Albertov 6, CZ 128 43, Prague, Czech Republic*

[b]*University of Chemistry and Technology, Department of Solid State Engineering, Technicka 5, CZ 16628, Prague, Czech Republic*

**Corresponding author*

E-mail address: jiri.barek@natur.cuni.cz (Jiri Barek)

Abstract

Gold nanolayers made by physical vapour deposition are well known and commonly used for many biophysical and material applications. However, their use for fabrication of working electrodes for electroanalytical purposes is less common. This paper focuses on the use of sputtered gold roughened nanolayers as working gold nanostructured film electrodes.

Gold 80 nm thin nanostructured films (GNF) were sputtered onto three types of treated thin (50 μm) PTFE substrates and applied as working electrodes. Important parameters of electrodes were characterized; the properties of electrode surface were examined and their behaviour towards measurements of standards was tested. The characterization of gold nanostructured film electrodes was carried out by examination of the electrode reaction of standard redox probes (ferrocyanide/ferricyanide, hydroquinone/benzoquinone) in different types of base electrolytes (buffers, KCl, KNO_3, H_2SO_4), by exploration of the electrode

surface by scanning electron microscopy and atomic force microscopy accompanied by elementary analysis and contact angle measurements. The testing of electrodes was complemented by calculations of their real surface areas from Randles-Sevcik equation. The applicability of the electrodes was verified by differential pulse voltammetric (DPV) determination of hydroquinone (HQ) as a one of the most commonly used standards of organic environmental pollutants. All results were compared to conventional bulk gold electrode.

Keywords: Gold film electrodes, Nanostructured electrodes, Gold sputtering, Grafting.

1. Introduction

Nanostructures are classified according to IUPAC as structures/electrodes made of nanoparticles whose at least one dimension falls in the range 1–100 nm [1]. The unique chemical and electrical properties of nanostructured electrodes depend more strongly on the size of nanoparticles and on their density rather than on the nature of the used material [2]. Nanostructured electrodes have received considerable attention and extensive development over the past few years in a broad variety of areas including electroanalytical chemistry, physical chemistry etc., where the interfacial nature of measurements favours the fabrication of miniaturized analytical devices. In this context, nano-thin-film technology is of great utility [3].

The properties of nanostructured electrodes are influenced by their fabrication process. In the case of nanostructured gold electrodes, many different manufacturing processes were developed. The gold nanostructured electrodes from gold nanoparticles (AuNPs) can be prepared by utilizing self-assembly of AuNPs at the surface of thiol spacer which is self-assembled at common bulk electrode serving as a conductor [4]. Other possible approaches to

the fabrication of gold nanostructured electrode are *in-situ* or *ex-situ* plating of AuNPs from the solution of $HAuCl_4$ onto selected substrate under certain potential (electrografting) [5, 6]. However, these procedures are very time consuming or require large amounts of chemicals and user experience. The deposition of AuNPs can be followed by deposition of mercury on the surface of substrate bulk electrode; deposition of AuNPs from the concentrated solution of $HAuCl_4$ can be followed by subsequent deposition of mercury from the concentrated solution of $Hg(NO_3)_2$ resulting in the gold nanostructured amalgam film electrode (hybrid) [7]. In the case of nanostructured gold film electrodes made by electrografting it is complicated to ensure that the thickness and shape of the gold layer will be completely identical for each thus prepared electrode, especially in nanoscale. To avoid this problem, gold nanostructured screen-printed electrodes can be used. During the preparation of nanostructured gold screen-printed electrodes, the electrode ink is applied on a suitable substrate, mostly made of plastic or ceramic and it is easier to ensure the same thickness for all electrodes. Another advantage of these film electrodes is very low cost in comparison with common conventional bulk electrodes; thus a new electrode can be used for each single measurement (disposable electrodes). Moreover, traditional three-electrode configuration printed on the same strip is also insurmountable advantage of any screen-printed electrodes [8]. Modern approach to fabrication of gold nanostructured film electrodes is physical vapour deposition of Au atoms using sputtering method. This fabrication process can be used in the case of the necessity to use a non-conventional reference electrode or different electrode arrangement, which cannot be satisfied when using screen printed electrode.

Advantage of sputtering lies in simplicity, reproducibility, and low price of final products. Moreover, it is considered as pollution free (“green”) method. Disadvantage of gold sputtering is that gold is one of the most inert metals and the adhesion between AuNP and a polymer substrate is poor. Film adhesion and electrical contact properties are strongly

influenced by the interface structure. Film adhesion can be changed when electrodes are exposed to some types of organic solvents or concentrated acids. Several modification techniques (physical, chemical or their combination) have been suggested for enhancing metal to polymer adhesion, for example treatment by plasma [9, 10] or fixing of AuNPs by thiol groups containing spacer [4, 9, 11].

Universally, nanostructured gold film electrodes offer unique physicochemical properties and advantages such as high surface-to-volume ratio, surface charge, possible change of the hydrophobicity or hydrophilicity, easy miniaturization and change of shape; they can be chemically modified and mechanically or electrochemically pre-treated to further improve their native properties [12]. The electrode material can be modified by addition of another nanoparticle (carbon or metal nanoparticles). Combination of two nanomaterials with different properties can provide a unique hybrid nanoparticle electrode with new properties [13]. In addition to that, it is possible to modify the electrode material by inorganic complexes [14], polysaccharides (chitosan) [15], conductive polymers [16], etc., if any special application is required.

Nanostructured gold electrodes made by various techniques has been used as voltammetric sensors for the determination of inorganic [17] and organic analytes [18], as well as metabolites of human body processes [19-21], pharmaceuticals [6, 22, 23] and for voltammetric studies of DNA [24]. Nanostructured gold electrodes are usable in a wide range of chemical disciplines such as impedance spectroscopy and chronopotentiometry in analytical chemistry [25], as an electrocatalytic mediator of luminescence in spectroscopy [26] or as biosensors in biochemistry [27, 28]. It is necessary to mention special usability of these electrodes in supercapacitors, in microelectronics and photovoltaics [29, 30].

This study is focused on the electrochemical characterization of three types of gold nanostructured film electrodes (GNFE) made by sputtering method which represent further

areas of applicability of gold nanomaterials and a new approach to the use of sputtered electrodes in analytical chemistry. Especially in the future, these GNFE should be used for the determination of oxidisable biomarkers in urine and of environmental pollutants in water as a final stage of next researches.

2. Experimental

2.1 Chemicals

The electrochemical behaviour of three types of nanostructured gold electrodes in electrolytes was studied using 0.1 mol L^{-1} sulfuric acid, 0.1 mol L^{-1} potassium chloride, 0.1 mol L^{-1} potassium nitrate, and 1 mmol L^{-1} potassium hexacyanoferrate in 1 mol L^{-1} potassium nitrate (all p.a. grade and obtained from Lach-ner, Czech Republic) as testing solutions.

Britton-Robinson (BR) buffers serving as testing medium and supporting electrolyte were prepared by mixing 0.2 mol L^{-1} solution of sodium hydroxide (Penta, Czech Republic) with a solution of phosphoric acid, boric acid and acetic acid (all Lach-ner, Czech Republic), 0.04 mol L^{-1} each. All chemicals used for buffer preparation were of analytical grade purity and were used without further purification.

The stock solution of 1 mmol L^{-1} hydroquinone (HQ) (Lach-ner, Czech Republic) was prepared by dissolving the exact amount of the substance in deionized water (Milli-Q-Gradient, Millipore, USA) and it was kept in the refrigerator. This solution was freshly prepared every week to avoid degradation due to spontaneous oxidation to benzoquinone.

2.2 Preparation of gold nanostructured film electrodes

For the fabrication of nanostructured gold film electrodes, 50 μm thick foil of polytetrafluoroethylene (PTFE, density 2.2 g cm^{-3}, Goodfellow, United Kingdom) was used as

a nonconductive substrate. PTFE substrate was chosen for its thermostability up to 300°C and robustness during measurement with organic solutions and good dielectrically properties. The gold nanolayers were deposited onto a patterned PTFE from Au target (purity 99.99 %, Safina, Czech Republic) in DC argon atmosphere (Ar, purity ≥99.996 %, Siad, Czech Republic). Gold nanolayers were deposited on three types of PTFE: pristine PTFE (GNFE-Pristine), plasma treated (GNFE-Plasma) and plasma treated and subsequently grafted with biphenyl-4,4′-dithiol (GNFE-BPD). The modification by plasma was performed by diode plasma discharge in etching mode on Balzers SCD 050 device (Pfaeffikon Balzers, Liechtenstein) for 240 s. DC Ar plasma treatment was performed under following conditions: discharge power of 8.3 W, Ar flow ~0.3 $dm^3 s^{-1}$, working pressure of 10 Pa, 50 mm distance between the electrode and the sample, area of electrodes 48 cm^2 and chamber volume about 1.0 dm^3. Subsequently, the PTFE was modified by 24 hours spontaneous grafting in methanolic solution of 0.1 mmol L^{-1} biphenyl-4,4′-dithiol (Sigma-Aldrich, USA) for improving the adhesion of gold nanolayers (if this process was required).

After BPD grafting, samples were rinsed with p.a. methanol. The deposition of gold was accomplished by sputtering of gold from Au target through contact mask on Balzers SCD 050 device (Pfaeffikon Balzers, Liechtenstein) in sputtering mode. Au nanolayers were prepared under following conditions: discharge power of 15 W (current 40 mA), working pressure of 5 Pa, deposition time 200 s.

Deposition mask parameters were: round shape head with 3 mm in diameter with connected tail 15 mm long and 1 mm thick; the tail was used for connection to potentiostat. The round shape head was isolated from the tail by non-conductive lacquer to ensure uniform electrode area.

2.3 Apparatus

Voltammetric measurements were performed with portable potentiostat PalmSens (Palm Instruments, Netherlands), controlled by PSTrace4.8 software. Voltammetric measurements were carried out with three types of nanostructured gold film electrodes with geometric area 7.1 mm^2 (Ø = 3 mm) (described in Section 2.2) or gold bulk electrode with the same geometric area (Metrohm, Czech Republic). A gel leakless Ag/AgCl reference electrode (3M KCl, Cypress Systems, Chelmsword, USA), to which all potentials values are referred, was used to avoid contamination by Cl^- ions from reference electrode. Platinum wire was used as an auxiliary electrode.

The pH of the solutions was measured with a pH meter Jenway 3510 (Jenway, United Kingdom) with a combined glass electrode.

The morphology of the prepared structures was investigated using scanning electron microscopy (SEM, Tescan Lyra dual beam microscope; Tescan, Czech Republic). Elemental composition was performed using an energy dispersive X-ray spectroscopy (EDS, analyzer X-MaxN, 20 mm^2 SDD detector, Oxford Instruments, United Kingdom). The samples were attached by carbon conductive tape to avoid sample charging. SEM-EDS and SEM measurements were carried out using accelerating voltages 10 kV and 2 kV, respectively.

The surface morphology and layer thickness was examined with atomic force microscope Dimension ICON (Bruker, USA) using ScanAsyst mode in Air. Silicon tip on nitride cantilever with spring constant 0.4 $N \cdot m^{-1}$ was used. NanoScope Analysis software was applied for data processing. The mean roughness values (Ra) represents the average deviations of the distance in the direction of the normal vector from the centre plane of the sample. Scan size was 2x2 μm^2.

Static contact angles (CA) of distilled water, characterizing structural and compositional changes caused by the gold deposition, were measured at room temperature at

two samples and at seven positions using a drop shape analyzer (DSA 100, KRÜSS, Germany). Drops of 2.0 ± 0.2 µl of water were deposited on the tested samples. Contact angles were evaluated using the DSA4 software.

2.4 Procedures

Parameters of the DPV potential program were: 0.1 s pulse width, 20 ms sampling time, 50 mV pulse height, 20 mV s^{-1} scan rate, and potential range from -100 to 1000 mV. Cyclic voltammetry (CV) was performed in the potential range from -100 mV to 1000 mV with 50 mV s^{-1} scan rate. Volume of the solutions applied on the surface of electrodes (head of electrode) for the measurement was 10 µL. All measurements were repeated five times and each measurement was performed with a new nanostructured gold film electrode, unless stated otherwise. In the case of gold bulk electrode, the surface of the electrode was renewed by polishing (30 s) on alumina slurry after each measurement. Calibration dependences were evaluated by the least squares linear regression method. The limits of quantification (*LOQ*) were calculated as the concentration of the analyte which gave a signal ten times higher than the standard deviation of the lowest evaluable concentration [31].

3. Results and discussion

3.1 Surface analysis

Morphology and chemical composition of the surface of the prepared GNFE was examined by scanning electron microscopy (SEM) combined with energy dispersive spectroscopy (EDS). SEM scans of GNFE are shown in Fig. 1. All types of GNFE exhibited homogeneous gold layer; however, small differences in coverage were observable. In the case of GNFE-Pristine, it is obvious that the gold layer exhibited extensive disruptions, gold layer was tattered with exposed PTFE surface (see upper part of Fig. 1A) and adhesion of gold layer was the weakest. In the case of other two electrodes (Fig. 1B, 1C), the gold layers were

more compact with higher adhesion to substrate. GNFE-Plasma exhibited the strongest adhesion of gold layer from all GNFEs; this corresponds to the higher levels of surface concentration of Au obtained by EDS measurement (Table 1). Besides, corrugation after the plasma treatment can be observed in Fig. 1B, 1C.

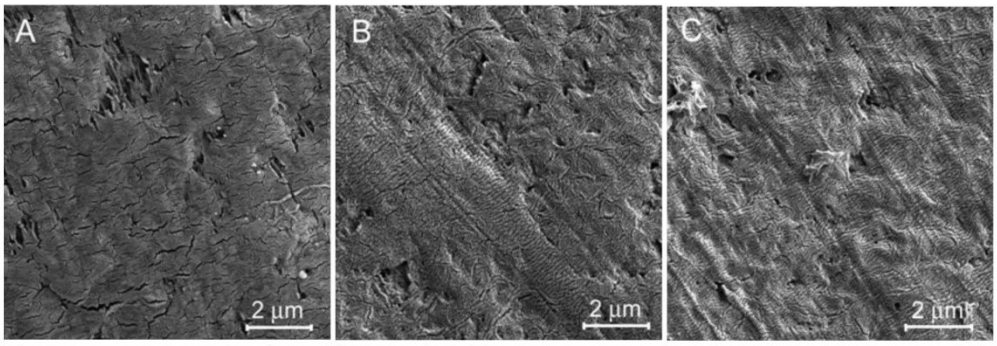

Fig. 1. SEM scans of (A) GNFE-Pristine, (B) GNFE-Plasma, and (C) GNFE-BPD.

Table 1 Element concentration (w %) determined by EDS analysis of surface of GNFE-Pristine, GNFE-Plasma, GNFE-BPD.

GNFE	[a] w_{Au}/%	w_C/%	w_F/%
Pristine	80.9±0.2	10.7±0.2	8.4±0.1
Plasma	84.4±0.2	9.9±0.2	5.7±0.1
BPD	82.9±0.2	9.7±0.2	7.4±0.1

[a]Element mass concentration ± standard deviation of the mean value

The results of AFM examination of the surface morphology of 80 nm thick Au layers of all types of GNFE are illustrated in Fig. 2. It is known that pristine PTFE exhibits different surface morphology and roughness than PTFE treated by plasma and after BPD treatment; the roughness increases [32]. This was confirmed by measured values of roughness of GNFE compared to values of pristine PTFE obtained during previous measurements of the same scientific group [9]. In the case of GNFE-Pristine (R_a = 16.7 nm), deposited gold layer caused smoothing and slight decrease of roughness compared to pristine PTFE (R_a = 17.7 nm). In the

case of GNFE-Plasma, the gold layer copied the laminar structure of the surface treated by plasma with R_a = 19.2 nm. GNFE-BPD exhibited a maximum surface roughness with R_a = 26.5 nm, because besides roughness caused by the plasma treatment and by grafting of BPD on the surface of PTFE, noticeable depressions can be seen caused by etching away low molecular weight oxidized structures of PTFE (LMWOS) by treatment of methanolic solution of BPD [10, 33] (Fig. 2C).

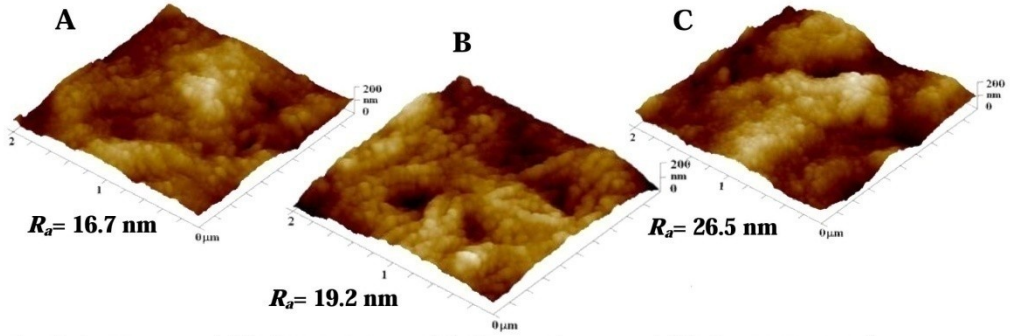

Fig. 2. AFM scans of (A) GNFE-Pristine, (B) GNFE-Plasma, and (C) GNFE-BPD with surface roughness in nm (R_a).

The results of measurement of water contact angle (surface wettability) follow the same trend as results of measurement of surface roughness. Values of water contact angles were 106.9° ± 2.2° for GNFE-Pristine, 107.7° ± 2.2° for GNFE-Plasma, and 110.5° ± 1.5° for GNFE-BPD. The small differences in those values are the function of surface roughness and chemical composition of the layer [9]. On the other hand, all values are not statistically significantly different and should not affect ways how to apply the aqueous sample on the surface of electrodes.

3.2 Electrochemical behaviour in electrolytes

The voltammetric behaviour of three GNFEs in several commonly used electrolytes was examined to find out, if there are any limitations regarding the electrolytes composition

or whether any interferents are present due to the manufacturing process. These electrolytes were: potassium chloride, potassium nitrate, sulphuric acid and BR buffers pH 2, 7 and 12. All the obtained results were compared with a measurement on gold bulk electrode.

Recorded voltammograms in anodic potential window can be seen in Fig. 3 and Fig. 4; maximum accessible potentials are summarized in Table 2. Typical electrochemical behaviour of gold electrodes was observed during measurement in acidic medium (H_2SO_4 and BR pH 2). In the case of GNFE, peaks of alpha and beta gold oxides have a lower oxidation potential (0.5 and 0.7 V) than on gold bulk electrode with peaks potentials at 1.1 and 1.3 V. It was probably caused by the strongly acidic environment which disrupted thin nanolayer of gold nanostructured electrode resulting in easier formation of the gold oxides [34, 35]. Acidic medium coupled with high inserted oxidation potential results in the decrease of the adhesion of thin nanolayer and fissures leading to the exposure of the surface of PTFE.

In alkaline medium (see BR buffer pH 12, Fig. 4) the conjunction of peaks of gold oxides was observed on all types of gold electrodes (0.6 V). On the other hand, peak of gold oxides was lower and the potential window was wider in the case of gold bulk electrode. Obviously, susceptibility to oxidation of the surface of gold bulk electrodes is generally lower.

Table 2 Maximal efficient potential (V) for anodic oxidation during the measurement on gold working electrodes in selected supportingelectrolytes.

	E/V					
Electrode	KCl	KNO_3	H_2SO_4	BR pH 2	BR pH 7	BR pH 12
GNFE - Pristine	0.8	0.9	0.4	0.4	0.8	0.5
GNFE - Plasma	0.8	0.9	0.4	0.4	0.9	0.5
GNFE - BPD	0.7	0.9	0.4	0.4	0.9	0.5
Bulk	0.8	1.1	1.1	1.1	1.1	0.5

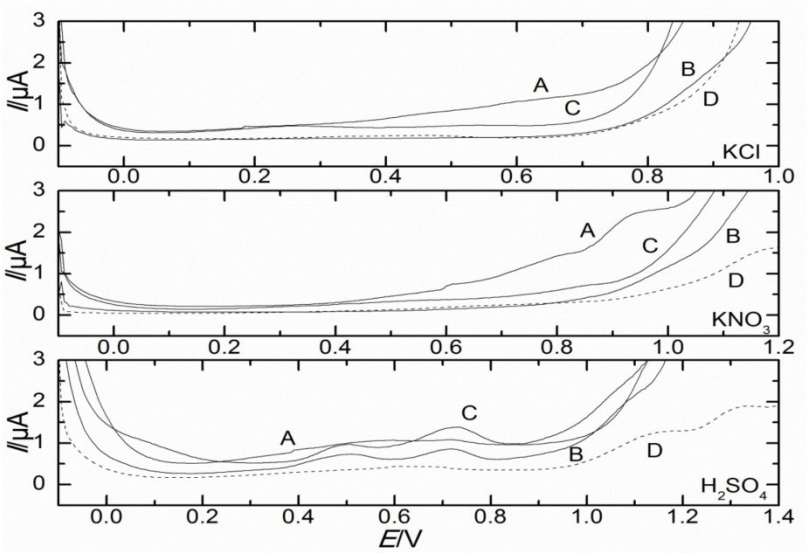

Fig. 3. DP voltammograms of selected electrolytes measured on (A) GNFE-Pristine, (B) GNFE-Plasma, (C) GNFE-BPD, and (D) gold bulk electrode.

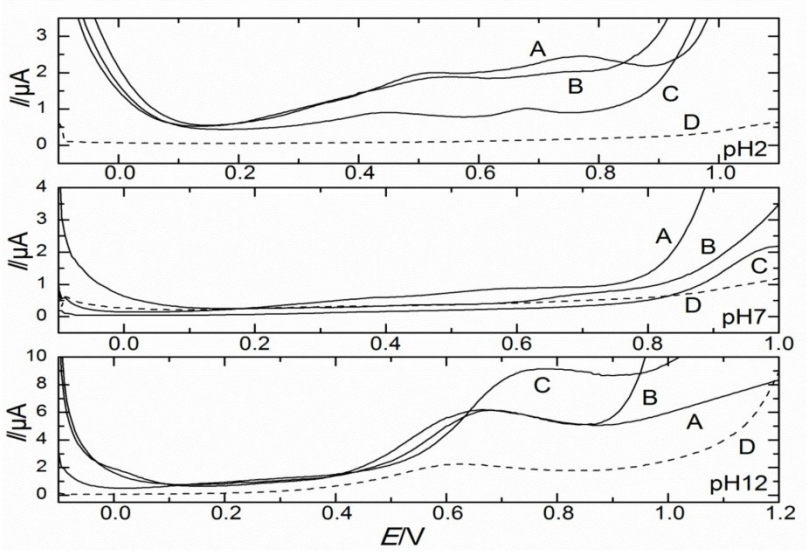

Fig. 4. DP voltammograms of BR buffer of various pH measured on (A) GNFE-Pristine, (B) GNFE-Plasma, (C) GNFE-BPD, and (D) gold bulk electrode.

As the consequence, a suitable media for voltammetric measurements with GNFE were potassium chloride, potassium nitrate and BR buffer pH 7, where peaks of gold oxides merged with the end of potential window and potential windows were wider. Generally, the gold oxides can be removed by polishing of the electrode (bulk electrodes), chemical cleaning of the electrode with organic or inorganic solvents or by fast cyclic voltammetric scanning in the wide range of positive and negative potentials (electrochemical cleaning) [36]. In our case, only gold bulk electrode was mechanically renewed, which was relatively easy. GNFE were not renewed due to low mechanical robustness and the electrodes were used as a disposable sensor. If it is necessary to renew GNFE, it might be possible to use chemical cleaning with concentrated ethanol.

For further measurements, potassium nitrate and BR buffer pH 7 were selected as optimum media.

During the measurement of potential windows widths, cathodic part of potential window was not evaluated. In the case of the measurement in the negative potential range, it would be necessary to find a way to successfully remove oxygen from the measured solution, which is complicated by a small volume of used sample (10 μL). Probably classical method based on working under nitrogen atmosphere can be used.

3.3 Electrochemical behaviour of ferrocyanide/ferricyanide redox system

Electrochemical behaviour of GNFE was studied by cyclic voltammetry of potassium hexacyanoferrate in potassium nitrate. Potassium hexacyanoferrate is the most commonly used probe for the characterization of electrochemical behaviour of electrodes in aqueous solutions. Repeatability of measurements, reversibility of one electron reaction (Table 3) and the dependence of electrode response on scan rate (Fig. 5, Table 4) was investigated and

complemented by calculations of real surface areas of electrodes from Randles-Sevcik equation (Table 3) [37].

Voltammetric studies at different scan rates were performed in 1 mmol L^{-1} potassium hexacyanoferrate in 1 mol L^{-1} potassium nitrate at scan rates from 10 to 500 mV s^{-1}. Repeatability of measurements, reversibility of one electron reaction and real surface areas of electrodes were determined from 10 CV measurements at scan rate 50 mV s^{-1}.

Voltammetric studies resulted in a linear relation between the anodic peak current values and the square root of scan rate (Fig. 5). In comparison to gold bulk electrode, all types of GNFE showed lower repeatability of heights of the peaks in the measured range of scan rates (Table 3) and higher standard deviation of the regression line (SD, Table 4).

Table 3 Parameters of GNFE and gold bulk electrode obtained from CV measurements of potassium hexacyanoferrate in potassium nitrate.

Electrode	ΔE_{peak}/mV	I_A/I_C	$RSD_{Anod.}$/%	$RSD_{Cath.}$/%	[a]Surface $Area_{real}$/mm^2
GNFE - Pristine	100±5	1.2	4.5	3.7	7.4±0.5
GNFE - Plasma	71±3	1.0	1.1	1.2	8.4±0.2
GNFE - BPD	98±10	1.0	6.7	8.5	7.3±0.5
Bulk	75±10	0.9	2.8	1.9	7.1±0.2

[a]Active surface area ± calculated confidence intervals.

Table 4 Parameters of dependences of peak heights of potassium hexacyanoferrate in potassium nitrate on square root of scan rate measured by CV at GNFE and gold bulk electrode.

Electrode	Slope/μA $mV^{-1/2}$ $s^{1/2}$	Intercept/μA[a]	SD/μA[a]	R^2
GNFE - Pristine	1.8	-2.3	0.5	0.996
GNFE - Plasma	1.9	-1.1	0.4	0.998
GNFE - BPD	1.1	1.3	0.4	0.993
Bulk	0.7	0.2	0.1	0.999

[a]The standard deviation of the regression line (random errors in *y*-direction), intercept is statistically significantly different from zero (a = 0.05).

However, similar determination coefficient confirmed the linearity of the obtained curves. Slopes of the dependences of peak heights on the square root of scan rate for all types of GNFE were higher than those slopes at gold bulk electrode. Nevertheless, order of values of slopes did not follow expected trend (plasma>BFD>pristine). The highest value of those slopes was found at GNFE-Plasma, which corresponded to the highest amount of electroactive gold material (Table 1) on the surface of working electrode and to higher active area of the electrode. But GNFE-Pristine should have the lowest value of the slope, if it depends only on the concentration of electroactive material. However, this assumption has not been fulfilled and the results are dependent on the type of selected probe (see next chapter). Difference in the slope of GNFE-Pristine is probably caused by the different kinetics of electrochemical reaction on the surface of electrode with lower adhesion and homogeneity of gold nanolayer (section 3.1) but full explanation is unclear yet.

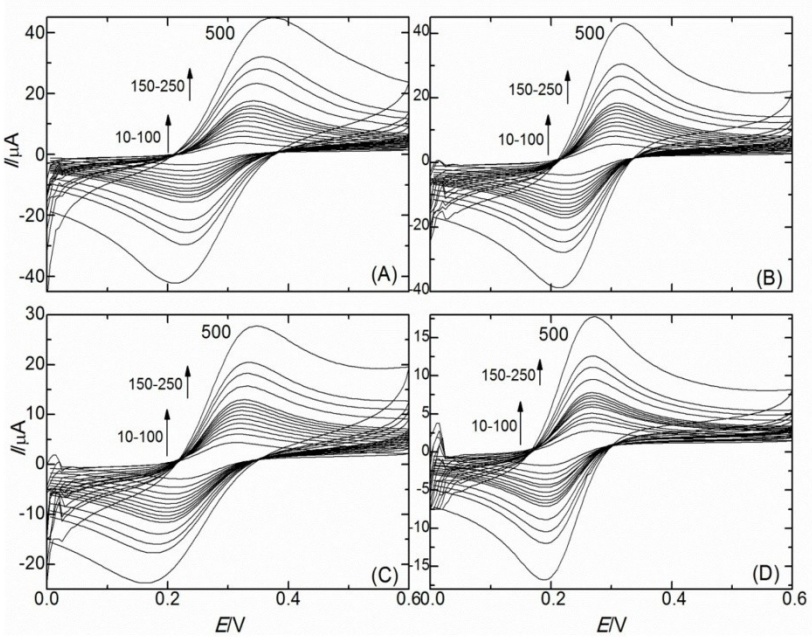

Fig. 5. Cyclic voltamogramms of 1 mmol L^{-1} potassium hexacyanoferrate in BR Buffer pH 7 measured on (A) GNFE-Pristine, (B) GNFE-Plasma, (C) GNFE-BPD, and (D) gold bulk electrode at different scan rates (from 10 to 500 mV s^{-1}).

Otherwise, the values for ΔE_p were higher than predicted for typical Nernstian reversible one electron reaction (59 mV), but the values did not exceed commonly obtained values on gold electrodes [36]. Repeatability of all types of GNFE was from 1.1 % to 8.5 % for the height of anodic peak as well as cathodic peak. At GNFE-Plasma the obtained repeatability was better than for other two GNFE, which should correspond with the highest amount of electroactive material, the most homogenous Au layer, and therefore stable fast electron transfer. The kinetics of the reaction was fast and almost reversible, which was proved by values for the ratio I_A/I_C calculated as the average for all measurements (Table 3). Obtained results for GNFE-Pristine and GNFE-BPD were mainly influenced by weaker adhesion (in comparison to GNFE-Plasma) of gold nanoparticles to the surface of PTFE,

where the gold layers were not fully homogeneous and exhibited smaller or bigger fissures, as described in Section 3.1 (fig. 1A, 1C). It led to an increase of electric resistance and impairment of the reversibility of electrochemical reaction.

Active areas of all types of GNFE were calculated from the Randles–Sevcik equation (Table 4),

$$I_p = 2.69\times10^5 n^{3/2} A D_0^{1/2} v^{1/2} c_o$$

where I_p is the anodic peak current, n is the number of exchanged electrons, A is the active electrode area in cm^2, D_0 is the diffusion coefficient for potassium hexacyanoferrate in potassium nitrate, v is the scan rate (50 mV s^{-1}) and c_0 is the concentration of potassium hexacyanoferrate (mol mL^{-1}).

The diameter of all used electrodes was 3 mm; therefore, their geometric area was 7.1 mm^2. Active areas ± confidence intervals 7.4 ± 0.5 mm^2, 8.4 ± 0.2 mm^2, 7.3 ± 0.5 mm^2 were calculated for GNFE-Pristine, GNFE-Plasma, and GNFE-BPD, respectively. In the case of GNFE-Plasma, the increase of active area by plasma treatment was observed; otherwise, the calculated active areas of other GNFEs were not statistically significantly different in agreement with obtained values and order of slopes (mentioned above). It is necessary to mention that the electrochemical reaction is almost reversible; however, Randles-Sevcik equation requires fully reversible, ideal parameters and behaviour of electrochemical system [36]. This requirement was almost satisfied, so the deviations from the ideal behaviour are noticeable in resulting calculated values of confidence interval and it also affected the overall analytical performance of resulting devices. Nevertheless, all obtained results demonstrated acceptable usability of sputtered GNFE in comparison with gold bulk electrode.

3.4 Electrochemical behaviour of HQ/BQ redox system

Electrochemical behaviour of GNFE towards a model organic probe was studied by cyclic voltammetry of hydroquinone in BR buffer pH 7. Hydroquinone was chosen as an organic compound representing typical environmental pollutant [38]. Electrochemical behaviour including dependence of electrode response on scan rate (Fig. 6, Table 5), and repeatability of measurements of heights of anodic and cathodic peaks with reversibility of two electron reaction (Table 6) was investigated.

Table 5 Parameters of dependences of peak heights of hydroquinone in BR buffer pH 7 on square root of scan rate measured by CV at GNFEs and gold bulk electrode.

Electrode	Slope/μA $mV^{-1/2}$ $s^{1/2}$	Intercept/μA[a]	SD/μA[b]	R^2
GNFE - Pristine	2.5	2.8	0.5	0.998
GNFE - Plasma	1.6	1.7	0.6	0.995
GNFE - BPD	2.1	1.7	0.7	0.996
Bulk	1.2	2.1	0.9	0.991

[a]Intercept is statistically significantly different from zero (a = 0.05), [b]the standard deviation of the regression line (random errors in *y*-direction).

Table 6 Parameters hydroquinone/benzoquinone system at GNFEs and gold bulk electrode obtained from CV in BR buffer pH 7.

Electrode	ΔE_{peak}/mV	I_A/I_C	$RSD_{Anod.}$/%	$RSD_{Cath.}$/%
GNFE - Pristine	428±5	1.1	3.8	3.8
GNFE - Plasma	451±10	1.2	4.0	3.8
GNFE - BPD	455±5	1.1	6.8	7.3
Bulk	248±5	1.1	3.2	3.3

Voltammetric studies at different scan rates were performed in 1 mmol L^{-1} hydroquinone in BR buffer pH 7, where HQ (pK_a = 10) exists in protonated form [39] at scan

rates from 10 to 500 mV s^{-1}. Repeatability of measurements and reversibility of two electron reaction were determined from 10 CV measurements at 50 mV s^{-1} scan rate.

Voltammetric studies resulted in a linear relation between the anodic peak current values and the square root of scan rate with determination coefficient higher than 0.99 (Table 5) indicating the diffusion behaviour without adsorption (Fig. 6). Therefore, the oxidation of hydroquinone is a simultaneous two-electron transfer process leading to benzoquinone, which is remarkably quasireversible under many conditions at most solid electrodes. Only at the pH extremes the HQ/BQ redox system is fairly reversible [36]. The relationships of log I_p vs log v were constructed (not shown) and the slope values about 0.45 for all electrodes were close to the theoretical value of 0.5, which proved again that the electrode reaction was a diffusion controlled process with non-reversible behavior.

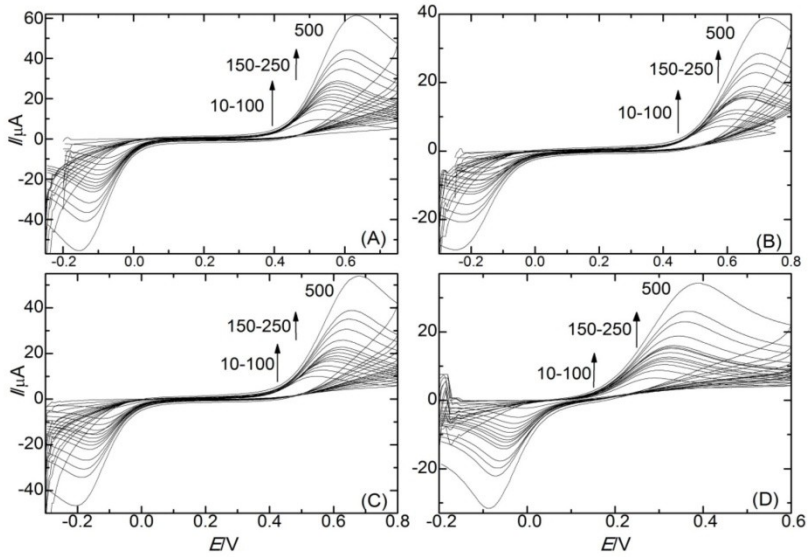

Fig. 6. Cyclic voltamogramms of 1 mmol L^{-1}hydroquinone in 1 mol L^{-1} potassium nitrate measured on (A) GNFE-Pristine, (B) GNFE-Plasma, (C) GNFE-BPD, and (D) gold bulk electrode at different scan rates (from 10 to 500 mV s^{-1}).

Slopes of the dependencies at all types of GNFE were higher than the slopes at gold bulk electrode, nevertheless, the order of values of slopes did not follow expected trend of results and also the trend in the measurement of ferro/ferri redox system (Table 3) was not the same. These results indicate diversity of behaviour of organic and inorganic probes and molecular size of probes with chosen electrolyte can influence electrochemical behaviour of the system on the electrode surface (HQ is three times smaller molecule than ferrocyanide), but full explanation is unclear yet and this problem needs further research.

The effect of passivation during repeated measurements was not observed. On the other hand, backward reduction peak was 10 % lower than oxidation peak (I_A/I_C, Table 6); it points to EC mechanism of the reaction and to the involvement of electrochemical side reactions where different product is formed [40]. Repeatability of all types of GNFE was from

3.8 % to 7.3 % for the height of anodic peak as well as cathodic peak; these results are comparable to the performance of gold bulk electrode.

The peak-to-peak separation values (ΔE_p) were higher than predicted for Nernstian reversible simultaneous two electron reaction (30 mV). On all types of GNFE, a pair of well-defined redox peaks appeared with the ΔE_p from 430 to 450 mV. Bulk electrode exhibited the best reversibility and smaller peak-to-peak separation with 250 mV difference. This smaller peak potential difference can be attributed to the most compact gold material of bulk electrode without disruptions with low value of electric resistance [36]. Another explanation was provided by Compton et al.; it can be caused by low value of k^0 (standard electrochemical rate constant) and α (transfer coefficient describing symmetry between the forward and reverse electron transfer steps), when electrochemical behaviour is not directly related by the Nernst equation. The current behaviour may be described in terms of Butler-Volmer equation then. Hence, it was necessary to measure with relatively large overpotential of the GNFE to provide sufficient energy for the redox reaction [40].

3.5 Concentration dependence of hydroquinone

To explore the possible application of the proposed GNFE in determination of oxidisable environmental pollutant, DPV concentration dependences of hydroquinone were investigated in the concentration range from 10 to 100 μmol L^{-1} (Table 7). The oxidation peak currents of HQ increased linearly with the concentration. Coefficients of determination and variability of all GNFE were similar and not statistically significantly different. Values of intercept of GNFE-Pristine and GNFE-BFD refer to a presence of side reaction or impurities in solution. Repeatability was 9 % for GNFE-Pristine, 7 % for GNFE-Plasma and 11 % for GNFE-BPD for the lowest measured concentration in the calibration curve (n = 10). Low value of slope and high value of repeatability explains higher LOQ in the case of GNFE-BPD.

Achieved quantification limits of hydroquinone were 4.3 μmol L^{-1} for GNFE-Pristine, 4.2 μmol L^{-1} for GNFE-Plasma, and 9.0 μmol L^{-1} for GNFE-BPD, In comparison with other DPV determinations on various nanostructured gold electrodes and bulk electrodes [41, 42], developed GNFE offer higher LOQ and it is necessary to improve structure and fabrication process to obtain more compact gold layers without disruptions and with higher content of Au, where all electrode reactions should be more reversible anb faster and the background of measurement should be lower (better *S*/*N* ratio).

Table 7 Parameters of hydroquinone concentration dependences measured by DVP at GNFE in BR buffer pH 7.

Electrode	Slope/A L mol^{-1}	Intercept/μA	R^2	LOQ/ μmol L^{-1}
GNFE - Pristine	0.008	-0.057[a]	0.990	4.3
GNFE - Plasma	0.007	0.004[b]	0.993	4.2
GNFE - BPD	0.005	- 0.011[b]	0.994	9.0

[a]Intercept is statistically significantly different from zero (a = 0.05), [b]Intercept is not statistically significantly different from zero (a = 0.05).

4. Conclusion

Important electrochemical and surface parameters of three types of 80 nm thick gold nanostructured films electrodes made by sputtering were characterized.

Gold nanolayers were deposited on three types of PTFE: Pristine PTFE, plasma treated PTFE and plasma treated PTFE subsequently grafted with biphenyl-4,4′-dithiol. All types of GNFEs exhibited homogeneous gold layer. However, small differences in coverage were observable, especially in the case of GNFE-Pristine where the gold layer exhibited disruptions and slightly exposed PTFE surface. The highest level of surface concentration of Au was obtained by GNFE-Plasma (84.4±0.2 %, w_{Au}). Pristine PTFE (R_a = 16.7 nm) exhibit different surface morphology and roughness than PTFE treated by plasma (R_a = 17.7 nm) and grafted by biphenyl-4,4′-dithiol (R_a = 19.2 nm); roughness increased by 15 %.

The voltammetric behaviour of all types GNFE in potassium chloride, potassium nitrate, sulphuric acid and BR buffers pH 2, 7 and 12 electrolytes was evaluated. For further measurements, potassium nitrate and BR buffer pH 7 were selected as optimum medium. Other electrolytes were excluded from further experiments for insufficient width of anodic potential window due to early formation of gold oxides or supporting electrolyte decomposition.

During study of electrochemical behaviour of two selected probes (ferrocyanide/ferricyanide, hydroquinone/benzoquinone) and construction of calibration dependences of hydroquinone, all GNFEs showed acceptable electrochemical parameters, which are comparable to parameters of gold bulk electrodes and all the acquired parameters and the results of measurements on the electrodes were satisfactory for further use in electroanalytical chemistry. Moreover, the increase of current response due to the increase of surface area by sputtering of Au atoms (resulting in nanolayer) was observed and confirmed; thus, the use of plasma treatment connected with Au sputtering method increased surface of working electrodes, which can be useful for electroanalytical chemistry. On the other hand, this electrochemical arrangement cannot yet compete with low limits of quantification of modern nanostructured gold electrodes or of factory-made gold electrodes. However, these sputtered films have been until now primarily intended for different utilization than for electroanalytical chemistry and there is a possibility to improve these electrodes and their fabrication to obtain their better performance. For example, the improvement of fabrication process is possible by extension of the deposition time and changes in the conditions of deposition of Au atoms, which can lead to more compact gold layers without disruptions and with a higher content of Au.

In can be concluded that disposable working GNFEs made by sputtering are able to provide reliable analytical results together with easy fabrication process using modern

technologies. Of course, the improvement in GNFEs needs further research, testing and characterizing to eliminate existing drawbacks. Nevertheless, gold electrodes made by sputtering offer certain advantages like short time of analysis, small volume of used sample, many possible ways of modification, easy miniaturization, and also "green" method of fabrication.

Acknowledgements

This research was realized in the frame of specific university research SVV. The authors are grateful for the financial support of the Czech Science Foundation from projects: M.L., J.Z., J.B. and H.D. - Project P206/12/G151, A.R. - Project 17-00939S and V.S. - Project P108/12/G108.

Reference

[1] A.D. McNaught, A. Wilkinson, I.U.o. Pure, A. Chemistry, Compendium of Chemical Terminology: IUPAC Recommendations, Blackwell Science1997.
[2] P. Diao, M. Guo, Q. Zhang, How does the particle density affect the electrochemical behavior of gold nanoparticle assembly?, Journal of Physical Chemistry C, 112 (2008) 7036-7046.
[3] A.I. Lopez-Lorente, M. Valcarcel, The third way in analytical nanoscience and nanotechnology: Involvement of nanotools and nanoanalytes in the same analytical process, Trac-Trends in Analytical Chemistry, 75 (2016) 1-9.
[4] J.B. Raoof, A. Kiani, R. Ojani, R. Valiollahi, S. Rashid-Nadimi, Simultaneous voltammetric determination of ascorbic acid and dopamine at the surface of electrodes modified with self-assembled gold nanoparticle films, Journal of Solid State Electrochemistry, 14 (2010) 1171-1176.
[5] I. Svancara, M. Matousek, E. Sikora, K. Schachl, K. Kalcher, K. Vytras, Carbon paste electrodes plated with a gold film for the voltammetric determination of mercury(II), Electroanalysis, 9 (1997) 827-833.
[6] A. Aflhami, A. Bahiraei, T. Madrakian, Gold nanoparticle/multi-walled carbon nanotube modified glassy carbon electrode as a sensitive voltammetric sensor for the determination of diclofenac sodium, Materials Science & Engineering C-Materials for Biological Applications, 59 (2016) 168-176.
[7] C.M. Welch, O. Nekrassova, X. Dai, M.E. Hyde, R.G. Compton, Fabrication, characterisation and voltammetric studies of gold amalgam nanoparticle modified electrodes, Chemphyschem, 5 (2004) 1405-1410.
[8] R. Garcia-Gonzalez, M.T. Fernandez-Abedul, A. Pernia, A. Costa-Garcia, Electrochemical characterization of different screen-printed gold electrodes, Electrochim. Acta, 53 (2008) 3242-3249.

[9] A. Reznickova, Z. Kolska, V. Hnatowicz, V. Svorcik, Nano-structuring of PTFE surface by plasma treatment, etching, and sputtering with gold, Journal of Nanoparticle Research, 13 (2011) 2929-2938.
[10] D.J. Wilson, R.L. Williams, R.C. Pond, Plasma modification of PTFE surfaces Part I: Surfaces immediately following plasma treatment, Surface and Interface Analysis, 31 (2001) 385-396.
[11] J. Siegel, O. Lyutakov, V. Rybka, Z. Kolska, V. Svorcik, Properties of gold nanostructures sputtered on glass, Nanoscale Research Letters, 6 (2011).
[12] M.L.C. Passos, P. Pinto, J.L.M. Santos, M. Saraiva, A. Araujo, Nanoparticle-based assays in automated flow systems: A review, Analytica Chimica Acta, 889 (2015) 22-34.
[13] A.I. Lopez-Lorente, B.M. Simonet, M. Valcarcel, Analytical potential of hybrid nanoparticles, Analytical and Bioanalytical Chemistry, 399 (2011) 43-54.
[14] M.J. Li, C.Q. Zhan, Y.M. Zheng, G.N. Chen, X. Chen, Simple and Selective Sensing of Cysteine Using Gold Nanoparticles Modified by Ruthenium(II) Complexes, Journal of Nanoscience and Nanotechnology, 11 (2011) 3578-3585.
[15] S.R. Bhattarai, B.K.C. Remant, S. Aryal, N. Bhattarai, S.Y. Kim, H.K. Yi, P.H. Hwang, H.Y. Kim, Hydrophobically modified chitosan/gold nanoparticles for DNA delivery, Journal of Nanoparticle Research, 10 (2008) 151-162.
[16] M.A. Tabrizi, M. Shamsipur, A. Mostafaie, A high sensitive label-free immunosensor for the determination of human serum IgG using overoxidized polypyrrole decorated with gold nanoparticle modified electrode, Materials Science & Engineering C-Materials for Biological Applications, 59 (2016) 965-969.
[17] X. Dai, R.G. Compton, Gold nanoparticle modified electrodes show a reduced interference by Cu(II) in the detection of As(III) using anodic stripping voltammetry, Electroanalysis, 17 (2005) 1325-1330.
[18] M. Tominaga, T. Shimazoe, M. Nagashima, I. Taniguchi, Electrocatalytic oxidation of glucose at gold nanoparticle-modified carbon electrodes in alkaline and neutral solutions, Electrochemistry Communications, 7 (2005) 189-193.
[19] C.R. Raj, T. Okajima, T. Ohsaka, Gold nanoparticle arrays for the voltammetric sensing of dopamine, Journal of Electroanalytical Chemistry, 543 (2003) 127-133.
[20] L. Wang, J.Y. Bai, P.F. Huang, H.J. Wang, L.Y. Zhang, Y.Q. Zhao, Self-assembly of gold nanoparticles for the voltammetric sensing of epinephrine, Electrochemistry Communications, 8 (2006) 1035-1040.
[21] L. Agui, C. Pena-Farfal, P. Yanez-Sedeno, J.M. Pingarron, Electrochemical determination of homocysteine at a gold nanoparticle-modified electrode, Talanta, 74 (2007) 412-420.
[22] P.K. Kalambate, M.R. Biradar, S.P. Karna, A.K. Srivastava, Adsorptive stripping differential pulse voltammetry determination of rivastigmine at graphene nanosheet-gold nanoparticle/carbon paste electrode, Journal of Electroanalytical Chemistry, 757 (2015) 150-158.
[23] M.B. Gholivand, M.H. Parvin, Voltammetric study of acetazolamide and its determination in human serum and urine using carbon paste electrode modified by gold nanoparticle, Journal of Electroanalytical Chemistry, 660 (2011) 163-168.
[24] C.Y. Tsai, T.L. Chang, C.C. Chen, F.H. Ko, P.H. Chen, An ultra sensitive DNA detection by using gold nanoparticle multilayer in nano-gap electrodes, Microelectronic Engineering, 78-79 (2005) 546-555.
[25] X.Q. Ding, M. Yang, J.B. Hu, Q.L. Li, A. McDougall, Study of the adsorption of cytochrome c on a gold nanoparticle - modified gold electrode by using cyclic voltammetry, electrochemical impedance spectroscopy and chronopotentiometry, Microchim. Acta, 158 (2007) 65-71.

[26] H. Cui, Y. Xu, Z.F. Zhang, Multichannel electrochemiluminescence of luminol in neutral and alkaline aqueous solutions on a gold nanoparticle self-assembled electrode, Analytical Chemistry, 76 (2004) 4002-4010.
[27] J.M. Pingarron, P. Yanez-Sedeno, A. Gonzalez-Cortes, Gold nanoparticle-based electrochemical biosensors, Electrochim. Acta, 53 (2008) 5848-5866.
[28] F.H. Zhang, S.S. Cho, S.H. Yang, S.S. Seo, G.S. Cha, H. Nam, Gold nanoparticle-based mediatorless biosensor prepared on microporous electrode, Electroanalysis, 18 (2006) 217-222.
[29] S. Mandal, A. Pal, R.K. Arun, N. Chanda, Gold nanoparticle embedded paper with mechanically exfoliated graphite as flexible supercapacitor electrodes, Journal of Electroanalytical Chemistry, 755 (2015) 22-26.
[30] B. Ankamwar, P. Das, U.K. Sur, Graphene-gold nanoparticle-based nanocomposites as an electrode material in supercapacitors, Indian Journal of Physics, 90 (2016) 391-397.
[31] J. Inczedy, Compendium of Analytical Nomenclature (Definitive Rules 1997), Blackwell Science, Santa Fe, 1998.
[32] V. Svorcik, A. Reznickova, Z. Kolska, P. Slepicka, V. Hnatowicz, Variable surface properties of PTFE foils, E-Polymers, (2010).
[33] A. Reznickova, Z. Kolska, J. Siegel, V. Svorcik, Grafting of gold nanoparticles and nanorods on plasma-treated polymers by thiols, Journal of Materials Science, 47 (2012) 6297-6304.
[34] U. Oesch, J. Janata, Electrochemical Study of Gold Electrodes with Anodic Oxide-Films 1. Formation on reduction behavior of anodic oxides on gold, Electrochim. Acta, 28 (1983) 1237-1246.
[35] U. Oesch, J. Janata, Electrochemical Study of Gold Electrodes with Anodic Oxide-Films 2. Inhibiton of electrochemical redox reactions by monolayers of surface oxides, Electrochim. Acta, 28 (1983) 1247-1253.
[36] R.N. Adams, Electrochemistry at solid electrodes, Marcel Dekker Inc., New York, 1969.
[37] J.E.B. Randles, A Cathode Ray Polarograph 2. The Current-voltage Curves, Transactions of the Faraday Society, 44 (1948) 327-&.
[38] H.S. Yin, Q.M. Zhang, Y.L. Zhou, Q.A. Ma, T. Liu, L.S. Zhu, S.Y. Ai, Electrochemical behavior of catechol, resorcinol and hydroquinone at graphene-chitosan composite film modified glassy carbon electrode and their simultaneous determination in water samples, Electrochim. Acta, 56 (2011) 2748-2753.
[39] J.G. Goldsmith, Modern Analytical Chemistry, 1st Edition (Harvey, David), Journal of Chemical Education, 77 (2000) 705.
[40] R.G. Compton, C.E. Banks, Understanding voltammetry 2nd edition, Imperial College Press, London, 2011.
[41] S. Hu, Y.H. Wang, X.Z. Wang, L. Xu, J. Xiang, W. Sun, Electrochemical detection of hydroquinone with a gold nanoparticle and graphene modified carbon ionic liquid electrode, Sensors and Actuators B-Chemical, 168 (2012) 27-33.
[42] X.M. Ma, Z.N. Liu, C.C. Qiu, T. Chen, H.Y. Ma, Simultaneous determination of hydroquinone and catechol based on glassy carbon electrode modified with gold-graphene nanocomposite, Microchim. Acta, 180 (2013) 461-468.

10. Appendix IV

Large-scale ultrasensetive, highly reproducible and regenerative smart SERS platform based on PNIPAm grafted gold grating

Guselníkova Olga, Postnikov Pavel, Kalachyova Yevgeniya, **Libánský Milan.**, Zima Jiří, Kolská Zdeňka, Švorčík Václav, Lyutakov Oleksiy

ChemNanoMat,

Volume 3, Year 2016, Pages 135-144.

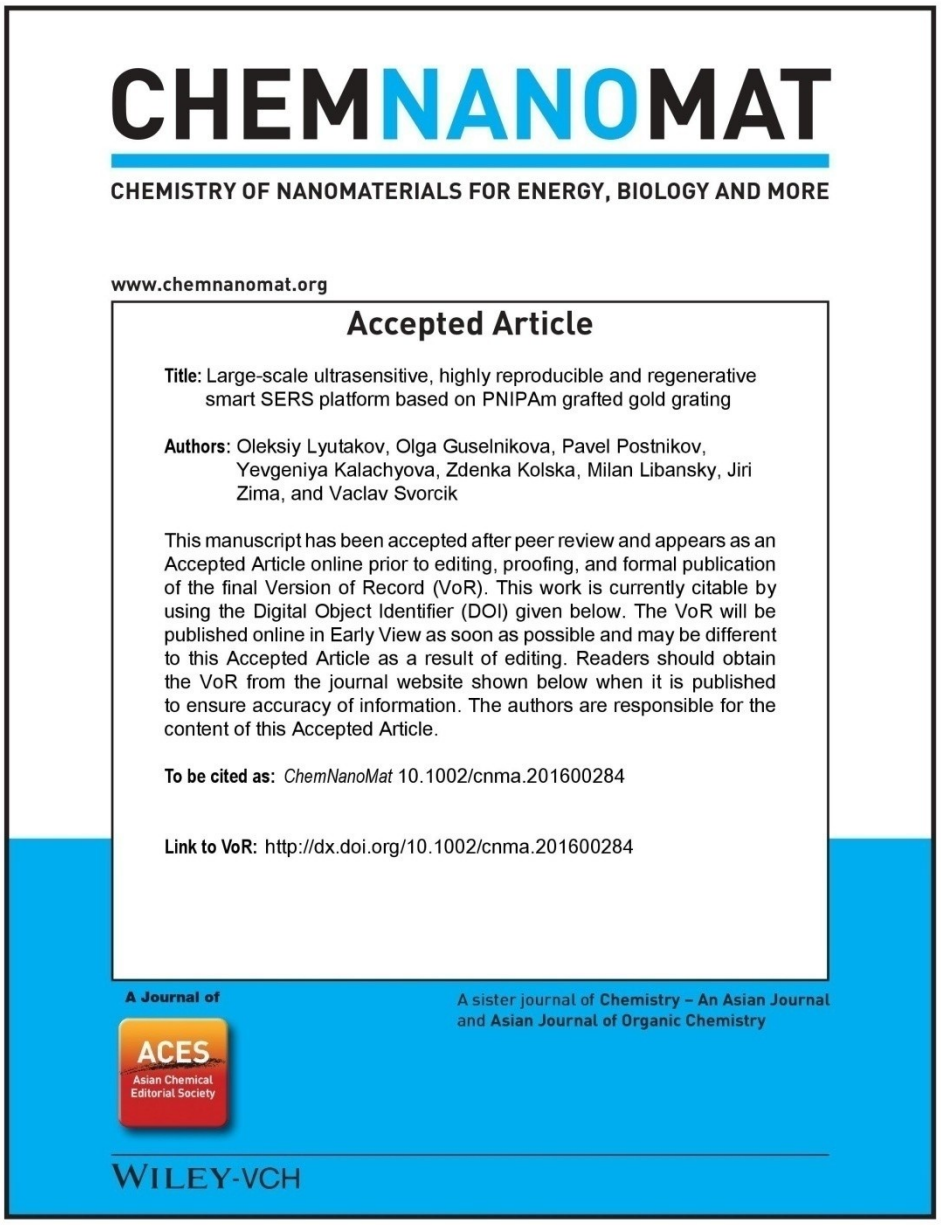

CHEMNANOMAT

CHEMISTRY OF NANOMATERIALS FOR ENERGY, BIOLOGY AND MORE

www.chemnanomat.org

Accepted Article

Title: Large-scale ultrasensitive, highly reproducible and regenerative smart SERS platform based on PNIPAm grafted gold grating

Authors: Oleksiy Lyutakov, Olga Guselnikova, Pavel Postnikov, Yevgeniya Kalachyova, Zdenka Kolska, Milan Libansky, Jiri Zima, and Vaclav Svorcik

To be cited as: *ChemNanoMat* 10.1002/cnma.201600284

Link to VoR: http://dx.doi.org/10.1002/cnma.201600284

A Journal of

ACES Asian Chemical Editorial Society

A sister journal of **Chemistry – An Asian Journal** and **Asian Journal of Organic Chemistry**

WILEY-VCH

ChemNanoMat 10.1002/cnma.201600284

Large-scale ultrasensetive, highly reproducibile and regenerative smart SERS platform based on PNIPAm grafted gold grating

O. Guselnikova [a,b], P. Postnikov *[b], Y. Kalachyova [a,b], Z. Kolska[c], M. Libansky[d], J. Zima[d], V. Svorcik[a], O. Lyutakov *[a,b]

* Corresponding author: lyutakoo@vscht.cz

[a] Department of Solid State Engineering, University of Chemistry and Technology, 16628 Prague, Czech Republic

[b] Department of Technology of Organic Substances and Polymer Materials, Tomsk Polytechnic University, Russian Federation

[c] Faculty of Science, J. E. Purkyne University, Usti nad Labem, Czech Republic

[d] UNESCO Laboratory of Environmental Electrochemistry, Department of Analytical Chemistry, Faculty of Science, Charles University in Prague, Czech Republic

Abstract

The design of the smart plasmonic sensor, based on the periodical gold gratings grafted with PNIPAm was proposed and realized. Periodical gold structure was created on the polymer backing modified by excimer laser (1x2 cm^2 modified area) and subsequently covered by thin gold film. In the next step 7 nm thick PNIPAm layer was grafted to gold surface through two step procedure: covalent attachment of 4-carboxybenzil groups followed by carboxyl groups activation and their coupling with amino-terminated PNIPAm. Surface properties of the prepared structure and their switchable behaviour were investigated using refractometry, wettability measurements, AFM in water medium, cyclic voltammetry, pH and temperature-dependent z-potential. The structure enables effective entrapping and SERS detection of azo dyes, significant reduction of minimal detectable concentration of target molecules and detection limit down to femtomolar concentrations. Excitation of plasmons on well ordered surface structure also shows excellent reproducibility of SERS system along the particular sample surface and between different samples too. Additionally, the reversible switching of wettability under repeated temperature changes on gold plasmonic platform allows multiple use of the developed system.

Keywords: *gold grating, surface grafting, PNIPAm, SERS, ultrasensitive, reproducible, regenerative*

ChemNanoMat 10.1002/cnma.201600284

Introduction

Plasmonic-active metal nanostructures become a key element in the variety of scientific and technical fields. [1-3] Their unique interaction with light enables the preparation of optically triggerable catalytic systems, extremely sensitive sensor platform, and photonic modulators with unprecedented speed. [4-7] The plasmon-based sensors are especially favourable due to extremely low detectable concentration and remarkable versatility of analyte molecules, varying from inorganic ions to biomolecules. [8-10] Imposition of the electromagnetic field on the plasmon-active surface of metallic nanostructures can significantly amplify the Raman signal from the surrounding analyte.

In order to further improve the performance of plasmonic sensors, the metal surface can be decorated with a broad range of functional groups, with specific properties for selective binding or entrapping of small molecules and biological targets. [5, 6, 11] Moreover, surface modification of metal nanostructures opens the potential for design and creation of the new generation of sensors devices, related to the area of so-called smart plasmonic systems. The design of such systems implements the introduction of significant and reproducible response to external stimuli, satisfying the growing demand for fine modulation of the plasmonic response. [12] As an example of this fascinating research area, polymer-coated colloidal AuNPs with reversible control of their properties by surrounding temperature or pH changes [13,14] can be mentioned. The establishment of this general approach is an important step forward for development and wide application of smart nanomaterials in catalysts, actuators, sensors and biomedicine. [15]

For the introduction of smart response to plasmonic nanostructures, its surface should be modified with intelligent molecules, commonly polymers. One of the most applicable intelligent polymers, is poly(N-isopropyl acrylamide) (PNIPAAm), with its temperature-dependent variation of thermodynamic state, has been extensively used as a key component in smart materials field. [16-18] The PNIPAm-based dynamic SERS substrates were designed to tune MeNPs distances or substrate-MeNPs coupling, which can significantly enhance SERS signals. [19] Additionally, phase transition of PNIPAAm from swollen to collapsed state can be used for analyte molecules entrapping. [20, 21] Typical model analytes for SERS (usually dye, such as Rhodamin 6G, methylene blue, crystal violet and so on) have been used to demonstrate of PNIPAm-based dynamic SERS systems in several works. [19, 20, 22] However, several key issues remain unclear or needs to be still resolved, e.g. decrease of minimal inhibition concentration up to real-application significant level, reproducibility of SERS signal (between different samples or along one sample surface) and development of reasonably simple SERS substrate preparation procedure.

ChemNanoMat 10.1002/cnma.201600284

In this work, we propose the covalent grafting of PNIPAAm to the surface of plasmon active gold grating through diazonium chemistry approach. The combination of signal enhancement by periodical surface and unique properties of PNIPAM allows the detection of prohibited azo dyes (crystal violet, metanil yellow, disperse red I) in the extremely low concentration and excellent reproducibility and homogeneity of related SERS signal.

Experimental

Materials and samples preparation

Materials: acetic acid (reagent grade, ≥ 99 %), diethyl ether, deionized water, ethanol (puriss. p.a., absolute, ≥ 99.8% (GC)), DCM, N,N′-Dicyclohexylcarbodiimide (99 %), N-Hydroxysuccinimide (98%), 4-aminobenzoic acid (ReagentPlus®, ≥ 99 %), p-Toluenesulfonic acid monohydrate (ACS reagent, ≥98.5%), Poly(N-isopropyl acrylamide) amine terminated (average Mn 2,500), O-(2-Aminoethyl)polyethylene glycol (average Mn 3,000) (PEG) were purchased from Sigma-Aldrich and used without further purification.

Grating preparation Polymer films (Solution of epoxy resin - photoresist, Su-8, purchased from Microchem) were spin-coated (1000 rpm) from a solution onto freshly cleaned glass substrates (supplied by Glassbel Ltd, CR) during 30 min. The prepared samples were dried at 50°C for 24 h and irradiated by UV-source for 30 min. After that, the UV-irradiated samples were dried at 90°C for 2 h. Pattering procedure of Su-8 film was described in our previous works [3, 7]. Briefly, the flat polymer surface was patterned by KrF excimer laser (COMPexPro 50F, Coherent, Inc., wavelength 248 nm, pulse duration 20-40 ns, repetition rate 10 Hz). The laser beam was polarized linearly with a cube of a UV-grade fused silica with an active polarization layer. The samples were irradiated with 3500 laser pulses with laser fluencies 9 mJ cm^{-2}. The angle of laser beam incidence with respect to the sample surface normal was 50° and the aperture with the area of 5×10 mm^2 was used. As a result, the periodic surface structures were created on the Su-8 surface with 1x2 cm^2 patterned area size. Then gold was deposited onto a patterned surface by vacuum sputtering (DC Ar plasma, gas purity of 99.995 %, a gas pressure of 4 Pa, a discharge power of 7.5 W, sputtering time 200 s, and thickness approx. 25 nm). The deposition of gold was accomplished from Au target (purity of 99.99 %, provided by Safina, Czech Republic).

Surface functionalization

Diazonium modification: 4-carboxybenzenediazonium tosylate (ADT-COOH) was prepared according to published procedure. [23] The obtained gratings were spontaneously modified by soaking in 1 mM freshly prepared aqueous solution of ADT-COOH for 10 min. After modification

ChemNanoMat 10.1002/cnma.201600284

gold substrates were rinsed under sonication sequentially with water, ethanol, and acetone for 10 min and dried in desiccator for 3 hours

Grafting of PNIPAM: surface modified gratings were immersed in a mixture of freshly prepared DCM solution of 0.4 M N,N'-Dicyclohexylcarbodiimide (DCC) solution and 0.1 M N-hydroxysuccinimide (NHS) solutions in a 1:1 volume ratio during 6 hours. Afterward, the gratings were thoroughly rinsed with DCM and ethanol 3 times. Prepared gold gratings were immersed in 1mM solution of PNIPAM-NH_2 overnight. Then the gratings were washed with DCM and acetone 3 times and dried in a desiccator for 3 hours.

Grafting of PEG: surface modified gratings were immersed in a mixture of freshly prepared DCM solution of 0.4 M N,N'-Dicyclohexylcarbodiimide (DCC) solution and 0.1 M N-hydroxysuccinimide (NHS) solutions in a 1:1 volume ratio during 6 hours. Afterward, the gratings were thoroughly rinsed with DCM and ethanol 3 times. Prepared gold gratings were immersed in 1mM solution of PEG-NH_2 overnight. Then the gratings were washed with DCM and acetone 3 times and dried in a desiccator for 3 hours.

Raman – dye entrapping: Typically, PNIPAM-modified gold gratings were immersed in aqueous solution of azo dyes (crystal violet, metanil yellow, disperse red I, 10^{-8}M concentration in all cases) rapidly heated above LCST for 5 min, washed with the hot water three times, cooled down to room temperature and dried on air. For crystal violet detection in 10^{-12} and 10^{-14} M concentration gratings were immersed in the dye solution for 15 and 30 min corresponding. The SERS measurements were conducted in air. Raman scattering was measured on Nicolet Almega XR spectrometer (Laser power 15 mW) Raman spectrometers with 785 nm excitation wavelengths, all spectra of trapped azo dyes were PNIPAM baseline corrected. Spectra were measured 10 times, each of them with 30 s accumulation time.

Multiply regeneration and utilization of PNIPAM-modified gold grating: To verify the regenerative properties of proposed SERS system, followed set of measurements was performed:

(1) – entrapping of CV from 10^{-14} M solution, SERS measurement

(2) – removement of CV, SERS measurement

(3) – entrapping of ME from 10^{-14} M solution, SERS measurement

(4) – removement of ME, SERS measurement

(5) – entrapping of DR1 from 10^{-14} M solution, SERS measurement

(6) – removement of DR1, SERS measurement

All measurements were performed on the same sample. Entrapping of dyes was performed by sample immersion into appropriate solution at room temperature and heating above LCST, followed

ChemNanoMat 10.1002/cnma.201600284

by sample washing three time with hot water. Dyes removement was performed by sample immersion in the distilled water for 15 min. at room temperature.

Measurement techniques

Water contact angles were measured by goniometer Surface Energy Evaluation System (Masaryk University, Czech Republic) with distilled water at room temperature and under gradual heating with simultaneous control of sample surface temperature, 72 h after surface modification.

X-ray photoelectron spectroscopy (XPS) was used to determine the surface chemical composition. The spectra were recorded using an Omicron Nanotechnology ESCAProbeP spectrometer fitted with monochromated Al K Alpha X-ray source. The analyzed area had dimensions of 2x3 mm^2. Concentrations of elements were calculated in at. % using the manufacturer's sensitivity factors.

Refraction spectra of functionalized grating were determined in-situ under gradual heating (1°C/min) from 24 to 35°C in 250–750 nm spectral range using refractometer Avaspec 2048. After the set of measurements the wavelength 620 nm, corresponding to maximal change of refraction intensity was determined and used as a characteristic one.

For characterization of the sample surface and nanomechanical mapping before and after surface modification, the peak force AFM technique was used. Surface mapping was performed with Icon (Bruker) set-up on 6x6 μm^2 areas in water at two different temperatures: 25 °C and 45°C.

As an inorganic probe, potassium ferrocyanide (p.a., Lachema, Czech Republic) was used for investigation of the electrochemical behaviour of the system with PNIPAm grafted onto the surface of the nanostructured gold layer. Electrochemical characterization of gold surfaces was performed by cyclic voltammetry (CV) with scan rate 0.05 V s^{-1} in the potential range from -0.1 V to 0.6 V, where the measurement is not affected by gold oxides formation on gold surfaces. Cyclic voltammograms on pristine and PNIPAm modified gold films were measured using solution containing 1 mmol L^{-1} potassium ferrocyanide diluted in potassium nitrate (both p.a., Lachema, Czech Republic) (10 µL). Cyclic voltammetry was carried out with gold film as working electrode. Platinum wire auxiliary electrode and miniaturized gel Ag/AgCl reference electrode (3M KCl, Cypress Systems, Chelmsword, MA, USA) to which all potential values are referred, were used. Voltammetric measurements were performed with portable potentiostat PalmSens 2 (Palm Instruments, Netherlands), controlled by PSTrace 4.8.0 software (Firmware 4.4). All measurements were repeated three times with five scans in each measurement.

Electrokinetic analysis (zeta potential) of all samples were determined by SurPASS Instrument (Anton Paar GmbH, AT). Samples were studied inside the adjustable gap cell with an

ChemNanoMat 10.1002/cnma.201600284

electrolyte of 0.001 M KCl. All samples were measured four times at constant pH 6.3 and at room temperature. For zeta potential determination the streaming current method and Helmholtz-Smoluchowski (HS) equation were used with an experimental error of 5 %.

UV-Vis spectra of azo dyes (CV, ME, DR1) solutions in 10^{-8} M concentration were measured using Spectrometer Lambda 25 (Perkin-Elmer) in 300-1100 nm wavelength range.

Results and Discussion

Preparation of plasmon-active gold grating were performed according to the previously reported procedure. [3, 7, 24, 25] The schematic of the grating surface functionalisation with PNIPAm is shown in the Fig. 1. In the first step, the diazonium chemistry approach was used for covalent grafting of C6H4-COOH to the gold surface. In order to prepare closed to monomolecular layer of organic functional groups (OFGs), [26] a spontaneous approach for surface modification with arenediazonium tosylates (ADTs) was chosen. [23,27] In the next step, the amino-terminated PNIPAm was coupled with carboxyl group using the DCC/NHS activation procedure. Both steps of surface grafting were checked using Raman spectroscopy and XPS analysis.

Results of Raman spectroscopy are presented in the Fig. S1 with detailed peak affiliation in the Table S1. Briefly, appearance of characteristic adsorption bands at 2930 cm^{-1} (H-bonded O-H stretch), 1580, 1780 cm^{-1} (C=O stretch), 1360, 1245 cm^{-1} (O-H in-plane bending) confirms the grafting of ADT-COOH. Moreover, weak adsorption band at 420 cm-1 arised after modification, corresponding to covalent Au-C bonds. [28] After the coupling of carboxyl group with amino-terminated PNIPAm, new adsorption bands appear, revealing formation of amide between carboxylic groups and PNPAm-NH_2:635 cm^{-1} (C-S stretch), 1185, 1245, 1376 cm^{-1} (C-N stretch) and 1590 cm^{-1} (N-H deformation).

Results of XPS measurement, also enabling to monitor grafting process, are presented in the Figs. S2-S4 and Table S2. On the spectra of pristine gold grating (Fig. S2) the composition of sputtered onto Su-8 gold films with apparent Au-related peaks and underlying polymer-related oxygen and carbon peaks are observed [22]: Au 4f (84.1 eV, 52.2 at. %), C1s (284.9 eV, 32 at. %), O1s (532.1 eV, 15.8 at. %). On the ADT-COOH grafted sample an increase of C1s peak to 42.3 at. % and O1s to 19.6 at.%, indicates successful grafting of OFGs. Further coupling with PNIPAM-NH2 results in the appearance of N1s peak and following final composition: Au 4f (84.5 eV, 6.28 at. %), C1s (282.1-290.5 eV, 69.8 at. %), O1s (532.1 eV, 21.5 at. %), N1s (*ca.* 400 eV, 2.42 at. %). As XPS is a highly surface-specific technique with a typical analysis depth of only 10 nm, it can be concluded that the polymer layer thickness is less than 10 nm. Estimation of the thickness of grafted

ChemNanoMat 10.1002/cnma.201600284

polymer layer can be done from the Au $4f_{7/2}$ (84.1-84.5 eV). According to the previously described methodology for calculation of gold films thickness [22] and density of PNIPAM (1.1 $g.cm^{-3}$), the thickness of PNIPAAM layer is 6.9 nm (with consideration of only PNIPAM density) (see SI for calculations). By considering the density of PNIPAM (1.1 $g.cm^{-3}$), calculated layer thickness (6.9 nm) and average molecular weight (2500 $g.mol^{-1}$) grafting gives a surface coverage **Γ** of $3.04x10^{-10}$ $mol.cm^{-2}$

Refractometry: It was expected, that the grafting of PNIPAm will introduce stimuli-responsive properties to functionalized surface due to polymer reversible phase transition, from a swollen to a collapsed state at about 32°C in water. However, it is well known, that constraints for lateral swelling affect the transition temperature of the surface-attached PNIPAm molecules. [29-32] Refraction spectra of PNIPAm functionalized gold grating were measured with the aim to determine the temperature range of polymer phase transition. The detailed experimental set-up is presented in the S5. Functionalized gold gratings were immersed in the water and slowly heated with permanent measurements of their refraction spectra (Fig. S6). During the heating procedure the changes in the refracted light intensity were observed and heating was stopped when the intensity did not change anymore with increasing temperature and remained constant over a several degree range. The wavelength, where the more apparent changes of refraction intensity occur was chosen as a probe one (Fig. S6 – 620 nm wavelength), and the dependence of reflected light intensity was plotted versus temperature in the Fig. 2. There are three apparent sections on the measured curve: (i) up to temperature 27°C the refraction intensity remains constant; (ii) rapid decrease of light intensity occurs in the 27-30°C temperature range; (iii) at higher temperature, the refraction spectra do not change significantly (Fig. S6). The range of rapid intensity decrease can be associated with PNIPAm phase transition. Observed temperature range of phase transition is located lower, than in the case of bulk PNIPAm (typical temperature of bulk PNIPAm swelling is 32°C [33]). Apparently, in this case, covalent attachment of PNIPAm molecules affects the phase transition due to the lateral restrictions mentioned above. Simultaneously phase transition range is wider than in the case of bulk polymer (bulk PNIPAm phase transition usually occurs in the 1.0-1.5°C temperature range). That fact can be attributed to additional dispersion of PNIPAm inter/inside chain interaction due to the restriction on chains mobility because of their covalent immobilization.

Wettability experiments: Phase transition of PNIPAm is closely related to the polymer wettability: the water contact angle, measured below LCST, when the polymer is in a soluble state, is significantly low then that above LCST. [34] To check the wettability-temperature dependence, the two sets of experiments were performed, i.e. measurements of water contact angle dependence on the temperature and on the repeated cycles of polymer heating cooling. Fig. 3 demonstrates the

ChemNanoMat 10.1002/cnma.201600284

changes of water contact angle (CA) with increasing temperature. Similarly to refraction data, three obvious sections can be established: constant value of water contact angle (≈ 34°) in the 24-26 °C temperature range, rapid increase of CA in 26-30°C temperature range and constant CA (85°) at the temperatures higher than 31°C. The first observed section corresponds to PNIPAm in a soluble state, the second section characterizes the phase transition of polymer and the third can be attributed to the collapsed and insoluble state of PNIPAm chains. It may be concluded that the temperature dependences of CA and refraction intensities are in good agreement.

The reversible change in the wettability induced by repeated thermo-control cycles is documented in the Fig. 4. It is seen that the PNIPAm-modified gold film exhibits the maximum CA value of 85° at the temperature 34°C and the minimum one 32° at 24°C. The reversibility of system was checked through 10 cycles in temperature with no significant deviations in CA (variations less than 5 %), indicating the excellent stability of system. Observed reversibility and stability indicates a possibility for utilisation of proposed material for the switching between hydrophilic/hydrophobic states, e.g. in self-cleaning optical component.

AFM quantitative mapping of surface topography and nanomechanical properties. AFM measurements of grafted surfaces were performed in water at two temperatures, attributed to swollen and collapsed states of PNIPAm (25 and 45°C). Results are presented in the Fig. 5, which gives the topography scans and corresponding nanomechanical maps (adhesion and deformation properties). From the topographical scans the grating structure is apparent at both working temperatures. On the other hand, rather pronounced differences between maps of mechanical properties measured at two temperatures are evident. The mapping performed at 45°C gives the distribution of mechanical properties closed to topography image. In this case the interaction of AFM tip with surface is apparently affected by the surface topography. Measurements performed at 25°C gives different result – distribution of mechanical properties seems to be roughly homogeneous in the case of surface deformation and only weak trace of periodical structure is evident on adhesion scans. The corresponding graphs of the values of AFM tip-surface adhesion forces and surface deformation under tip oscillation are also given in the Fig. 5. In the measurements of adhesion forces performed below LCST single peak located at 1.5 nN on the measured distribution, is seen. This peak is shifted to higher value and simultaneously widened when the temperature of water exceeds the PNIPAm LCST. So, swollen PNIPAm chains introduce repulsive forces between the AFM tip and sample surface, decreasing the adhesion interaction. When the polymer is converted to collapsed state, the adhesion interaction becomes more pronounced and the peak wider. This may reflect the inhomogeneities of PNIPAm grafting, as was detected from CVA measurements, when the PNIPAm do not block surface homogeneously and

ChemNanoMat 10.1002/cnma.201600284

there are many "free" places. On the other hand, surface undergoes more significant deformation under the interaction with oscillated AFM tip, when the grafted PNIPAm chains are in swollen state (Fig. 5 – deformation maps). This could be expected since the swollen polymer chains are more rigid. Oppositely, temperature induced conversion of PNIPAm into collapsed state leads to increase of surface mechanical resistivity and widening of local point surface deformation distribution. The last phenomenon can also be attributed to the inhomogeneities in the PNIPAAm grafting – due to the high volume of PNIPAm molecule and sterical hindering the modified surface cannot be fully covered in-principle.

Zeta potential Further characterization of surface properties was performed using z-potential and cyclic voltammetry methods. The results of z-potential measurements are presented as the dependences of surface charge on the pH of flowing solution, taken at two temperatures: 25°C and 40°C (Fig. 6). There is no difference in the z-potential measured at 25° C and 40° C for pH values greater than 4.7. Oppositely, apparent dependence of z-potential on temperature is observed for pH<4.7. Schematic of the observed phenomenon shown in the Fig. 6 deserves more detailed discussion. Probably, at pH<4.7 H_3O^+ ions can effectively interact with PNIPAm amine groups. This interaction, which is enhanced by further pH decrease, affects the value of z-potential (surface charge). Accessibility of PNIPAm amine groups is a function of polymer state. At higher temperature PNIPAm is collapsed and screening effect of enclosed PNIPAm state leads to less pronounced dependence of z-potential (i.e. surface charge) on the pH. (see Fig. 6). Al lower temperature PNIPAm is swollen, its amine groups are more exposed and z-potential becomes more pronounced function of pH (Fig. 6).

Cyclic voltammetry The gold grating surface blocking by PNIPAm-grafting was examined using cyclic voltammetry, also performed at two temperatures. Results are presented in the Fig 7A, where typical reduction and oxidation behaviour of potassium ferrocyanide is evident. The electrochemical behaviour did not change with the increase of the temperature, and moreover, there are no differences between the curves, measured on pristine and grafted gold surface. So, regardless of the PNIPAm state the sample surface is not blocked. It should be also noted that the pristine grating demonstrates sufficient repeatability (under 5 %) and reversibility (ΔE_p = 90 mV, I_{anod}/I_{cathod} = 1.1) of one electron reaction. The similar electrochemical behaviour was observed during the measurement on PNIPAm-grafted gold gratings at 25 °C (ΔE_p = 95 mV, I_{anod}/I_{cathod} = 1.1).

On the other hand, a significant change of the electrochemical behaviour was observed during the measurement of repeated scans at 45°C (Fig. 7B). Surprisingly, the each next scan results in increased height of the slightly shifted peak. This phenomenon can be explained by PNIPAm collapsing at the electrode surface, resulted in the deviation of the whole process from a diffusion-

ChemNanoMat 10.1002/cnma.201600284

controlled mechanism. Molecules of ferrocyanide are entrapped and accumulated in the PNIPAm layer and observed increase of the signal occurs. Similar effects on PNIPAm-modified surfaces were observed previously. [35, 36]

In general, observed CV results demonstrate that the grafting of PNIPAm substrate does not lead to blocking of gold layer surface, which remains electrochemically available. Nevertheless, the temperature induced change of PNIPAm structure affects the typical diffusion-controlled process CV process.

SERS activity: PNIPAm functionalized plasmon-active surfaces have the great potential in the various application fields, e.g. in food or ecology safety or medical diagnostics. [8, 9, 37] The capture function of the grafted polymers, i.e. their ability to accommodate various chemicals, dyes, enzymes, etc. is explored for the substantial extension of plasmon-active surface functions. In this work PNIPAm-grafted gold grating is applied as sensors for the detection of azo dyes by surface enhanced Raman spectroscopy (SERS). In particular, crystal violet (CV), disperse red 1 (DR1), and metanil yellow (ME) is used as model dyes, taking into account the recommendation of EU and USA to avoid utilization these dye in several practical fields. [38, 39]

In order to evaluate the efficiency of proposed sensor system, the PNIPAm-grafted gold gratings were immersed in the dyes solutions in 10^{-8} M concentration at room temperature (24°C), rapidly heated above LCST and dried on air. It was proposed, that the dye will effectively diffuse into the PNIPAm layer and after the temperature increase will be entrapped by polymer. In this way, the "effective" concentration of dye, as well as the Raman response, will be increased by many orders of magnitude. After entrapping of dyes, Raman spectra (at 785 nm excitation wavelength) were recorded and the results are presented in the Fig. 8. All spectra were baseline corrected on pristine PNIPAm sample (also given in the Fig. 8), measured before the dye incorporation. According to the measured data, the excellent response in all cases was achieved, appearance of characteristic bands of dye with perfect resolution of characteristic bands position should be noted. Full assignation of Raman peaks is in excellent agreement with previously published data (see Table S3). [40-42]

It must be additionally noted, that UV-Vis absorption spectra (Fig. S6) demonstrated that the maxima of dyes adsorption is far from excitation wavelength (593 nm, 427 nm and 438 nm for CV, DR1 and ME respectively; 785 nm excitation wavelength), so observed Raman response can be considered as a non-resonant. [43] Therefore, the high measured signal is attributed to the excitation of dye through the grating plasmon resonance, arising from the proximity of dye and gold surface, but not from intrinsic dye absorption at used Raman wavelength.

ChemNanoMat 10.1002/cnma.201600284

Influence of gold grating structure on SERS activity: In order to further examine impact of periodical structure of gold grating and PNIPAm on SERS effectivity of prepared sensing system, several Raman spectra were recorded from DR1 on PNIPAM-modified gold grating, from PNIPAm- modified plain gold film (with the same gold thickness as that on grating) and drop-deposited DR1 on unmodified gold grating (DR1 concentration 10^{-8} M in all cases). It is clear from Fig. S7 (A) that dried DR1drop on unmodified gold grating does not exhibit good signal-to-noise-ratio and assignation of peaks is complicated in this case. For PNIPAM-modified plain gold film (Fig SI B), captured molecules of DR1 and characteristic peaks become quite well detectable. In the last case (Fig SI C), we observe further enhancement of Raman signals and excellent signal-to-noise-ratio. Thus, SERS signal enhancement originates from combination of highly periodical structure of gold grating and unique behaviour of PNIPAm layer.

Control experiments were also performed with the aim of estimation the "smart" effect of PNIPAm triggering and elimination of the potential impact of samples cooling/heating. As a control, the gold grating grafted with PEG was used. Results are presented in the Fig. S8, which demonstrates the SERS activity of CV entrapped from water solution (10^{-8} M) on the gold grating surface grafted with PNIPAm or PEG. As shown in the Fig. S8, significantly stronger SERS response was observed in the case of smart sensor structure (PNIPAM grafted gold grating).

Minimal detectable concentration: For determination of minimal detectable concentration we measured SERS response for three different concentrations of CV solution: 10^{-8}, 10^{-12} and finally extremely small concentration 10^{-14} M. Received SERS response show a perfect signal-to-noise ratio and well visible Raman peaks (Fig 9). The dependence of the peak intensity on the dye concentration (determined on 1535 cm^{-1} peak – Fig. 9 insert) is nearly linear, as is typical for SERS measurements. The developed system can detect azo dyes down to femtomolar concentration in linear response regime. Moreover, Raman spectra measured on 3 different samples at 10 different spots demonstrate show minimal deviations, and indicate excellent reproducibility too, which are key requirements for an ideal SERS sensor (discussed below). The measurements at 10^{-15} M CV concentration did not show any detectable characteristic peaks, so that 10^{-14} M CV concentration can be considered as a detection limit in this particular case. Observed improvement of the SERS system and its low detection limit compared to previously reported systems (Tab. 1) can be explained by the following advantages of the system: (i) high affinity of dye-PNIPAm compounds; (ii) smart nature of used system (similar results were for example, observed by Serpe group for so-called etalon device [45, 46]); (iii) well-defined distribution of SPP intensity along the full "active" sample area (since the SERS response is achieved through the surface plasmon-polariton excitation, which provides homogeneous distribution of plasmon intensity near the metal surface [3]); (iv)

ChemNanoMat 10.1002/cnma.201600284

proposed system allows the dye entrapping in the area corresponding to "high" value of plasmon evanescent wave through the PNIPAm collapsing. It must also be noted that several reported system allow the dye detection limit down to 10^{-21} M concentration. Their implementation, however, involves technologically complex steps, such as the application of electron lithography or sophisticated nanoparticles synthesis procedure. [19, 45-48]

Multiply regeneration and SERS reproducibility: After detection limit examination, the possibility of multiply regeneration and utilization of one sample was studied (Fig 10). The sample from previous experiment (treated by 10^{-14} M CV) was subsequently washed and treated with ME in 10^{-14} M and 10^{-14} M solution of DR1 for analyte loading. For sample processed in this way the same characteristic adoption bands as in 10^{-8} M concentration was observed (Fig. 8, Fig 10, Table S1), confirming established MDC. These results demonstrate that PNIPAm-modified gold grating can be cleaned from azo dyes and subsequently used for further detection. Such sensor system gives excellent response in several cycles of azo dyes entrapping at 10^{-14} M concentration level.

Spot-to-spot Raman intensity variation along the single sample surface, intensity variations between the different samples and the influence of subsequent dye entrapping, washing and entrapping again on the Raman signal were measured too. Results of these measurements are presented in the Fig. 11, where the intensities of 1430 cm^{-1} Raman peak measured on four samples (at ten positions at each sample along the full grating area – 1x2 cm^2) and samples repeatedly washed and treated in 10^{-8} M DR1 solution are shown. The error bars on the columns give the information about the measuring uncertainty along the sample surface. In this case, the peak intensity variation was found to be less than 3%. The average height of the columns indicates the SERS signal homogenity from different samples which is better than 4.5 %. Finally, the column height in each set was used to evaluate the variation of Raman response in the dye entrapping-removing-entrapping cycles. The cycle-to-cycle coefficient of variation was found to be about 5 %. So, it can be concluded that presented modification procedure for gold grating results in high reproducibility between substrates, which is one of the key requirements for perfect sensing system. It must also be noted that the well-defined distribution of surface plasmon-polariton intensity along the SERS-active sample area allows the quantification of SERS results (Fig. 9 - insert).

Comparison with other PNIPAM-based SERS systems: The present minimal detectable concentrations (MDC) can be compared with published data on other PNIPAm based sensor systems. Results of literature analysis are summarized in the Table 1. It is evident, that only nanomolar detection limits for R6G and CV was achieved by self-assembly of AuNPs onto a gold/silica-coated silicon substrate covered by PNIPAM through chemisorption. [20] Even the systems based on the interaction between AuNPs and metal film with PNIPAm as a spacer do not

ChemNanoMat 10.1002/cnma.201600284

lead to a significant MDC reduction. [19, 22] It may be concluded that the present system consisting of the gold periodical grating and thermo-responsive PNIPAm overcome all other PNIPAM-based structures in sensitivity and it allows detection of selected dyes down to femtomolar concentrations.

Conclusion

Plasmonically-active gold gratings grafted with PNIPAm were prepared trough stepwise procedure, combining excimer patterning of Su-8 polymer, gold deposition, diazonium chemistry based covalent attachment of carboxyl group and their further coupling with amino-terminated PNIPAm. Value of PNIPAm phase transition temperature and broadening of phase transition range after polymer grafting were confirmed by the refractometry and contact angle measurement. Impact of the grafting procedure on the surface properties was studied by measuring the wettability, CVA, AFM in water, and z-potential at the temperatures corresponding to swollen and collapsed PNIPAm states.

The smart SERS activity of prepared structures was applied for sensing of several azo dyes: CV, DR1, and ME. Switching of PNIPAm between swollen and collapsed state allows effective entrapping of targeted molecules from the model dyes solutions. Low detection limit and high signal-to-noise ratio were demonstrated for the present system over the all grating area – 1x2 cm^2. The highly periodical structure of gold gratings and thermo-responsive nature of PNIPAm result in the extremely low detection limit down to femtomolar concentrations and very good homogeneity of Raman signal measured on the different spots on one sample within active area (2 cm^2), as well as between several samples. Additionally, reversibility in the phase transitions induced by temperature changes , makes possible to use the present system repeatedly.

Acknowledgement

This work was supported by the GACR under the projects Nos. 15-19485S, 15-19209S, P108/12/G108, and P206/12/G151; and by the RFBR under the project no. 16-33-00351.

References

[1] J. N. Anker, W. P. Hall, O. Lyandres, N. C. Shah, J. Zhao, R. P. Van Duyne, *Nat. Mater.* **2008**, *7*, 442.

[2] E. Katz, I. Willner, *Angew. Chem. Int. Ed.* **2004**, *43*, 6042.

ChemNanoMat 10.1002/cnma.201600284

[3] Y. Kalachyova, D. Mares, O. Lyutakov, M. Kostejn, L. Lapcak, V. Švorčík, *J. Mater. Chem. C* **2015**, *119*, 9506.

[4] J. Svanda, Y. Kalachyova, P. Slepicka, V. Svorcik, O. Lyutakov, *ACS Appl. Mater. Interfaces* **2016**, *8*, 225.

[5] W. S. Cai, J. S. White, M. L. Brongersma, *Nano Let.* **2009**, *9*, 4403.

[6] K. F. MacDonald, N. I. Zheludev, *Laser Photon. Rev.* **2010**, *4*, 562.

[7] Y. Kalachyova, D. Alkhimova, M. Kostejn, P. Machac, V. Svorcik, O. Lyutakov, *RSC Adv.* **2015**, *5*, 92869.

[8] C. L. Wong, M. Olivo, *Plasmonics* **2014**, *9*, 809.

[9] S. Unser, I. Bruzas, J. He, L. Sagle, *Sensors* **2015**, *15*, 15684.

[10] R. Wilson, *Chem. Soc. Rev.* **2008**, *37*, 2028.

[11] A. C. Manikas, F. Causa, R. Della Moglie, P. A. Netti, *ACS Appl. Mater. Interfaces* **2013**, *5*, 7915.

[12] M. F. Maitz, U. Freudenberg, M. V. Tsurkan, M. Fischer, T. Beyrich, C. Werner, *Nat. Commun.* **2013**, *4*, 2168.

[13] M. A. C. Stuart, W. T. S. Huck, J. Genzer, M. Muller, C. Ober, M. Stamm, G. B. Sukhorukov, I. Szleifer, V. V. Tsukruk, M. Urban, F. Winnik, S. Zauscher, I. Luzinov, S. Minko, *Nat. Mater.* **2010**, *9*, 101.

[14] M. S. Yavuz, Y. Cheng, J. Chen, C. M. Cobley, Q. Zhang, M. Rycenga, J. Xie, C. Kim, K. H. Song, A. G. Schwartz, L. V. Wang, Y. Xia, *Nat. Mater.* **2009**, *8*, 935.

[15] D. D. Diaz, D. Kuhbeck, R. J. Koopmans, *Chem. Soc. Rev.* **2011**, *40*, 427.

[16] L. Wang, X. Zhao, Y. Zhang, W. Zhang, T. Ren, Zh. Chen, F. Wang, H. Yang, *RSC Adv.* **2015**, *5*, 40437.

[17] C. Fernández-López, L. Polavarapu, D. M. Solís, J. M. Taboada, F. Obelleiro, R. Contreras-Cáceres, I. Pastoriza-Santos, J. Pérez-Juste, *ACS Appl. Mater. Interfaces* **2015**, *7*, 12530.

[18] T. Ding, Ch. Rüttiger, X. Zheng, F. Benz, H. Ohadi, G. A. E. Vandenbosch, V. V. Moshchalkov, M. Gallei, J. J. Baumberg, *Adv. Opt. Mater.* **2016**, *4*, 877.

[19] M. Nguyen, A. Kanaev, X. Sun, E. Lacaze, S. Lau-Truong, A. Lamouri, J. Aubard, N. Felidj, C. Mangeney, *Langmuir* **2015**, *31*, 12830.

[20] Y. Zheng, A. H. Soeriyadi, L. Rosa, S. H. Ng, U. Bach, J. J. Gooding, *Nat. Comm.* **2015**, *6*, 8797.

[21] Q. Zhou, G. Meng, P. Zheng, S. Cushing, N. Wu, Q. Huang, Ch. Zhu, Zh. Zhang, Zh. Wang, *Sci. Rep.* **2015**, *5*, 12865.

ChemNanoMat 10.1002/cnma.201600284

[22] H. Gehan, L. Fillaud, M. M. Chehimi, J. Aubard, A. Hohenau, N. Felidj, C. Mangeney, *ACS Nano* **2010**, *4*, 6491.

[23] V. D. Filimonov, M. E. Trusova, P. S. Postnikov, A. E. Krasnokutskaya, Y. M. Lee, H. Y. Hwang, H. Kim, K.-W. Chi, *Org. Lett.* **2008**, *18*, 3961.

[24] Y. Kalachyova, O. Lyutakov, P. Slepicka, R. Elashnikov, V. Svorcik, *Nanoscale Res. Lett.* **2014**, *9*, 591.

[25] Y. Kalachyova, D. Mares, V. Jerabek, K. Zaruba, P. Ulbrich, L. Lapcak, V. Svorcik, O. Lyutakov, *J. Phys. Chem. C* **2016**, *120*, 10569.

[26] A. Mesnage, X. Lefèvre, P. Jégou, G. Deniau, S. Palacin, *Langmuir* **2012**, *28*, 11767.

[27] O. A. Guselnikova, A. I. Galanov, A. K. Gutakovskii, P. S. Postnikov, *Beilstein J. Nanotechnol.* **2015**, *6*, 1192.

[28] L. Laurentius, S. R. Stoyanov, S. Gusarov, A. Kovalenko, R. Du, G. P. Lopinski, M. T. McDermott, *ACS Nano* **2011**, *5*, 4219.

[29] M. E. Harmon, D. Kuckling and C. W. Frank, *Macromolecules* **2003**, *36*, 162.

[30] M. E. Harmon, D. Kuckling, P. Pareek and C. W. Frank, *Langmuir* **2003**, *19*, 10947.

[31] I. Tokarev, S. Minko, *Soft Matter* **2009**, *5*, 511.

[32] M. E. Harmon, T. A. M. Jakob, W. Knoll and C. W. Frank, *Macromolecules* **2002**, *35*, 5999.

[33] X. Z. Zhang, Y. Y. Yang, T. S. Chung, K. X. Ma, *Langmuir* **2001**, *17*, 6094.

[34] R. A. Alvarez-Puebla, R. Contreras-Caceres, I. PastorizaSantos, J. Perez-Juste, L. M. Liz-Marzan, *Angew. Chem., Int. Ed.* **2009**, *48*, 138.

[O35] Y. Zhou, J. Cao, J. Zhao, Y. Xie, J. Fei, Y. Cai, *Microchim. Acta* **2016**, *183*, 2501.

[36] Y. Dou, J. Han, T. Wang, M. Wei, D. G. Evans, X. Duan, *Langmuir* **2012**, *28*, 9535.

[37] J. Song, P.Huang, H. Duan, X. Chen, *Acc. Chem. Res.* **2015**, *48*, 2506.

[38] P. Mpountoukas, A. Pantazaki, E. Kostareli, P. Christodoulou, D. Kareli, S. Poliliou,. *Food Chem. Toxicol.* **2010**, *48*, 2934.

[39] M S. Khehra, H. S. Saini, D. K. Sharma, B. S. Chadha, S. S. Chimni, *Dyes Pigm.* **2006**, *70*, 1.

[40] F. Casadio, K. Mauck, M. Chefitz, R. Freeman, *Appl. Phys. A* **2010**, *100*, 885.

[41] B. Lee, J. H. Kang, I. Jo, D. Shin, B. H. Hong, Phys. *Chem. Chem. Phys.* **2016**, *18*, 3413.

[42] S. Dhakal, K. Chao, W. Schmidt, J. Qin, M. Kim, D. Chan, *Foods* **2016**, *5*, 36.

[43] E. C. Le Ru, E. Blackie, M. Meyer, P. G. Etchegoin, *J. Phys. Chem. C* **207**, *111*, 13794.

[44] Y. Lu, G. L. Liu, L. P. Lee, *Nano Lett.* **2005**, *5*, 5.

[45] L. Hu, M. J.Serpe, *ACS Appl. Mater. Interfac.* **2013**, *5*, 11977.

[46] J. B. Smiley-Wiens, M. J. Serpe, *Colloid Polym. Sci.*, **2013**, *291*, 971.

ChemNanoMat 10.1002/cnma.201600284

[47] L. Rodríguez-Lorenzo, R. A. Álvarez-Puebla, I. Pastoriza-Santos, S. Mazzucco, O. Stéphan, M. Kociak, L. M. Liz-Marzan, F. J. García de Abajo, J. Am. Chem. Soc. 2009, 131, 4616.

[48] A. Dandapat, T. K. Lee, Y. Zhang, S. K. Kwak, E. C. Cho, D.-H. Kim, *ACS Appl. Mater. Interfaces* **2015**, *7*, 14793.

Figure caption

Fig. 1 Schematic representation of plasmon-active grating functionalization by PNIPAm.

Fig. 2 Dependence of the refraction coefficient (measured at 632 nm wavelength) of functional gold grating on the temperature

Fig. 3 Dependence of the water contact angle measured on the gold grating grafted with PNIPAm on the temperature

Fig. 4 Effect of repeated cycles of heating/cooling on the water contact angle measured on functional gold grating

Fig. 5 Surface topography, mechanical and adhesion properties of gold grating grafted with PNIPAm, measured at 25 and 45°C in water medium.

Fig. 6 Z-potential measured on the functional metal surface at the different pH and temperatures above and below PNIPAm phase transition.

Fig. 7 Cyclic voltammograms of potassium ferrocyanide (c =1 mM) in potassium nitrate (c = 0.1 M) (A) at two different temperatures (25 and 45°C) at a plain gold film electrode and at gold film electrodes with grafted pNIPAM and (B) at gold film electrodes with grafted pNIPAM (serial number of scan is displayed below the curve).

Fig. 8 SERS spectra of several dyes entrapped from solution and pressed against the plasmonically-active gold surface by the PNIPAm phase transition.

Fig. 9 Raman spectra of CV entrapped by PNIPAm phase transition from solution with different dye concentration.

Fig. 10 SERS activity at the different stages of the sensing scheme (from top to bottom): analyte trapped (CV in concentration 10^{-14} M), washed by heating above LCST, analyte trapped (ME in concentration 10^{-14} M), washed by heating above LCST, trapped (DR1 in concentration 10^{-14} M), washed by heating above LCST,

Fig. 11 Cycling SERS activity (3 cycles of entrapping and washing for every sample) of PNIPAM-modified gold grating with entrapped DR1 at 10^{-8} M concentration

ChemNanoMat 10.1002/cnma.201600284

Table 1

Samples	Target molecules	MDC, mol.l^{-1}	Reference
PNIPAM film-Ag NPs coated by oleic acid and oleylamine	Rhodamin 6G	10^{-5}	[44]
PNIPAM coated AuNPs	1-naphtalenethiol,, Nile Blue A, 1-naphthol	10^{-6}	[34]
Au-coated silicon wafers-PNIPAM-AuNPs	Methylene blue	10^{-4}	[22]
Au triangles-PNIPAM-Au NRs	Nile Blue A	10^{-6}	[19]
AuNRs-PNIPAM-ZnONTs coated by AgNPs	p-aminothiophenol, Rhodamin 6G	10^{-6}	[21]
Au-coated silicon wafers-AuNPs-PNIPAM	Rhodamin 6G, crystal violet	10^{-9}	[20]
Au grating-PNIPAM	***Crystal violet, metanil yellow, disperse red I***	***10^{-14}***	***This work***

ChemNanoMat 10.1002/cnma.201600284

TOC

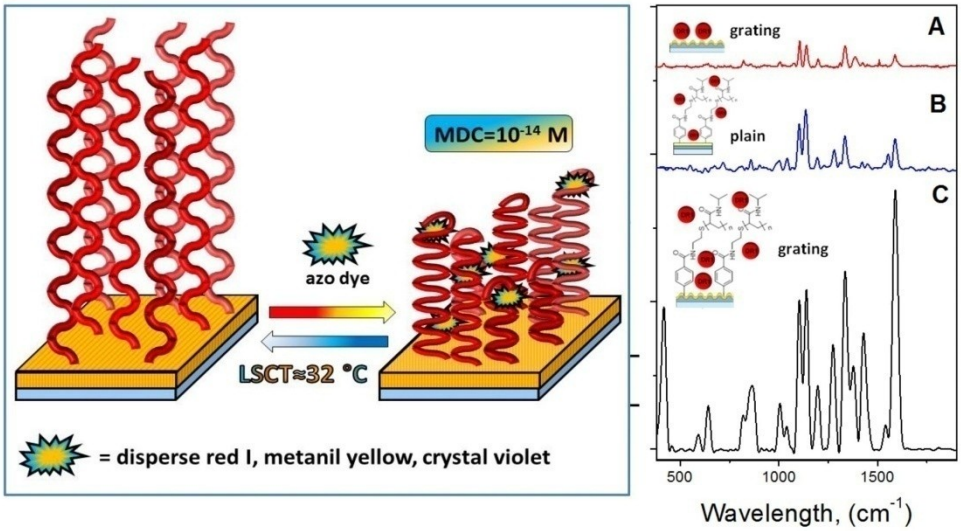

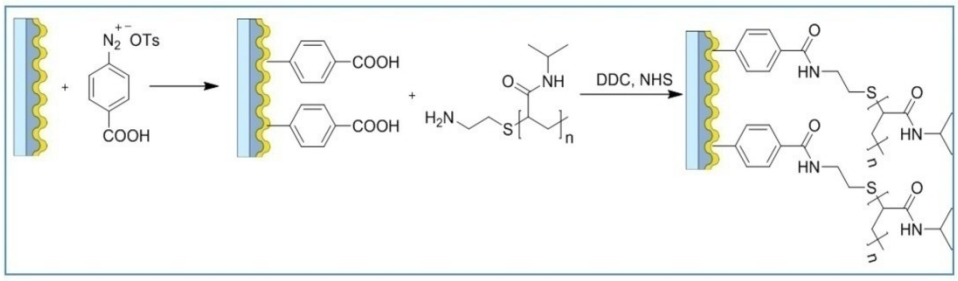

Fig. 1

ChemNanoMat 10.1002/cnma.201600284

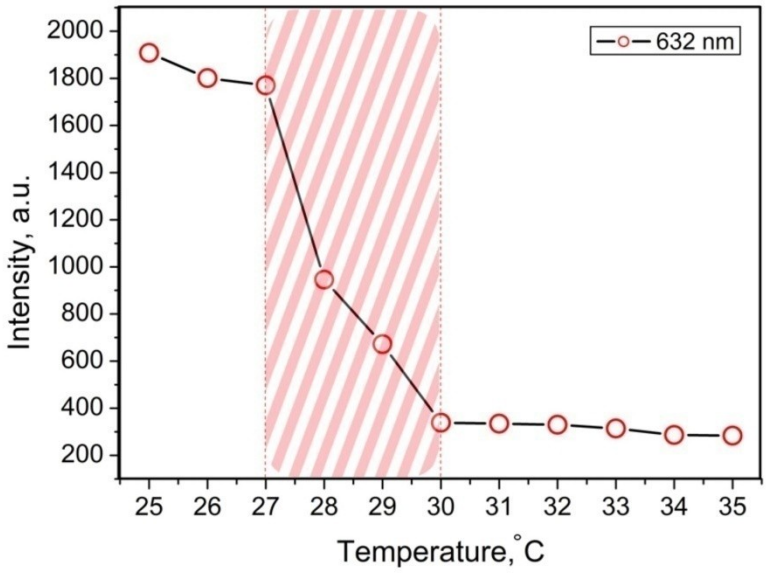

Fig. 2

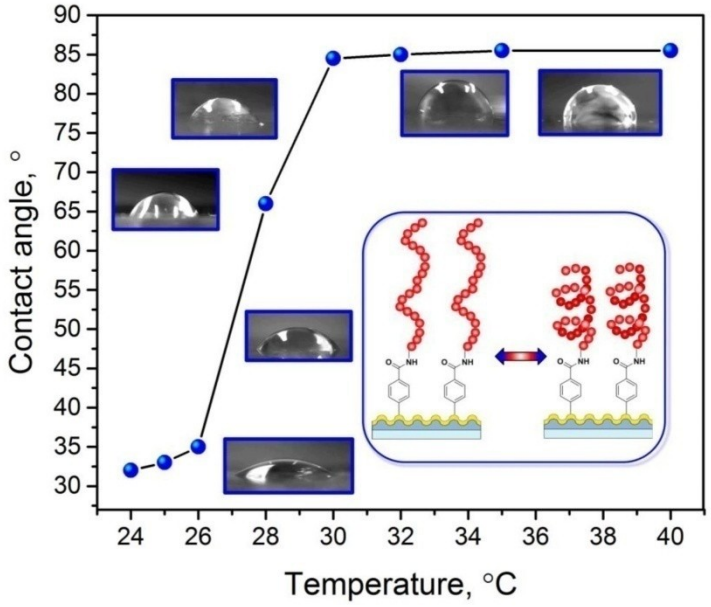

Fig . 3

ChemNanoMat 10.1002/cnma.201600284

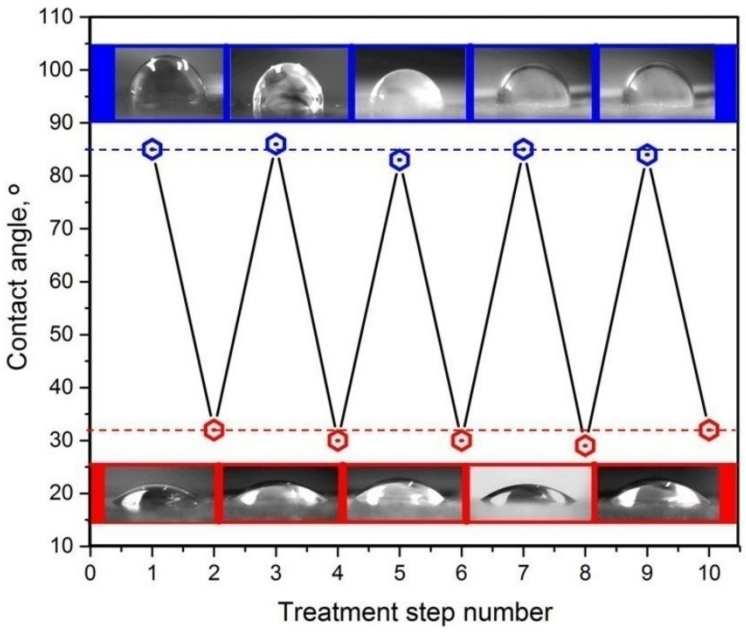

Fig. 4

ChemNanoMat 10.1002/cnma.201600284

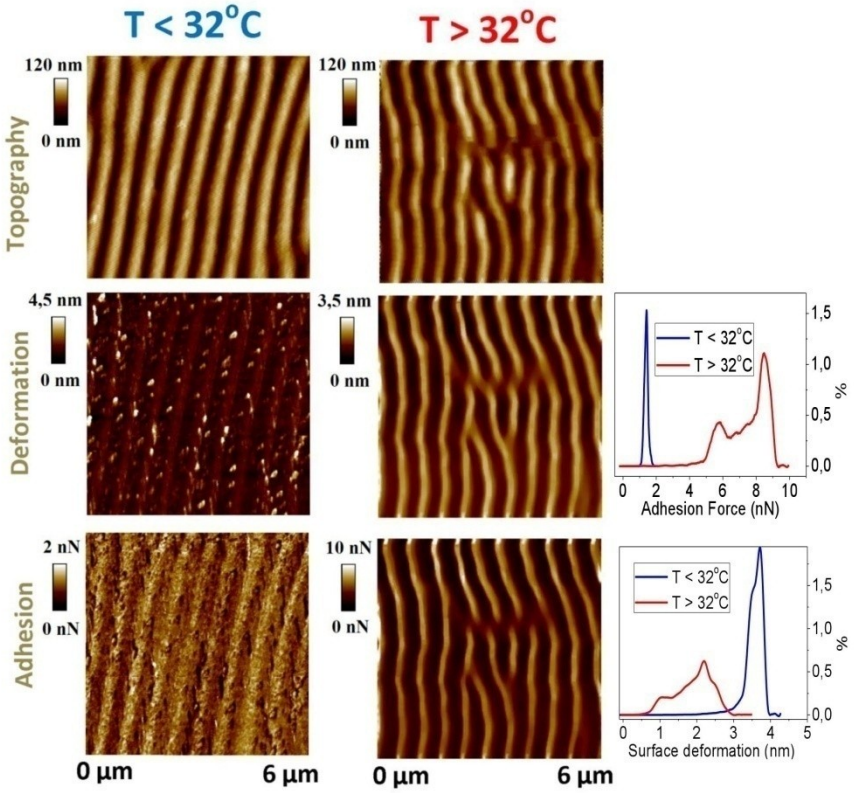

Fig. 5

ChemNanoMat 10.1002/cnma.201600284

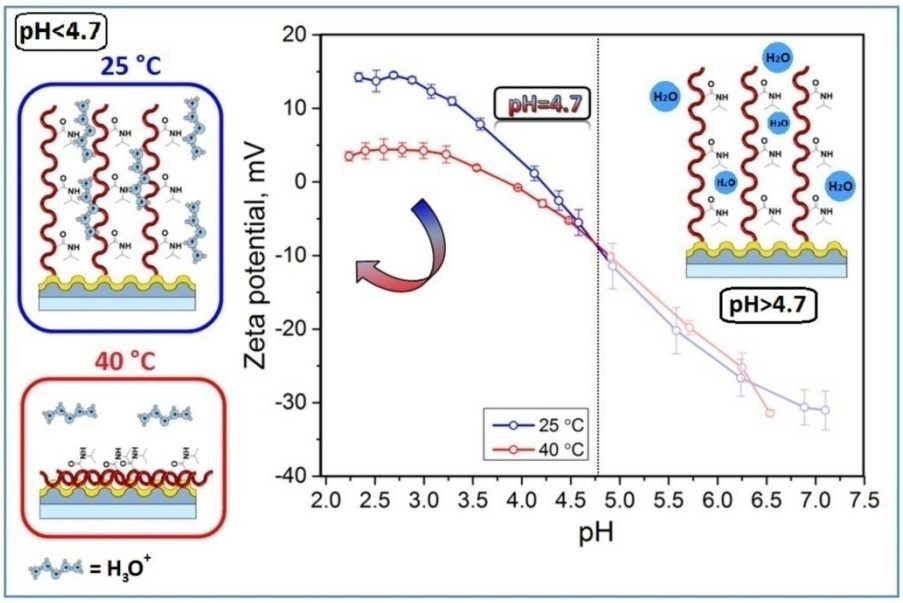

Fig. 6

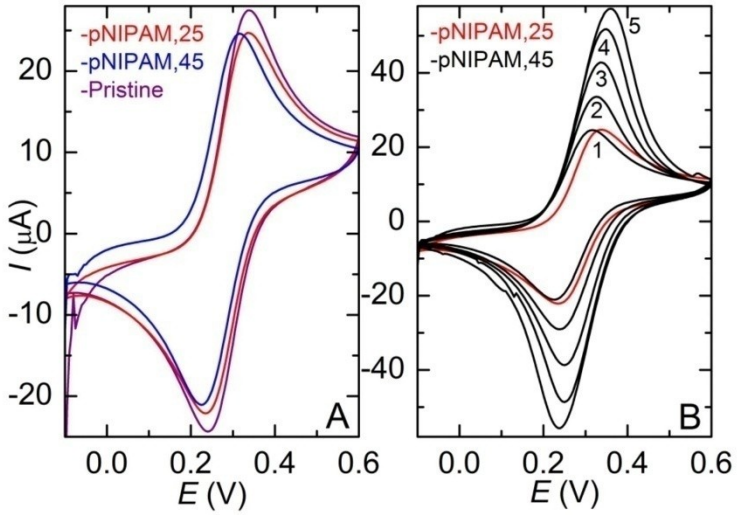

Fig. 7

ChemNanoMat 10.1002/cnma.201600284

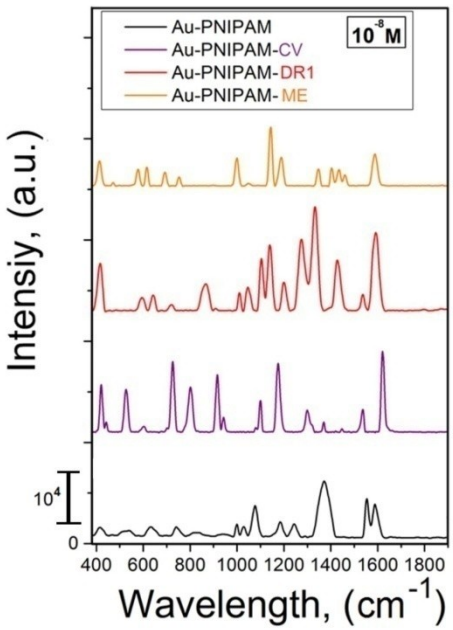

Fig. 8

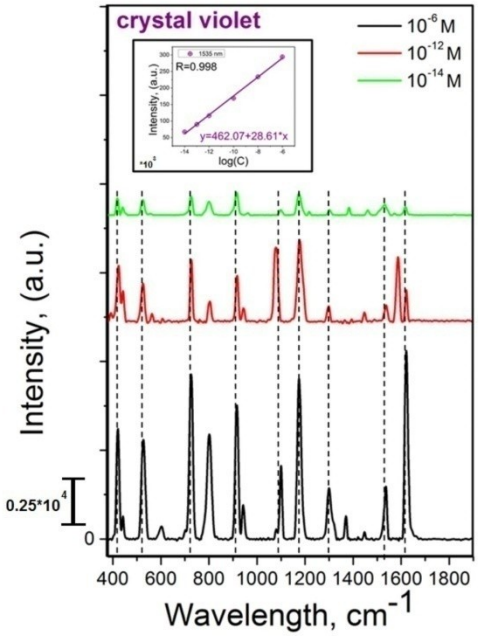

Fig. 9

ChemNanoMat 10.1002/cnma.201600284

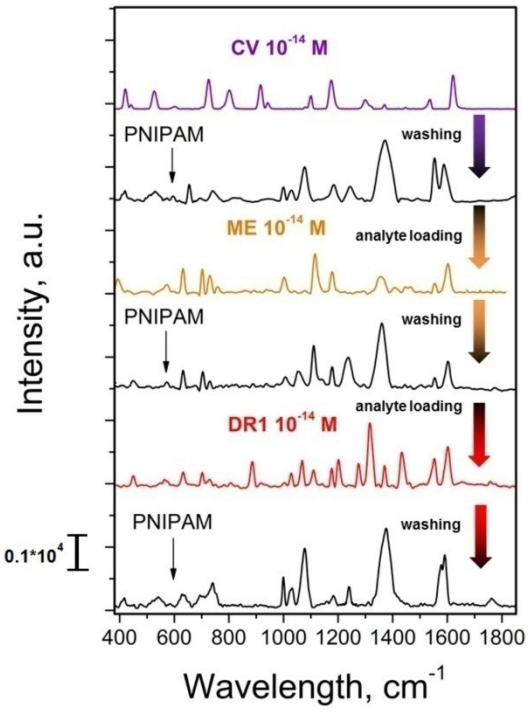

Fig. 10

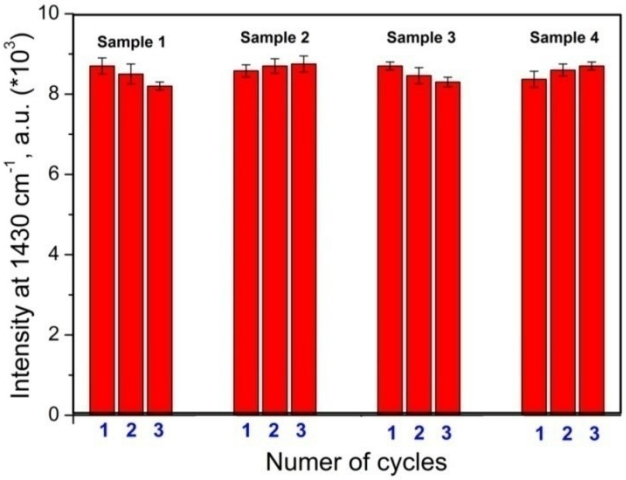

Fig. 11

11. Appendix V

Surface modification of Au and Ag plasmonic thin films via diazonium chemistry: evaluation of structure and properties

Guselnikova Olga, Postnikov Pavel, Elashnikov Roman, Trusová Monika, Kalachyova Yevgeniya, **Libánský Milan**, Barek Jiří, Kolská Zdeňka, Švorčík Václav, Lyutakov Oleksiy

Colloids and Surfaces A: Physicochemical Engineering Aspects

In Press, Year 2016

Accepted Manuscript

Title: Surface modification of Au and Ag plasmonic thin films via diazonium chemistry: evaluation of structure and properties

Author: O. Guselnikova P. Postnikov R. Elashnikov M. Trusova Y. Kalachyova M. Libansky J. Barek Z. Kolska V. Švorčík O. Lyutakov

PII: S0927-7757(16)31083-4
DOI: http://dx.doi.org/doi:10.1016/j.colsurfa.2016.12.040
Reference: COLSUA 21247

To appear in: *Colloids and Surfaces A: Physicochem. Eng. Aspects*

Received date: 10-10-2016
Revised date: 19-12-2016
Accepted date: 22-12-2016

Please cite this article as: O.Guselnikova, P.Postnikov, R.Elashnikov, M.Trusova, Y.Kalachyova, M.Libansky, J.Barek, Z.Kolska, V.Švorčík, O.Lyutakov, Surface modification of Au and Ag plasmonic thin films via diazonium chemistry: evaluation of structure and properties, Colloids and Surfaces A: Physicochemical and Engineering Aspects http://dx.doi.org/10.1016/j.colsurfa.2016.12.040

Surface modification of Au and Ag plasmonic thin films via diazonium chemistry: evaluation of structure and properties

O. Guselnikova[a,b], P. Postnikov[b*], R. Elashnikov[a], M. Trusova[c], Y. Kalachyova[a], M. Libansky[d], J. Barek[d], Z. Kolska[e], V. Švorčík[a], O. Lyutakov[a,b*]

[a] *Department of Solid State Engineering, University of Chemistry and Technology Prague, Czech Republic*

[b] *Department of Technology of Organic Substances and Polymer Materials, Tomsk Polytechnic University, Russia*

[c] *Department of Bioengineering and Organic Synthesis, Tomsk Polytechnic University, Russia*

[d] *UNESCO Laboratory of Environmental Electrochemistry, Department of Analytical Chemistry, Faculty of Science, Charles University in Prague, Czech Republic*

[e] *Faculty of Science, J. E. Purkyne University, Usti nad Labem, Czech Republic*

** Corresponding author: lyutakoo@vscht.cz, postnkov@tpu.ru*

Graphical Abstract

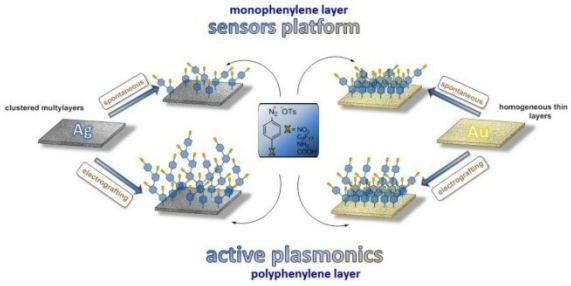

Highlights

- The Au and Ag thin films were modified using diazonium approach.
- In particular, spontaneous and electrochemically grafting methods were investigated.
- The modified surfaces were investigated with a variety of techniques.
- The possibility to tune the surface properties of metals into desired range was demonstrated.

Abstract

Plasmon-active noble metals nanostructures based on Ag and Au thin films become widely applied in the field of plasmonics and related sensing technologies. For improvement of the metal interaction with different media, metals surface can be functionalized in order to increase/decrease hydrophilicity, lipophilicity or introduce/change the surface charge. In this paper, the surface functionalization of plasmon-active Au and Ag films using arenediazonium tosylates was described. The surface functionalization was performed in the aqueous medium by the spontaneous and electrically induced mechanisms. Functionalized surfaces were characterized by the Raman and UV-Vis spectroscopies, AFM nanomechanical mapping, SEM (EDX), XPS, CVA, zeta- potential, and water contact angle measurement techniques. It was founded that the key difference between reactivity of gold and silver films is distributional behavior of grafted organic functional groups: silver has higher tendency to form clustered, island-like structure while gold is covered more homogeneously. Spontaneous modification forms approximately monomolecular thick films of organic compounds and can be used in the field of SPR or SERS sensors. Electrochemically induced activation produces thick polyphenylene layer on the metal surface and can find application in the field of tunable plasmonic devices or plasmon-based lasers.

Keywords: surface modification; plasmonic thin films; surface properties; diazonium chemistry

1. Introduction

The light interaction with free electrons confined in the metal nanostructures leads to the surface plasmon excitation and focusing of light into small, subwavelength, closed to surface volumes. The typical wavelengths of surface plasmon lie in the nanometers range and the plasmon intensity decays exponentially in the direction of the metal-dielectric boundary.[1] This spatial concentration and localization of light provide various interesting applications of plasmonics: surface-enhanced optical spectroscopies, sensor technologies, energy harvesting and super-resolution optical imaging.[2] These plasmonic opportunities became fundamentals for sensor platforms based on SEF (surface-enhanced fluorescence), SPR (surface plasmon resonance) and SERS (surface enhanced Raman scattering) for the detection of trace molecules in chemistry and biology,[3-7] ultrasmall plasmonic lasers,[8] ultracompact nanophotonic optical circuits,[9] tunable plasmonics switchers with ultrafast response,[10-12] or optical tweezers working at low light intensity.[13]

Considering the plasmon excitation by visible light, collective electronic motions in the noble metals nanostructures (especially Au and Ag) are most appropriate for plasmonic applications .[14] Gold surfaces are a common choice because of high stability and well-known versatile chemistry, based on the formation of surface attached monolayer.[15] However, gold substrates can be used only in the longer-wavelength part of the visible light spectrum because of the interbands electron transition.[16] Oppositely, silver nanostructures demonstrate a sharper angular resonance in comparison with gold and give enhanced plasmon properties. Unfortunately, poor stability of silver restricts its applications in the plasmonic field. Immobilization of organic compounds on the silver surface can increase the stability of metal plasmon-active structure against oxidation and aging.[17, 18] Functionalization of noble metal surfaces by organic molecules is used not only for increasing of plasmonic structures stability. Also, deposition of additional layers on the plasmon-active substrate can significantly increase the amount of the attached analyte molecules decreasing the minimum of detectable concentration and increasing the reproducibility of SERS and SPR.[19, 20] Organic molecules provide a wide range of stimuli-responsive properties, where the dielectric function of such molecules can be changed by the external stimuli.[21] These responsive properties are used for a broad range of tunable plasmonic devices, in order to shift plasmon wavelength position or to affect its amplitude.[21, 22] Also, additional promising application is the preparation of plasmon-based lasers using immobilization of optically active organic compounds.[23]

Taking into account the distribution of plasmon intensity, coverage of surface by organic molecules is standing out as a key point for successful plasmonic device realization. The thickness of organic layer must be carefully chosen, depending on the different applications scenarios. In particular, the SERS and SPR applications requires surface functionalization by the thin molecular

layer, to conserve the maximal interaction of plasmon with analyte, which interacts with modified metal surface.[20, 24] Oppositely, for plasmonic laser or switches large thickness of attached organic molecules is desired.[21-23] Thus, development of surface modification method with controllable resulting thickness of organic layer is still challenging for plasmonic metal surfaces.[25] Chemical functionalization by thiol derivatives is one of the most commonly used approaches for the decoration of plasmonic substrates with organic functional groups (OFGs).[26, 27] However, a number of authors underlined some disadvantages of this strategy - moderate stability (including thermal) of metal-thiol bonds, formation of only monolayers, reversibility and possibility of displacement by other thiols.[28, 29]

An attractive alternative to thiol's chemistry is the grafting of OFGs by arenediazonium salts (ADSs) because high reactivity of the aryl radicals results in the generation of aryl layers strongly covalently bounded to metal surface.[30-33] Surface diazonium chemistry is well-proven for a wide range of materials, including metal substrates (gold, silver, iron, copper, zinc, nickel etc.).[34, 35] Most of the actual works report functionalization of electrodes or bulk metals using electrografting or spontaneous attachment of diazonium salts. [36-38] On the other hand, diazonium chemistry has not been widely employed for functionalization of plasmonic active thin metal films. McCreery and coworkers reported only spontaneous (not electrochemical) attachment of nitroazobenzene by chemisorption on plasmonic silver films in acetonitrile[39,40] and the influence of modification method (spontaneous or induced) on optical properties of thin metal films has not been examined yet. Continuing with gold films, there are quite a lot of works about modification of gold surfaces by diazonium salt in acetonitrile. Diazonium derived nitrophenyl groups were deposited by spontaneous reaction with gold films surfaces (50-150 nm). [29] Modification of 100 nm thick gold-coated silicon wafers was demonstrated by the electrografting of acetonitrile solutions containing a diazonium salt and an alkyl iodide.[41] However, optical and plasmonic properties of both prepared materials have not been discussed. One of the most interesting example of thin gold film modification is preparation of antifouling surface coating by electrografting of 4-phenylalanine on 50 nm gold film, where antifouling properties were monitored by SPR.[42] Owing to great promises of covalently modified noble metal thin films in field of plasmonic component and devices, there is a need for detailed examination of bonded organic layers structure and mechanism of its attachment using diazonium salts.

In this work the surface modification of thin silver and gold films by spontaneous reaction or electrochemical reduction of water-soluble arenediazonium tosylates (ADTs) was demonstrated (Figure 1). After grafting the surface and optical properties were characterized by the wide range of techniques. We have conducted detailed comparative research of surface properties on prepared materials and hypothesized appropriate modification conditions for certain optical application.

2. Experimental

2.1 Materials

Silver and gold were deposited onto glass surface (Thermo Scientific), covered by transparent titanium layer (thickness ca 10 nm), using vacuum sputtering method (DC Ar plasma, gas purity - 99.995 %, gas pressure 4 Pa, discharge power 7.5 W, sputtering time 120 sec, resulted thickness 18.5 nm for Au and 14.1 for Ag). Targets for metals deposition (purity of metals 4 N) were purchased from Safina. 4-nitrobenzenediazonium tosylate, 4-carboxybenzenediazonium tosylate, 4-aminobenzenediazonium tosylate and 4-(heptadecafluorooctyl)benzenediazonium tosylates were prepared according to published procedure.[43]

2.2 Sample preparation

The 4-nitrophenyl, 4-carboxyphenyl, 4-aminophenyl and 4-(heptadecafluorooctyl)phenyl organic functional groups (OFGs) were grafted spontaneously by soaking of the freshly obtained Ag and Au films in 1 mM freshly prepared solutions of corresponding arenediazonium tosylates in deionized water for 10 min (for 4-(heptadecafluorooctyl)benzenediazonium tosylate mixture of water/ethanol (3/1) was used). Electrografting of Ag and Au was performed in 1mM fresh water solutions of corresponding diazonium salts (for 4-(heptadecafluorooctyl)benzenediazonium tosylate mixture of deionized water/ethanol (3/1) was used) without addition of any electrolytes under the potential -2 V for 10 min with a platinum counter electrode. After modification metal substrates were rinsed under sonication sequentially with deionized water, ethanol, and acetone for 10 min and dried in desiccator for 3 hours.

2.3 Measurement techniques:

2.3.1 Wettability

Water contact angles were measured by goniometer Surface Energy Evaluation System (Masaryk University, Czech Republic) at 10 positions with distilled water at room temperature 24 h after surface modification. The deviation between measurements was used for the calculation of measurements errors.

2.3.2 Atomic-force microscopy

For characterization of sample surface and nanomechanical mapping before and after surface modification, the peak force AFM technique was applied. Surface mapping was performed with Icon (Bruker) set-up on the areas of 1.5x1.5 μm^2. Conducted measurements were performed in Peak Force AFM mode, using the Pt/Pd coated tip with constant voltage (3V). Tuna current parameter was evaluated. AFM scratch test was carried out on metal films by profiling across a scratch at an angle of 90 degrees relative to the surface. Then the sample was cleaned by washing in an acetone bath for a few seconds, dried with nitrogen gas, and imaged with the AFM. The reported

film thicknesses are the means of at least 16 values obtained from three scratches, and the uncertainty is the standard deviation of the mean.

2.3.3 X-ray photoelectron spectroscopy

X-ray photoelectron spectroscopy (XPS) was used to determine the surface chemical composition. The spectra were recorded using an Omicron Nanotechnology ESCAProbeP spectrometer fitted with monochromated Al K Alpha X-ray source. The pass energy was set at X (eV) and Y as intensity (cps) for the survey and high resolution spectra, respectively. Since the metal films were deposited on the glass substrates the law energy compensation (up to 2eV) was applied during measurements. The energy resolution was 0.4 eV for the measurement of full XPS spectrum and 0.1 eV for the measurement of individual peak detail. The analyzed area had dimensions of 2x3 mm^2. Concentrations of elements were calculated in at. % using the manufacturer's sensitivity factors.

2.3.4 Scanning electron microscopy

The scanning electron microscopy (SEM) (LYRA3 GMU, Tescan, CR) was used for the study of morphology and elements distribution of the pristine and modified Au and Ag films. SEM images and mapping were performed using an energy dispersive spectroscopy (EDX, analyser X-MaxN, 20 mm2 SDD detector, Oxford instruments). The samples were attached by carbon conductive tape to avoid sample charging. SEM-EDX and SEM measurements were carried out using accelerating voltages 10 kV and 2 kV respectively. The obtained EDX mappings were processed using the software ImageJ.

2.3.5 Cyclic voltammetry

Cyclic voltammograms (CV) of pristine and modified films were obtained using 1 mM potassium hexacyanoferrate (II) in 0.1 M potassium chloride (p.a., Lachema, Czech Republic) for gold films and with 1 mM Hexaammineruthenium (III) chloride (98%, Sigma Aldrich, USA) in 0.1 M potassium sulphate (p.a., Lachema, Czech Republic) for silver films. Volume of the drop, deposited for the measurement was 10 µL. Cyclic voltammetry was carried out with working gold film electrodes with an exposed area of 3 mm^2 with deposited thin tail, when contact to potentiostat was connected. Voltammetric measurements were performed with portable potentiostat PalmSens (Palm Instruments, Netherlands), controlled by PSTrace 4.6.1 software (4.4 firmware). Parameters of the CV potential program were: 50 mV s^{-1} scan rate and potential range from -100 mV to 600 mV for the gold films and from 50 mV to -300 mV for the silver films. CV measurements were carried out with platinum wire auxiliary electrode and miniaturized Ag/AgCl (3 M KCl) gel leakless reference electrode (EE009, ESA Cypress Systems, Massachusetts, USA), to which all potentials

values are referred. All measurements were repeated three times with five scans for each measurement, unless stated otherwise.

2.3.6 Electrokinetic analysis

Electrokinetic analysis (zeta potential) of all samples were determined by SurPASS Instrument (Anton Paar GmbH, AT). Samples were studied inside the adjustable gap cell with an electrolyte of 0.001 M KCl. All samples were measured four times at constant pH 6.3 and at room temperature. For zeta potential determination the streaming current method and Helmholtz-Smoluchowski (HS) equation were used with experimental error of 5 %.[44]

2.3.7 Optical measurements

UV-Vis spectra were measured using Spectrometer Lambda 25 (Perkin-Elmer) in 300-1100 nm wavelength range.

Raman scattering was measured on Nicolet Almega XR spectrometer (Laser power 15 mW) Raman spectrometers with 470 and 785 nm excitation wavelengths. Spectra were measured 10 times, each of them with 30 s accumulation time.

3. Results and Discussion

In the present work we report comprehensive study of structure and surface properties of plasmonic active Au and Ag films functionalized by ADTs (see Figure 1), which possess a key advantage over classical diazonium salts.[45, 46] ADTs demonstrate explosion safety, storage stability and good solubility in a wide range of organic solvents and water. Especially last property is favorable, since it allows the electrochemical and spontaneous grafting in water, without addition of some special electrolytes. In this work, we chose silver and gold metals, known as plasmonic active substrates. The main difference between them lies in „working wavelength". Silver has the plasmon resonance in 400-600 nm range, depending on the size and shape of nanostructures. For gold more typical plasmon resonance band lies at longer wavelength. Thus, both metals are complementary in the sense that they fully cover the optical wavelengths range.

Firstly, the metals surfaces were modified by 4-nitrobenzenediazonim tosylate (ADT-NO_2) and 4-(heptadecafluorooctyl)benzenediazonium tosylate (ADT-C_8F_{17}) as the model modification agent (due to a large basis of data about these compound grafting and significant changes of surface properties after introduction of perfluoro-derivatives).[47] Secondly, modification by 4-aminobenzenediazonium tosylate (ADT-NH_2) and 4-carboxy benzenediazonium tosylate (ADT-COOH) was performed and investigated, because these functional groups are able to create specific surface properties or selective sites for further modification.[36,38]

Taking into account different potential application of the plasmonic surface modification, which can require monomolecular or polyphenylene layers of grafted molecules, the surface modification was performed by two procedures, shown schematically in Figure 1. Modification mechanisms usually involve dediazoniation leading to spontaneously generation of reactive cations or radicals, which are able to graft spontaneously on electron-rich surfaces such as metals and form approximately monomolecular layers.[28, 29, 48] Oppositely, electrically induced process results in thicker and less ordered organic layers due to enhanced reduction of ADSs.[49, 50] Thus, application of spontaneous surface modification will lead to the formation of thin layer, suitable for sensor applications, and the electro-induced modification will create thicker layer applicable in plasmonic-based switchers or lasers.

3.1 XPS

The changes in surface elemental concentration after OFGs grafting was studied using XPS method. The results, presented in Table 1, show elemental surface concentrations on pristine and modified samples (full XPS graphs are given in the supporting information – Figure S1). On the pristine samples the presence of carbon and oxygen traces are apparent, indicating the metals deposition imperfection which is typical case for the sputtering procedure. Characteristic peaks for grafted OFGs are observed in XPS spectra in accordance with the results published previously.[29,51] As could be expected, the electrochemical grafting resulted in greater increase of carbon, nitrogen and fluorine concentrations comparing to spontaneous modification. Considering the Au and Ag surfaces, the changes in the carbon concentration are comparable. Grafting of ADT-NO_2 resulted in the appearance of nitrogen-related XPS peak. Surprisingly, we did not observe characteristic peak at 400 eV, corresponding to –N=N- group formation, which was observed previously.[33] Comparison between gold and silver surfaces shows slightly lower nitrogen concentration on the silver substrate. Grafting of ADT-C_8F_{17} groups has led to similar result: apparently higher concentration of fluorine in the case of electro modification.

3.2 AFM scratch test

Thicknesses of grafted organic layers were measured by scratch method using the AFM technique by profiling across a scratch in the film (Table 2). The reported film thicknesses are the means of at least 16 values obtained from three scratches. The surface roughness of metal films (Tab. S1, Fig. S4) allows the measurement of thickness with at least 0.2 nm precision. Table 2 gives the thickness variation for pristine, spontaneously and electrochemically modified by ADT-NO_2 and ADT-C_8F_{17} thin metal films. The layer thickness after modification with species of known molecular size enables one to discern the grafting of monophenylene or polyphenylene organic layer. As the length of 4-nitrobenzene molecule is ≈ 0.8 nm, the film prepared by spontaneous modification on gold is consistent with a multilayer structure comprising from 2 to 3 phenylene layers.[52] After spontaneous

modification of gold by ADT-C_8F_{17}, organic layer is close to a monophenylene layer, (length of 4-(heptadecafluorooctyl)benzene molecule is ≈ 1.6 nm) (Figure S2). Hence, we suppose that formation of monophenylene layer structure can be explained by hindered attack of formed on surface 4-(heptadecafluorooctyl)phenyl layers, i.e. the effect that is typical for sterically hindered molecules (Figure S2).[53] Therefore, even electrochemical modification of gold by ADT-C_8F_{17} has led to formation of thin polyphenylene layer (approximately 4 molecules). In the case of electrochemically grafted ADT-NO_2, we have observed formation of structures with more than 8 phenylene layers of nitrobenzene (7.1±0.3 nm), what is consistent with previously published data.[54] Similar results were obtained in the case of silver modification - formation of structures consisting of 2-3 phenylene layers of ADT-NO_2 and ADT-C_8F_{17} monophenylene layer in the case of spontaneous modification. Electrochemical modification of silver resulted in attachment of 11-12 phenylene layers of ADT-NO_2 and 6-7 phenylene layers of ADT-C_8F_{17}. According to scratch test, modification of silver resulted in the thicker organic films but XPS data demonstrate lower concentration of key elements, these findings point towards evidence of ”island-like” structured OFGs.

3.3 SEM-EDX

To verify these assumptions, spatial distribution of elements on the samples surface after OFGs grafting was determined using SEM-EDX methods, on the 1x1 μm^2 samples surface (Figure 2, Fig. S3). (It must be also noted, that present work is focused on the surface modification of plasmon-active metal films (i.e. noble metals film with a rough surface) and thus investigation of final grafted OFGs distribution by AFM topography images is restricted). Nitrogen and fluorine are specific markers for ADT-NO_2 and ADT-C_8F_{17} for the presented EDX maps of nitrogen (yellow) and fluorine (blue). Regions of EDX analysis are also presented in the Fig. 2 above the EDX maps.

In all cases the implementation of electro-induced modification mechanism has led to significantly greater concentration of nitrogen and fluorine. Moreover, difference between elements distribution on the gold and silver substrates was apparent. The gold surface was covered more homogeneously – the larger amount of small dots. Organic layer on the silver substrate showed the “island-like” structure – the fluorine and nitrogen appeared on limited number of larger dots. In order to prove these differences, we carried out the analysis of OFGs distribution. In assumption, that spot size on EDX-mapping correlates with element concentration at local places the spots size distribution for fluorine and nitrogen was calculated (the diagrams of distribution is presented in Figure S3). The results of analysis demonstrated that spontaneous reaction between ADTs and Ag surface led to formation of relatively large “islands” with narrow distribution. Conversely, in case of gold films, the reaction was conducted with formation of relatively small areas of OFGs with broad distribution. This tendency is kept during electrochemical process: the OFGs formed smaller areas

with broad distribution and larger areas with narrow distribution in case of gold and silver films correspondingly.

3.4 CVA

We supposed that observed differences in the structure of grafted organic layers are determined by the nature of metals, not by morphology of pristine metals films. To validate it, we carefully evaluated morphology of pristine films at different length scales using the AFM and 3D confocal techniques (results are presented in the Supplementary information – Figure S4, Table S1). Statistical analysis (R_a) did not show any significant difference between pristine Ag and Au films surface.

The surface blocking due to OFGs grafting was examined by CV methods performed using the solution of hexacyanoferrate (II) for gold and ruthenium (III) for silver (Figure 3) as the most relevant probes for these metals. On the CV curves, measured on pristine gold films the apparent positive and negative peaks located at 0.33 V are attributed to the Fe(II)/Fe(III) probe oxidation and reduction. After grafting of ADT-NO_2 by the spontaneous mechanism the peak becomes less pronounced, due to particular surface blocking by OFGs. When the electrochemically induced modification was applied, the Fe(II)/Fe(III) probe-related peaks fully disappeared, indicating the full blocking of surface, so that the hexacyanoferrate (II) cannot reach the metal surface. The situation was similar in the case of ADT-C_8F_{17} grafted by electrochemical mechanism when the Fe(II)/Fe(III) oxidation/reduction peak is also suppressed. However, spontaneous grafting of ADT-C_8F_{17} does not lead to full peak suppression (in the Fig. 3 the response of C_8F_{17} grafted surface are statistically the similar to pristine gold surface – the typical uncertainty of CV measurements is 5%, when solid metal electrodes are used), indicating the presence of unmodified electroactive surface.

CV curves of pristine and modified Ag films confirm the hypothesis about formation of organic layers with "island-like" structure. In case of unmodified silver, the surface is unblocked and broad peaks, associated with the electron transfer, due to efficient reduction (oxidation) of ruthenium (III) on the unprotected metal surface were observed. It should be noted that peak height slightly decayed on spontaneously and electrochemically modified film with a slight difference between each other. It is evident that both modification methods keep the surface electrochemically available. In comparison with gold films, electrochemical blocking does not occur in the case of electrochemically modified silver and electrochemical activity is conserved. The unexpected shift of the peak of ruthenium hexamine reduction/oxidation potential can be attributed to: (i) increase of the energy barrier and necessity to deliver more energy (potential) to cause a reaction on an electrode (the influence of grafting) or (ii) the decrease of reversibility of the redox system ($I_C/I_A \neq 1$). Similar shift of the peak maximum position was described in [55] and explained in terms

of the change electron transfer kinetics at the modified electrode surface. This potential shift highlighted the different morphology and different chemical behavior between the used electrodes.

3.5 Conductive AFM

Additional information, regarding the growth of OFGs on the Ag films through spontaneous or electrochemical mechanisms was taken using the conductive AFM technique (Figure S5 – supplementary information). Comparative analysis of graphs shows the conservation of significant conductivity of silver substrate after spontaneous modification and apparent decreasing of conductivity after electro-chemical grafting, which correlates well with XPS results – significantly greater amounts of OFGs grafted by electrochemical approach. However, in the last case several conductive spots were also detected (Figure S5) in good agreement with SEM –EDX and CVA results – some reduction/oxidation processes on the unprotected Ag surface is possible.

It may be concluded that XPS, EDX, and CV methods confirm grafting of ADTs to the thin metal films. In the case of spontaneous process, OFGs were grafted with formation of "island-like" structures, while electrochemical method resulted in thicker polyphenylene layers. The key difference between reactivity of gold and silver films is the distribution of grafted OFGs: silver tends to form clustered polyphenylene structure while gold is covered more homogeneously with thinner layers. The effect of radical size is more pronounced in the case of spontaneous modification, which leads to formation of monophenylene of attached molecules.

3.6 Oxidation experiments in water medium

Additional control experiments were performed by soaking of thin noble films in the deionized water for 15 min, in order to estimate the potential effect of interaction with water on film morphology and metal oxidation. We evaluated structure of water treated films using AFM and XPS techniques and results are given in SI (Figure S6, and Table S2). We observed that silver shows tendency to oxidation in water, while changes in gold films composition and structure are slightly detected. However, comparison with the data presented in the Tab. 1 indicates that metal oxidation is terminated by the formation of grafted organic layers. Additionally, soaking in the distilled water led to significant changes of silver thin film morphology, (corresponding Figure S6 is also given in the supplementary information). The observed effects confirm extremely high reactivity of diazo cations in reaction with noble metal surfaces. Modification reactions occurs significantly faster than interaction with water. Formed phenylene layers prevent the oxidation of metal surfaces, that is good agreement with CVA results.

3.7.Wettability

After confirmation of modification process, the possibility of the grafting of various "active" OFGs was studied (ADT-NH_2 and ADT-COOH). It is well known, that the diazonium salts attachment can significantly affect the surface properties.[56] First of all, the surface wettability

(contact angle) was measured in dependence on the grafted OFGs and results are presented in the Figure 4 for both metals. As could be expected, the presence of carboxyl groups decreases the water contact angle down to 46° and 32° for silver and to 55° and 33° for gold films, corresponding to spontaneous and electrochemical treatment, which is in good angreement with the results published for the various other surfaces, such as indium tin oxide, gold and glassy carbon electrode (contact angle was consistently reduced to 40.7°, 47.69° and 35.61° respectively) [57]. As can be expected, the contact angle increased by the grafting of more hydrophobic groups (nitro, amino). This trend was also demonstrated in several works.[58, 59] In the case of ADT-C_8F_{17} grafting, unexpected results were obtained: the grafting increased water contact angle significantly, but the effect is more pronounced in the case of spontaneous grafting, unlike to data published in work [51]. This fact can be explained by the distribution of grafted aryl layers – the non-homogenous structure of spontaneously grafted ADT-C_8F_{17} can be additional factors, affecting the contact angle. In general, all observed contact angles measured after modification are consistent with previously published data and trends.[51, 56-59, 62] Moreover, we suggest that changes of contact angles depend not only on the nature of attached radicals but also on the amount of OFGs, their distribution, and the methods used for metal surface modification.

The ability of carboxyl and amino groups to interact with protons or ions (as model system) was checked using their immersion into acidic (HCl) or basic (Na_2CO_3) solutions. Further treatment of amino and carboxyl groups respectively resulted in a contact angle decreasing due to salts formation. The increase of wettability on –C_6H_4-COOH grafted films to 42° (spontaneous) and 19° (electrochemical) for silver and 50° (spontaneous) and 25° (electrochemical) for gold was observed. Also, for –C_6H_4-NH_2 decrease of contact angle to 67° (76° before treatment), 72° (87° before treatment) for silver and 58° (65° before treatment), 49° (70° before treatment) for gold corresponding to spontaneous and electrochemical methods. A change in the contact angle after the treatment with amino and carboxylic groups enables one to assess the accessibility of OFGs for charging and acid-base properties.[60, 61] Additionally, the salts formation was confirmed using the Raman spectroscopy and corresponding graphs are shown in the supplementary information – Figure S7. Apparent changes in the peaks, related to amino and carboxyl groups due to the protonation/deprotonation, indicate the availability of these groups to further chemical interaction.

3.7. Zeta-potential

Results of electrokinetic analysis (zeta potential), confirming the change of surface chemistry and charge, are presented in the Figure 5. Previously it was expected[44] that the grafting of amino groups will shift the zeta potential to more positive values and the grafting with carboxyl groups will shift it to the more negative value. In the case of spontaneous modification, the above expectation was confirmed, i.e. zeta potential was shifted as expected and, like in the previous case,

the effect was more pronounced for silver. Similarly, grafting of carboxyl OFGs decreased the zeta potential, indicating the negative charge presented on the modified metal surface.

However, observed shifts in z potential are not so obvious for electrochemically induced modification (Figure 5). The tendency for amino and carboxylic groups remains the same as for spontaneous modification for both metals, but unexpectedly, grafting through electro-chemical mechanism leads to less pronounced changes in zeta potential response. This observation seems to be in some disagreement with the results of XPS and AFM that indicate the greater amount of attached OFGs in case of electrochemical modification. Probably, explanation lies in the steric nature of grafted OFGs layer, which restrict their interaction with analytical solution.

3.8. AFM investigations

Modification of surface topography, adhesion and deformation (the maximum deformation of the sample caused by the probe) were studied at nanoscale level using peak-force AFM technique. Such preparations of repellent surface are one of the main changes in plasmonics for non-invasive sensors, the studies were performed on the $–C_6H_4-C_8F_{17}$ modified silver and gold surfaces and results are presented in the Figure 6. It is evident, that sputtering of metals leads to formation of well-known cluster structure[63] with narrow distribution of mechanical and adhesive properties. Spontaneous modification conserved the surface topography, but dramatically changed surface mechanical properties. Adhesion significantly decreased and deformation increased as could be expected. Both effects were slightly more pronounced on the gold surface. The distribution of mechanical properties on silver was wider due to "island-like" structure of organic layers. Modification by electrochemically induced mechanism led to further changes of the surface properties. The surface topography was significantly changed due to formation of polyphenylene organic layers. The electrochemical modification also led to significant increase of adhesion. The source of the increased adhesion can be any attractive force between the tip and sample - the long grafted molecules can serve as a meniscus, leading to unexpected adhesion increase. For the same reason significant increase of surface deformation takes place since the hard metal surface is substituted by the rigid organics chains.

Additional measurements of the electrochemically grafted ADT-NO2 samples were performed with the aim to compare the SEM and AFM images. Their results are given in the Fig. S8. Observed thin films morphologies confirm the previous conclusion – high corrugation of grafted silver surface can be attributed to the formation of the island-like organic layer, when the gold surface is more flat, indicating more homogeneous covering by the organic layer.

3.9 Plasmonic activity

Finally, the plasmonics properties of the metal surface were tested using the UV-Vis and Raman spectroscopy. Results of UV-Vis measurements are presented in the Figure 7. It is well

known that the position of plasmon resonance depends on the dielectric constant of medium surrounding metal nanostructures, namely electron density in the nanostructure and electron scattering function on the metal/dielectric boundary. In the case of thin metal films the plasmon properties also depend on the film thickness and roughness. In turn, the thickness and surface roughness of sputtered noble metal thin films are the functions of deposition conditions: deposition rate, vacuum pressure, the temperature of the substrate and so on.[64, 65] In the present case both, thin film thickness and surface morphology are in good agreement with the results published in the literature (with similar deposition conditions).[66-68] In turn, the surface plasmon resonance position of thin noble metal film on is a strong function of the surface roughness.[67] Since the film morphology, measured on the pristine metal films are similar (the values of Ra are only slightly of silver and gold – Fig. S4), observed differences the plasmon resonance position for gold and silver could be attributed to the intrinsic metal parameters – concentration of free electrons and scattering constants. In the case of gold layer (Figures 7 A and B), the plasmon resonance peak appeared in the near IR range, which is typical for cluster structure of sputtered gold layer.[63] Modification of gold surface shifts the plasmon peak position to longer wavelength. The shift was more pronounced in the case of electrochemical modification because the larger part of plasmon evanescent wave is affected by the thicker organic film. Similar situation was also observed for cluster silver structure. Since the silver has higher electron density, its pristine plasmon peak is blue shifted relative to gold. Silver surface modification shifts the position of plasmon resonance to longer wavelength, too. As a rule, the shift was more pronounced for electrochemical modification. The only exception was the case of ADT-C_8F_{17}, where the long OFGs were enough to almost fully affect the plasmon evanescent way even in the case of monomolecular layer formation.

Typical proof of the plasmon activity is sufficient enhancement of OFGs Raman scattering, when they are closed to plasmon-active surface. Raman spectra were also collected in order to confirm the presence of corresponding OFGs on the surface of films (Figure 8). Taking into account of UV-Vis spectra of modified silver and gold (Figure 7), two excitation wavelengths, close to plasmon absorption band, were chosen: 475 nm for silver and 780 nm for gold. Spectra of pristine metals films did not show any significant Raman bands. After spontaneous and electrically induced modification of gold and silver by OFGs expected Raman peaks occurred (Figure 8). Detailed assignation of the peaks is presented in the supplementary materials (Table S3). The pronounced nature of the peaks in the Figure 8 indicates real enhancement of OFGs Raman scattering signal, due to significant energy focusing in the near-surface volume after photon-plasmon transition. The spectra of films after electrochemical treatment were significantly enhanced in comparison with spontaneous grafting due to the polyphenylene nature of OFGs layer. It should be also noted, that

low intensity bands at approximately 400 cm^{-1} correspond to covalent bond Au-C, which were also observed at 433 cm^{-1}. Their presence indicates the covalent binding of OFGs to metal surface.[33]

4. Conclusion

Thin films of plasmon-active metal (silver and gold) were grafted with various organic functional groups using ADTs spontaneous or electrochemically induced procedures. 4-nitrobenzediazonim tosylate and 4-(heptadecafluorooctyl)benzenediazonium tosylate were used as model modification agent and modification by 4-aminobenzenediazonium tosylate and 4-carboxybenzenediazonium tosylate was performed to induce the specific changes of surface properties or create specific and selective sites for further modification. After grafting the surface and optical properties were characterized by the wide range of techniques. The possibility of changing the thickness of organic layer, modification of surface charge and wettability, particular of full surface blocking or modification of adhesive or repellent surface properties were demonstrated. Different behavior of gold and silver was found: silver tends more to formation of clustered polyphenylene structure while gold is covered by more homogeneous and thinner layers. Spontaneous reaction creates the short, approximately monomolecular layer films of organic compounds and could be used in the field of SPR or SERS sensors. Electrochemically induced activation gives the thicker layer of the organic compounds on the metal surface and it could find application in the field of tunable plasmonic devices or plasmon-based lasers.

Acknowledgement

This work was supported by the GACR under the projects No. 15-19485S, 15-19209S and P206/12/G151. Pavel S. Postnikov is thankful to the Ministry of Education and Science of the Russian Federation (project "Science" no. 4.2569.2014/K). Olga A. Guselnikova is thankful to Russian Foundation for Basic Research (project no. 16-33-00351).

References

[1] P. K. Jain, K. S. Lee, I. H. El-Sayed, M. A. El-Sayed, Calculated absorption and scattering properties of gold nanoparticles of different size, shape, and composition: Applications in biological imaging and biomedicine, J. Phys. Chem. B 110 (14) (2006) 7238-7248.

[2] E. Ozbay, Plasmonics: Merging photonics and electronics at nanoscale dimensions, Science 311 (5758) (2006) 189-193.

[3] Y. Kalachyova, O. Lyutakov, M. Kostejn, M. Clupek, V. Svorcik, Silver Nanostructures: From Individual Dots to Coupled Strips for the Tailoring of SERS Excitation Wavelength from Near-UV to Near-IR. Electron. Mater. Lett. 11 (2) (2015) 288-294.

[4] Y. Kalachyova, D. Mares, O. Lyutakov, M. Kostejn, L. Lapcak, V. Svorcik, Surface Plasmon Polaritons on Silver Gratings for Optimal SERS Response, J. Phys. Chem. C 119 (17) (2015) 9506-9512.

[5] G. A. Baker, D. S. Moore, Progress in plasmonic engineering of surface-enhanced Raman-scattering substrates toward ultra-trace analysis, Anal. Bioanal. Chem. 382 (8) (2005) 1751-1770.

[6] Y. Kalachyova, O. Lyutakov, A. Solovyev, P. Slepicka, V. Svorcik, Surface morphology and optical properties of porphyrin/Au and Au/porphyrin/Au systems, Nanoscale Res. Lett. 8 (2013) 547.

[7] S. Quanwei, P. Manshu, W. Le, H. Dacheng, O. Jin, A fluorescent aptasensor for amplified label-free detection of adenosine triphosphate based on core–shell Ag@SiO2 nanoparticles, Biosens. Bioelectron. 77 (2016) 237–241.

[8] M. T. Hill, M. C. Gather, Advances in small lasers, Nat. Photon. 8 (2014) 908-918.

[9] M. Ohtsu, K. Kobayashi, T. Kawazoe, S. Sangu, T. Yatsui, Nanophotonics: Design, fabrication, and operation of nanometric devices using optical near fields IEEE, J. Selected Topics Quant. Electron. 8 (4) (2002) 839-862.

[10] K. Chen, E. S. P. Leong, M. Rukavina, T. Nagao, Y. J. Liu, Yu. Zheng, Active molecular plasmonics: tuning surface plasmon resonances by exploiting molecular dimensions, Nanophotonics 4 (1) (2015) 186–197.

[11] Y. Kalachyova, D. Alkhimova, M. Kostejn, P. Machac, V. Svorcik, O. Lyutakov, Plasmooptoelectronic tuning of optical properties and SERS response of ordered silver grating by free carrier generation, RSC Adv. 5 (113) (2015) 92869-92877.

[12] J. Svanda, Y. Kalachyova, P. Slepicka, V. Svorcik, V., O. Lyutakov, Smart Component for Switching of Plasmon Resonance by External Electric Field, ACS Appl. Mater. Inter., 8 (1) (2016) 225-231.

[13] M. Righini, A. S. Zelenina, Ch. Girard, R. Quidant, Parallel and selective trapping in a patterned plasmonic landscape, Nature Physics 3 (7) (2007) 477 – 480.

[14] K. Jain, X. H. Huang, I. H. El-Sayed, M. A. El-Sayed, Noble Metals on the Nanoscale: Optical and Photothermal Properties and Some Applications in Imaging, Sensing, Biology, and Medicine, Acc. Chem. Res. 41 (12) (2008) 1578-1586.

[15] M. Walter, J. Akola, O. Lopez-Acevedo, P. D. Jadzinsky, G. Calero, C. J. Ackerson, R. L. Whetten, H. Gronbeck, H. A. Hakkinen, A unified view of ligand-protected gold clusters as superatom complexes, Proc. Natl. Acad. Sci. U. S. A. 105 (27) (2008) 9157-9162.

[16] K. C. Grabar, R. G. Freeman, M. B. Hommer, M. J. Natan, Preparation and Characterization of Au colloid monolayer, Anal. Chem. 67 (4) (1995) 735-743.

[17] J. Kalbacova, R. D. Rodriguez, V. Desale, M. Schneider, I. Amin, R. Jordan, D. R. T. Zahn, Chemical stability of plasmon-active silver tips for tip-enhanced Raman spectroscopy, Nanospectroscopy 1 (2014) 12–18.

[18] L. Touahir, A. T. A. Jenkins, R. Boukherroub, A. C. Gouget-Laemmel, J.-N. Chazalviel, J. Peretti, F. Ozanam, S. Szunerits, Surface Plasmon-Enhanced Fluorescence Spectroscopy on Silver Based SPR Substrates, J. Phys. Chem. C 114 (51) (2010) 22582–22589.

[19] L. Touahir, J. Niedziolka-Jonsson, E. Galopin, R. Boukherroub, A. C. Gouget-Laemmel, I. Solomon, M. Petukhov, J. N. Chazalviel, F. Ozanam, S. Szunerits, Surface Plasmon Resonance on Gold and Silver Films Coated with Thin Layers of Amorphous Silicon-Carbon Alloys, Langmuir 26 (8) (2010) 6058–6065.

[20] R. J. C. Brown, M. J. T. Milton, Nanostructures and nanostructured substrates for surface-enhanced Raman scattering (SERS), J. Raman. Spectroscopy 39 (10) (2008) 1313-1326.

[21] D. Schaming, V. Q. Nguyen, P. Martin, J. C. Lacroix, Tunable Plasmon Resonance of Gold Nanoparticles Functionalized by Electroactive Bisthienylbenzene Oligomers or Polythiophene. J. Phys. Chem. C 118 (43) (2014) 25158-25166.

[22] I. Tokarev, S. Minko, Tunable plasmonic nanostructures from noble metal nanoparticles and stimuli-responsive polymers, Soft Matter. 8 (22) (2012) 5980-5987.

[23] R. F. Oulton, V. J. Sorger, T. Zentgraf, R. M. Ma, C. Gladden, L. Dai, G. Bartal, X. Zhang, Plasmon lasers at deep subwavelength scale, Nature 461 (7264) (2009) 629-632.

[24] L. Guerrini, V. J. Garcia-Ramos, C. Domingo, S. Sanchez-Cortes, Functionalization of Ag nanoparticles with dithiocarbamate calixarene as an effective supramolecular host for the surface-enhanced Raman scattering detection of polycyclic aromatic hydrocarbons, Langmuir 22 (26) (2006) 10924-10926.

[25] S. Unser, I. Bruzas, J. He, L. Sagle, Localized Surface Plasmon Resonance Biosensing: Current Challenges and Approaches, Sensors 15 (7) (2015) 15684-15716.

[26] L. Newton, Th. Slater, N. Clark, A. Vijayaraghavan, Self-assembled monolayers (SAMs) on metallic surfaces (gold and graphene) for electronic applications, J. Mater. Chem. C 1 (3) (2013) 376-393.

[27] T. A. J. Grell, A. M. Alabanza, K. Gaskell, K. Aslan, Microwave-Accelerated Surface Modification of Plasmonic Gold Thin Films with Self-Assembled Monolayers of Alkanethiols, Langmuir 29 (43) (2013) 13209−13216.

[28] D. M. Shewchuk, M. T. McDermott, Comparison of Diazonium Salt Derived and Thiol Derived Nitrobenzene Layers on Gold, Langmuir 25 (8) (2009) 4556–4563.

[29] A. Mesnage, X. Lefèvre, P. Jégou, G. Deniau, S. Palacin, Study of the spontaneous formation of organic layers on carbon neous Grafting of Diazonium Salts: Chemical Mechanism on Metallic Surfaces, Langmuir 28 (32) (2012) 11767−11778.

[30] L. Civit, A. Fragoso, C. K. O'Sullivan, Thermal stability of diazonium derived and thiol-derived layers on gold for application in genosensors. Electrochem. Commun. 12 (8) (2010) 1045–1048.

[31] R. Ahmad, L. Boubekeur-Lecaque, M. Nguyen, S. Lau-Truong, A. Lamouri, Ph. Decorse, A. Galtayries, J. Pinson, N. Felidj, C. Mangeney, Tailoring the Surface Chemistry of Gold Nanorods through Au−C/Ag−C Covalent Bonds Using Aryl Diazonium Salts, J. Phys. Chem. C 118 (33) (2014) 19098−19105.

[32] A. Adenier, C. Combellas, F. Kanoufi, J. Pinson, F. I. Podvorica, Formation of Polyphenylene Films on Metal Electrodes by Electrochemical Reduction of Benzenediazonium Salts, Chem. Mater. 18 (8) (2006) 2021-2029

[33] L. Laurentius, S. R. Stoyanov, S. Gusarov, A. Kovalenko, R. Du, G. P. Lopinski, M. T. McDermott, Diazonium-Derived Aryl Films on Gold Nanoparticles: Evidence for a Carbon Gold Covalent Bond, ACS Nano 5 (5) (2011) 4219-4227.

[34] A. A. Mohamed, Z. Salmic, Si A. Dahoumane, A. Mekki, B. Carbonnier, M. M. Chehimi, Functionalization of nanomaterials with aryldiazonium salts, Adv. Colloid Interf. Sci. 225 (2015) 16–36.

[35] D. J. Guo, F. Mirkhalaf, Modification of Nano-objects by Aryl Diazonium Salts. In Aryl Diazonium Salts: New Coupling Agents in Polymer and Surface Science, Chehimi, M. M., Ed.; Wiley-VCH: Weinheim, Germany, 2012, 103-125.

[36] J. J. Gooding, Advances in Interfacial Design for Electrochemical Biosensors and Sensors: Aryl Diazonium Salts for Modifying Carbon and Metal Electrodes, Electroanalysis 20 (6) (2008) 573–582.

[37] J. Pinson, F. Podvorica, Attachment of organic layers to conductive or semiconductive surfaces by reduction of diazonium salts, Chem. Soc. Rev. 34 (5) (2005) 429–439.

[38] M. Torrens, M. Ortiz, A. P. F. Turner, V. Beni, S. K. O'Sullivan, Amperometric detection of Francisella tularensis genomic sequence on Zn-mediated diazonium modified substrates, Electrochem. Commun. 53 (2015) 6–10.

[39] L.C. Shoute, A. J. Bergren, A. M. Mahmoud, K. D. Harris, R. L. McCreery, Optical interference effects in the design of substrates for surface-enhanced Raman spectroscopy, Appl. Spectrosc. 63 (2) (2009) 133-140.

[40] H. Liang, H. Tian, R. L. McCreery, Normal and Surface-Enhanced Raman Spectroscopy of Nitroazobenzene Submonolayers and Multilayers on Carbon and Silver Surfaces, App. Spectros. 61 (6) (2007) 613-620.

[41] D. Hetemi, H. Hazimeh, Ph. Decorse, A. Galtayries, C. Combellas, F. Kanoufi, J. Pinson, and F. I. Podvorica, One-Step Formation of Bifunctionnal Aryl/Alkyl Grafted Films on Conducting Surfaces by the Reduction of Diazonium Salts in the Presence of Alkyl Iodides, Langmuir 31 (19) (2015) 5406−5415.

[42] Q. Zou, L. L. Kegel, K. S. Booksh, Electrografted Diazonium Salt Layers for Antifouling on the Surface of Surface Plasmon Resonance Biosensors, Anal. Chem. 87 (4) (2015) 2488−2494.

[43] V. D. Filimonov, M. E. Trusova, P. S. Postnikov, A. E. Krasnokutskaya, Y. M. Lee, H. Y. Hwang, H. Kim and K.-W. Chi, Unusually Stable, Versatile, and Pure Arenediazonium Tosylates: Their Preparation, Structures, and Synthetic Applicability, Org. Lett. 10 (18) (2008) 3961–3964.

[44] Z. Kolská, A. Řezníčková, M. Nagyová, N. Slepičková Kasálková, P. Sajdl, P. Slepička, V. Švorčík, Plasma activated polymers grafted with cysteamine for bio-application, Polym. Degrad. Stabil. 101 (1) (2014) 1-9.

[45] P. S. Postnikov, M. E. Trusova, T. A. Fedushchak, M. A. Uimin, A. E. Ermakov, V. D. Filimonov, Aryldiazonium tosylates as new efficient agents for covalent grafting of aromatic groups on carbon coatings of metal nanoparticles, Nanotechnogies in Russia 5 (7-8) (2010) 446–449.

[46] O. A. Guselnikova, A. I. Galanov, A. K. Gutakovskii, P.S. Postnikov, The convenient preparation of stable aryl-coated zerovalent iron nanoparticles, Beilstein J. Nanotechnol. 6 (1) (2015) 1192–1198.

[47] L. Servinis, L. C. Henderson, L. M. Andrighetto, M. G. Huson, T. R. Gengenbachc, B. L. Fox, A novel approach to functionalise pristine unsized carbon fibre using in situ generated diazonium species to enhance interfacial shear strength, J. Mater. Chem. A 3 (2015) 3360-3371.

[48] A. Adenier, N. Barre, E. Cabet-Deliry, A. Chausse, Study of the spontaneous formation of organic layers on carbon and metal surfaces from diazonium salt, Surf. Sci. 600 (21) (2006) 4801–4812.

[49] J. Pinson, F. I. Podvorica, Attachment of organic layers to conductive or semiconductive surfaces by reduction of diazonium salts, Chem. Soc. Rev. 34 (5) (2005) 429-439.

[50] Th. Menanteau, E. Levillain, T. Breton, Electrografting via Diazonium Chemistry: From Multilayer to Monolayer Using Radical Scavenger, Chem. Mater. 25 (14) (2013) 2905−2909.

[51] M. M. Chehimi, A. Lamouri, M. Picot, J. Pinson, Surface modification of polymers by reduction of diazonium salts: polymethylmethacrylate as an example, J. Mater. Chem. C 2 (2) (2014) 356-363.

[52] P. A. Brooksby and A. J. Downard, Electrochemical and Atomic Force Microscopy Study of Carbon Surface Modification Via Diazonium Reduction in Aqueous and Acetonitrile Solutions, Langmuir 20 (12) (2004) 5038–5045.

[53] C. Combellas, F. Kanoufi, J. Pinson and F. I. Podvorica, Sterically Hindered Diazonium Salts for the Grafting of a Monolayer on Metals, J. Am. Chem. Soc. 130 (27) (2008) 8576–8577.

[54] M.-C. Bernard, A. Chaussé, E. Cabet-Deliry, M. M. Chehimi, J. Pinson, F. I. Podvorica, C. Vautrin-Ul, Organic layers bonded to industrial, coinage, and noble metals through electrochemical reduction of aryldiazonium salts, Chem. Mater. 15 (18) (2003) 3450–3462.

[55] N. Dekker, Electrochemistry at solid electrodes, New York, M. Dekker, 1969.

[56] B. Mrabet, A. Mejbri, S. Mahouche, S. Gam-Derouich, M. Turmine, M. Mechouet, Ph. Lang, H. Bakala, M. Ladjimi, A. Bakhrouf, S. Tougaard, M. M. Chehimi, Controlled adhesion of Salmonella Typhimurium to poly(oligoethylene glycol methacrylate) grafts, Surf. Interface Anal. 43 (11) (2011) 1436–1443.

[57] D.-J.Chung, S.-H. Oh, Sh. Komathi, A. I. Gopalan, K.-P. Lee, S.-H. Choi, One-step modification of various electrode surfaces using diazonium salt compounds and the application of this technology to electrochemical DNA (E-DNA) sensors, Electrochimica Acta 76 (2012) 394–403.

[58] F. Brisset, J. Vieillard, B. Berton, S. Morin-Grognet, C. Duclairoir-Poc, F. Le Derf, Surface functionalization of cyclic olefin copolymer with arenediazonium salts: A covalent grafting method, Appl. Surf. Sci. 329 (2015) 337-346.

[59] J. Wang, M. A. Firestone, O. Auciello, J. A. Carlisle, Surface Functionalization of Ultrananocrystalline Diamond Films by Electrochemical Reduction of Aryldiazonium Salts, Langmuir 20 (26) (2004) 11450-11456.

[60] M. Cheng, Q. Liu, G. Ju, Y. Zhang, L. Jiang, F. Shi, Bell-Shaped Superhydrophilic–Superhydrophobic–Superhydrophilic Double Transformation on a pH-Responsive Smart Surface, Adv. Mater. 26 (2) (2014) 306–310.

[61] M. N. Nguyen, T. Matrab, Ch. Badre, M. Turmine, M. M. Chehimi, Interfacial aspects of polymer brushes prepared on conductive substrates by aryl diazonium salt surface-initiated ATRP, Surf. Interface Anal. 40 (3-4) (2008) 412–417.

[62] B. Harnish, J. T. Robinson, Zh. Pei, O. Ramstrom, M. Yan, UV-Cross-Linked Poly(vinylpyridine) Thin Films as Reversibly Responsive Surfaces, Chem. Mater. 17 (16) (2005) 4092-4096.

[63] J. Siegel, O. Lyutakov, V. Rybka, Z. Kolska, V. Svorcik, Properties of gold nanostructures sputtered on glass, Nanoscale Res. Lett. 6 (1) (2011) 96-105.

[64] H. You, R. P. Chiarello, H. K. Kim, K. Q. Vandervoort, X-Ray Reflectivity and Scanning-Tunneling-Microscope Study of Kinetic Roughening of Sputter-Deposited Gold Films during Growth, Phys. Rev. Lett. 70 (19) (1993) 2900-2903.

[65] V. Kapaklis, P. Poulopoulos,V. Karoutsos, Th. Manouras, C. Politis, Growth of thin Ag films produced by radio frequency magnetron sputtering, Thin Solid Films 510 (1-2) (2006) 138–142.

[66] J.-Y. Kwon, T.-S. Yoon, K.-B. Kim, S.-H. Min, Comparison of the agglomeration behavior of Au and Cu films sputter deposited on silicon dioxide 93 (6) (2003) 3270-3278

[67] G. Xu, M. Tazawa, P. Jin, S. Nakao, Surface plasmon resonance of sputtered Ag films: substrate and mass thickness dependence Appl. Phys. A 80 (7) (2005)1535–1540

[68] K. L. Chopra, Growth of Sputtered vs Evaporated Metal Films J. Appl. Phys., 37 (9) (1966) 3405-3410

Figure caption

Fig. 1 Schematic representation of the proposed covalent modification of plasmon-active metal surface.

Fig. 2 SEM-EDX mapping of nitrogen (yellow) and fluorine (blue) on gold and silver modified films.

Fig. 3 Cyclic voltammograms measured on the Au and Ag thin films with covalently modified surface: Au and Ag thin films modified by ADT-NO_2 and ADT-C_8F_{17} through the spontaneous (-sp) or electrochemical (-el) grafting.

Fig. 4 Surface wettability (contact angle and water drop) of pristine and modified Au and Ag film by ADTs.

Fig. 5 Zeta potential measured on the Au or Ag thin films modified by ADT-NH_2 and ADT-COOH salts.

Fig. 6 Surface topography and mechanical properties of Au and Ag pristine and modified by ADT-C_8F_{17} surfaces.

Fig. 7 UV-Vis spectra of pristine Au and Ag thin films measured before and after covalent modification by ADTs.

Fig. 8 Raman spectra of ADTs covalently bounded to plasmon-active Au and Ag surfaces.

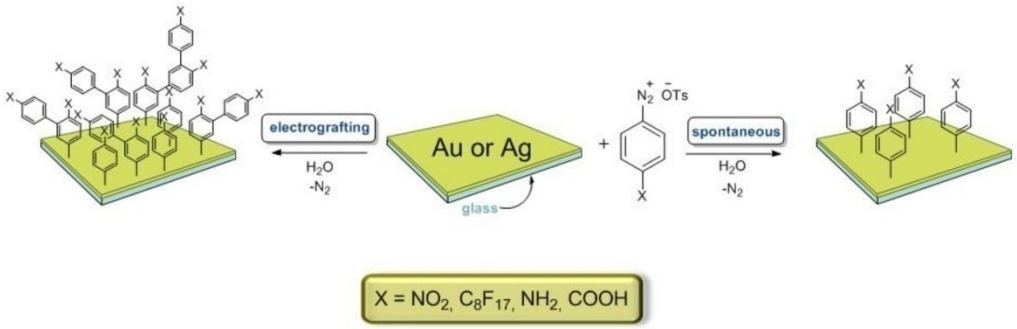

Fig. 1

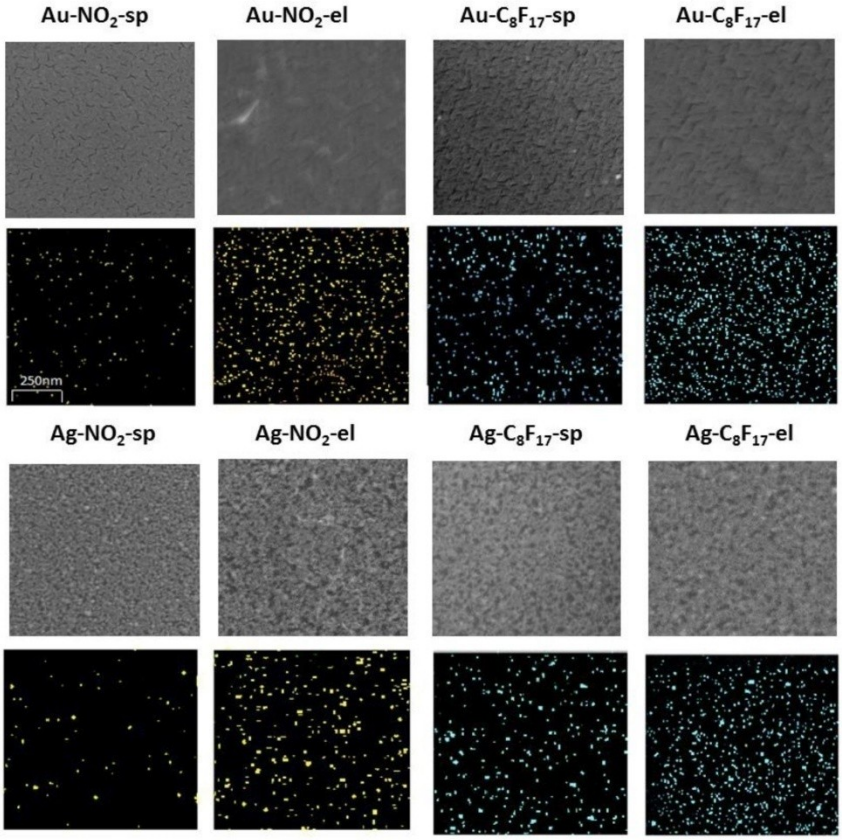

Fig. 2

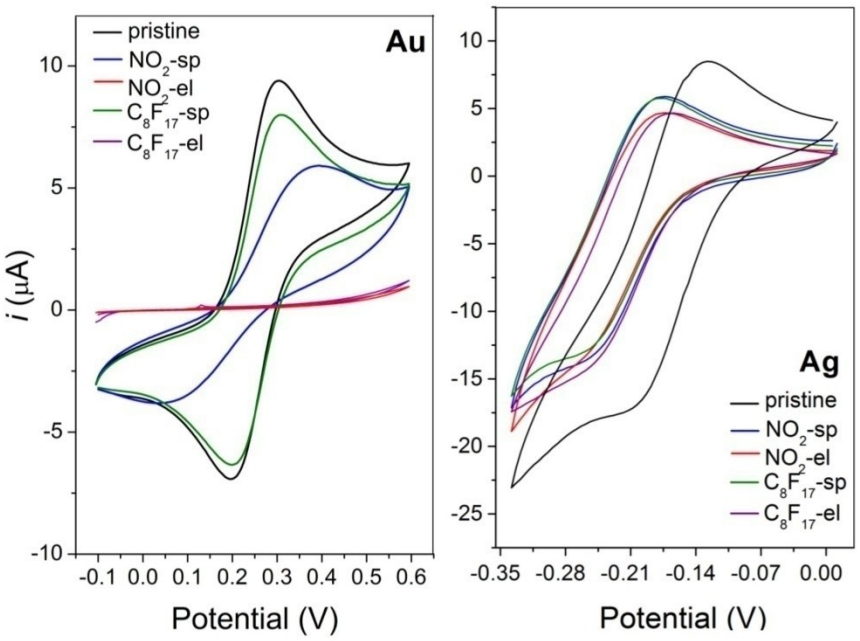

Fig. 3

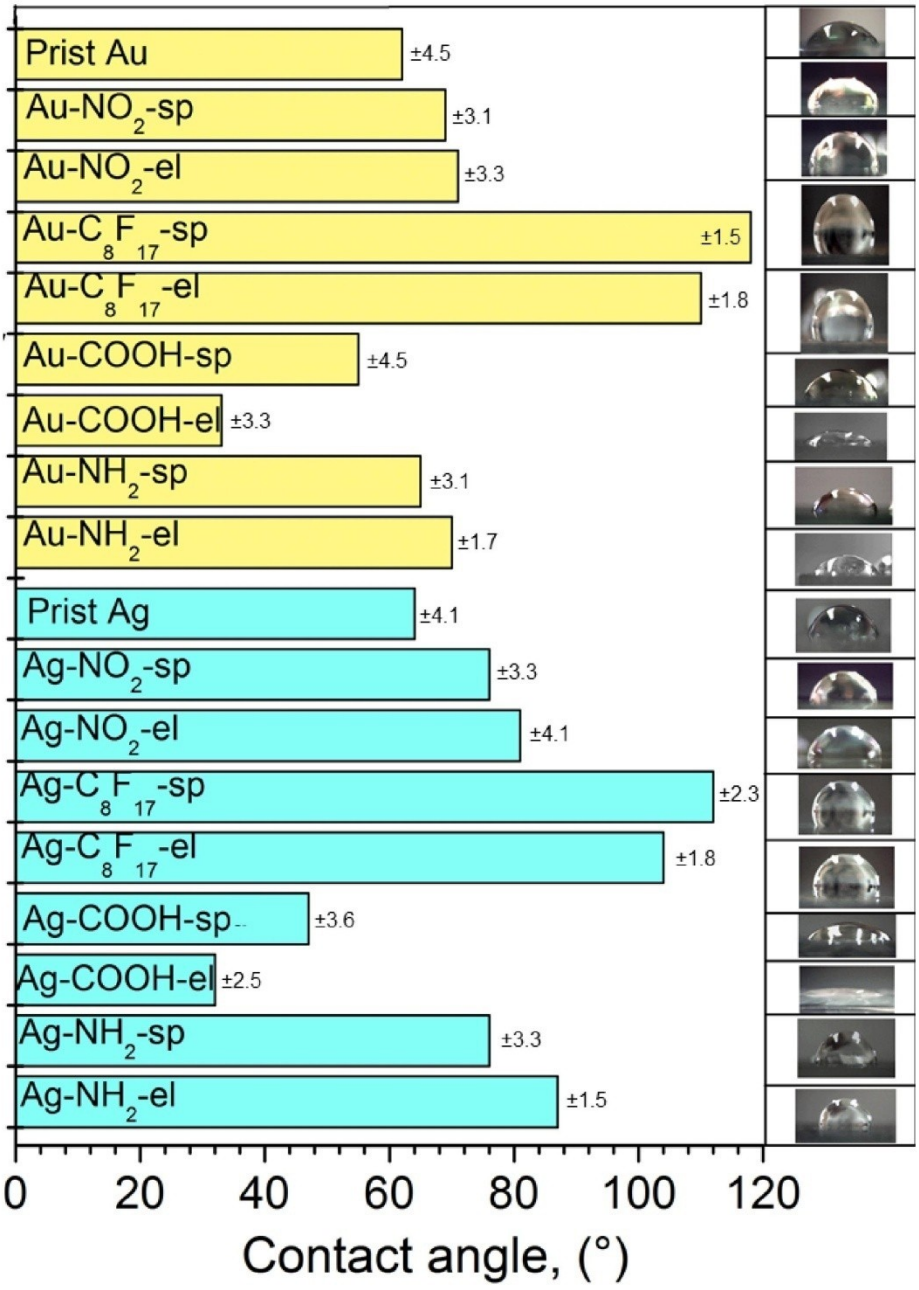

Fig. 4

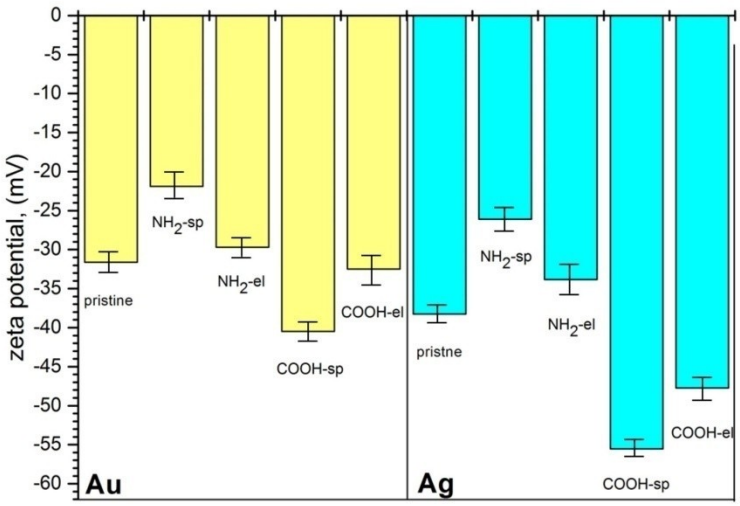

Fig. 5

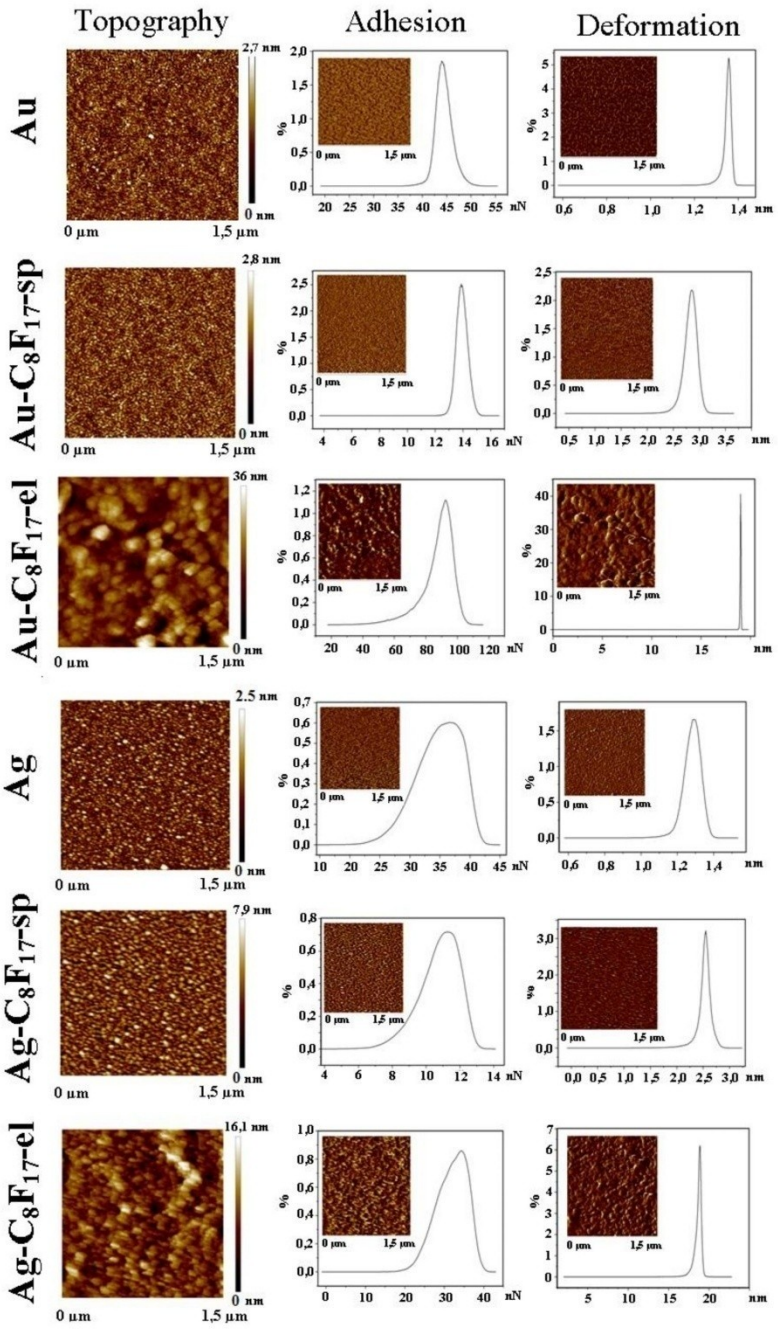

Fig. 6

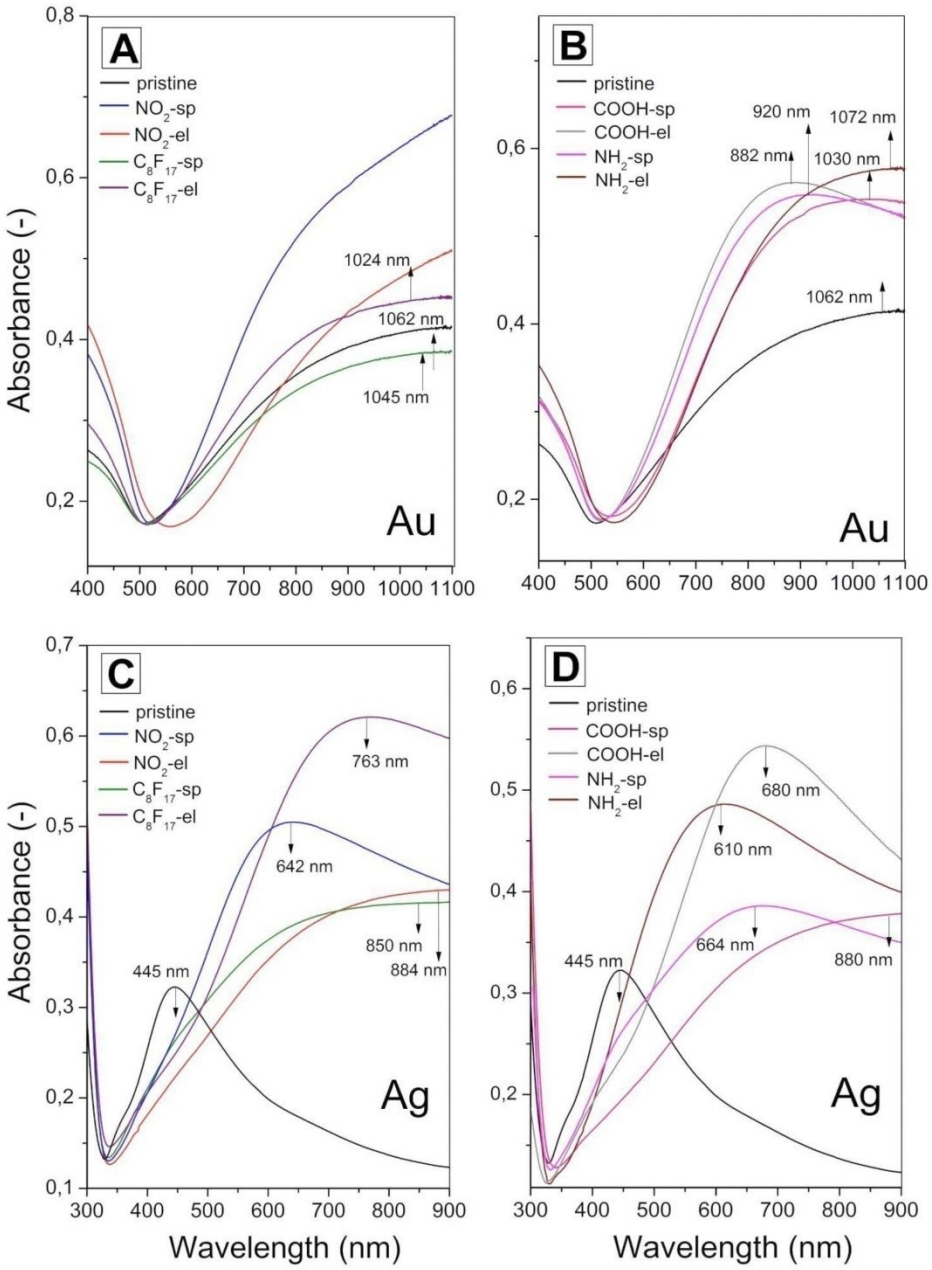

Fig. 7

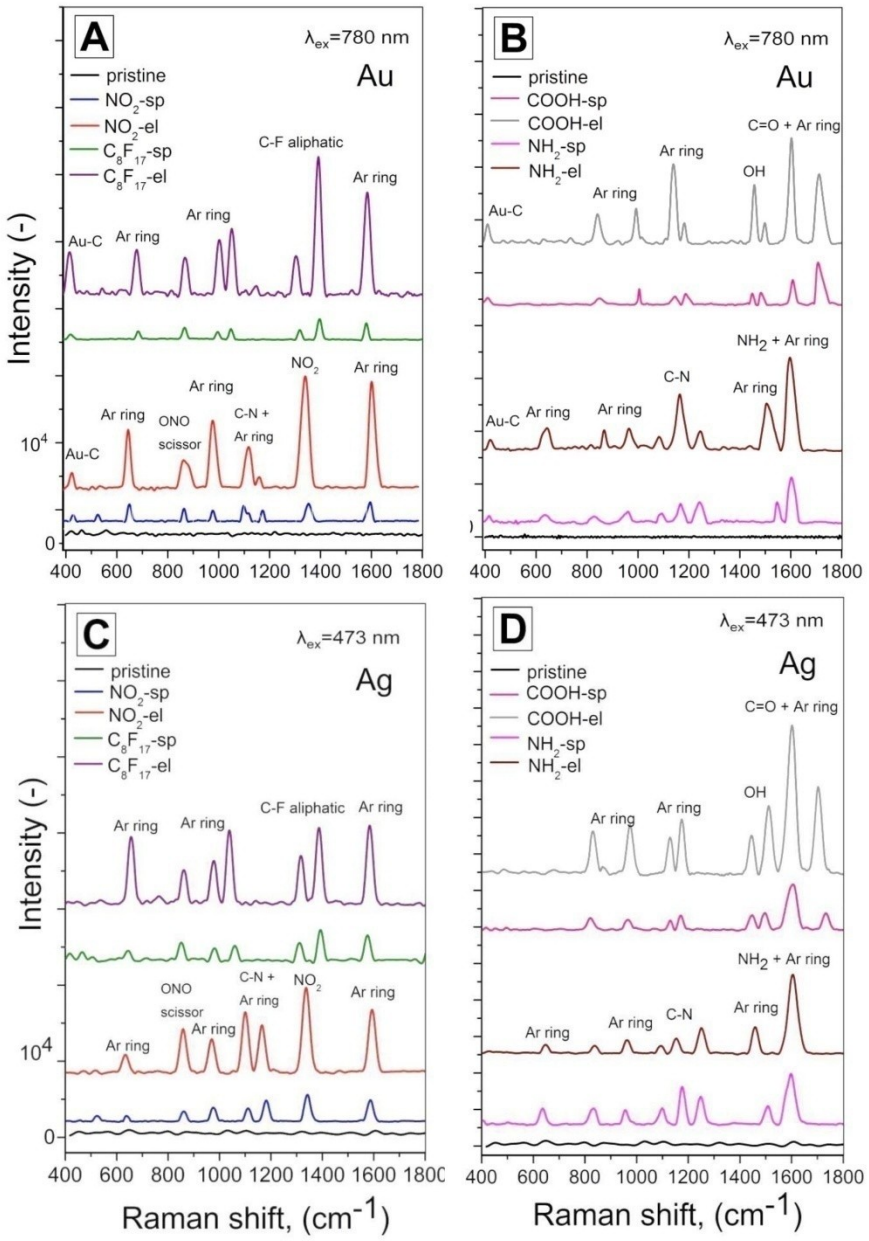

Fig. 8

Table 1

Surface atomic percentage element concentration calculated from XPS results study under 9º for gold and silver thin films modified with ADT-NO_2 and ADT-C_8F_{17}.

Sample	**Surface atomic element concentration** (at. %)					
	C(1s)	O(1s)	Au(4f)	Ag(3d)	N(1s)	F(1s)
Prist Au	32.0	15.8	52.2	-	-	-
Au-NB-sp	43.0	10.3	45.3	-	1.5	-
Au-NB-el	61.4	26.0	4.8	-	7.8	-
Au-CF-sp	37.5	11.7	33.4	-	-	17.4
Au-CF-el	44.3	9.6	4.0	-	-	42.1
Prist Ag	26.6	20.0	-	53.4	-	-
Ag-NB-sp	37.5	20.0	-	41.3	1.2	-
Ag-NB-el	47.0	39.0	-	8.6	5.4	-
Ag-CF-sp	39.7	11.9	-	22.7	-	25.7
Ag-CF-el	42.0	10.5	-	5.3	-	42.2

Table 2

Results of the scratch tests characterizing the changes of Ag and Au films after spontaneous or electrically induced modification with ADT-NO_2 and ADT-C_8F_{17} (*difference in thickness between pristine metal film and modified film).

Sample	**Thickness** (nm)	**Δ*** (nm)	**Molecular size** (nm)	**Approx. number of layers**
Prist Au	18.5±0.18	-	-	-
Au-CF-sp	20.3±0.2	1.8	1.6	1.1
Au-CF-el	24.8±0.15	6.3	1.6	4.0
Au-NB-sp	20.4±0.2	1.9	0.8	2.4
Au-NB-el	25.6±0.18	7.1	0.8	8.9
Prist Ag	14.1±0.1	-	-	-
Ag-CF-sp	16.2±0.2	2.1	1.6	1.3
Ag-CF-el	25.0±0.2	10.9	1.6	6.8
Ag-NB-sp	15.9±0.16	1.8	0.8	2.3
Ag-NB-el	23.4±0.2	9.3	0.8	11.6

12. Appendix VI

Functional SPP-based SERS sensor platform for lipoproteins detection

Guselnikova Olga, Kalachyova Yevgeniya, Faragova Karolína, **Libánský Milan**, Dejmková Hana, Švorčík Václav, Sajdl Petr, Lyutakov Oleksiy

Talanta

Prepared for submission, Year 2017

Experimental

Potassium ferrocyanide (p.a., Lachema, Czech Republic) was used as an inorganic probe for investigation of the electrochemical behaviour of gold layers. Electrochemical characterization of gold surfaces was performed by cyclic voltammetry (CV) at the potential range from -100 mV to 700 mV with scan rate 50 mV s^{-1}. Cyclic voltammograms of pristine and modified layers (film electrodes) were obtained using 1 mM potassium ferrocyanide (II) in 0.1 M potassium nitrate (p.a., Lachema, Czech Republic) as an aqueous medium and 1 mM potassium ferrocyanide in 0.1 M potassium nitrate with 50 % of methanol (*v/v*) as a mixed water-methanol medium. Volume of the solution used for the measurement was 10 µL. Cyclic voltammetry was carried out with working film electrodes with an exposed area of 3 mm^2 (vicinity of the area was isolated), platinum wire auxiliary electrode and miniaturized gel Ag/AgCl reference electrode (3M KCl, Cypress Systems, Chelmsword, MA, USA), to which all potentials values are referred.

Voltammetric measurements were performed with portable potentiostat PalmSens (Palm Instruments, Netherlands), controlled by PSTrace 4.8 software.

All measurements were repeated three times with five scans for each measurement.

Results and Discussion

The electrochemical response of inorganic probes is often used to evaluate the density of grafted substrates onto the surface of metal films. The surface blocking due to grafting of substrates and hydrophobicity of the surface was examined by cyclic voltammetry performed in the solution of potassium ferrocyanide in two commonly used electrolytes.

Figure 5A shows the response of ferrocyanide/ferricyanide system on the gold electrodes in the aqueous medium. The voltammogram measured on the pristine electrode without surface modification showed typical reduction and oxidation behaviour of a diffusion controlled redox couple. During the CV measurements on the plain electrode; sufficient repeatability (5 %) and reversibility (ΔE_p = 100 mV, I_{anod}/I_{cathod} = 1.1, I_{anod} = 9.5 µA) of the one electron reaction was achieved in comparison to common used gold bulk electrodes. However, the peaks become less pronounced and the electron transfer kinetics significantly slowed down when ADT-C_xH_n were grafted

onto the surface of the electrode, due to partial surface blocking. In the case of grafted – C_1H_3, only negligible blocking of ferrocyanide molecules with lower rate of reversibility of the electrochemical reaction was showed (ΔE_p = 200 mV, I_{anod}/I_{cathod} = 1.4, I_{anod} = 8.9 μA).

In the case of -C_4H_9 and -$C_{10}H_{21}$, partial blocking of ferrocyanide/ferricyanide electron transfer was observed and small redox peaks were observable (I_{anod} < 2.0 μA). On the other hand, when -$C_{16}H_{33}$ substrate was grafted, oxidation and reduction peak fully disappeared, indicating full blocking of surface so that the probe molecules cannot reach the metal surface. The organic substrate apparently exhibits different behaviour due to hydrofobicity so that in aqueous medium aliphatic organic chains can be bent and unevenly arranged.

Similar electrochemical behaviour with slight differences was observed during the measurements in the mixed aqueous-methanol medium (50 % *v*/*v*, Figure 5B). Pristine electrode and electrodes with -C_1H_3 and -C_4H_9 substrates exhibited oxidation peak at the same potential (the oxidation reaction is not distorted), but on the reduction peak of the analyte at the electrode with -C_1H_3 and -C_4H_9 substrates it was possible to observe a lower rate of reversibility of the electrochemical reaction with the shift of the potential of reduction peak. Otherwise, grafting of substrates with increasing carbon chain length did not lead to full peak suppression, indicating the influence of the used solvent. Despite the fact that the surface of the electrode with ADT-$C_{16}H_{33}$ substrate should be fully covered, small oxidation peak around the potential of 350 mV was observed. This is probably due to the organic solvent (methanol) which pushes inorganic probe through the inorganic substrate to the surface of gold electrode and the electron transfer controlled by diffusion could be completed; however, the electrochemical reaction is not reversible at all.

The attenuation of cyclic voltammograms and slower electron transfer kinetics confirmed that used substrates for grafting can block almost the entire surface of the gold film. Nevertheless, electron reaction can be promoted by the change of the solvent or co-solvent (to mixed aqueous-methanolic medium) which leads to revelation of defects where molecular layer of organic substrate is not sufficiently thick to block electron transfer and the gold surface is electrochemically available.

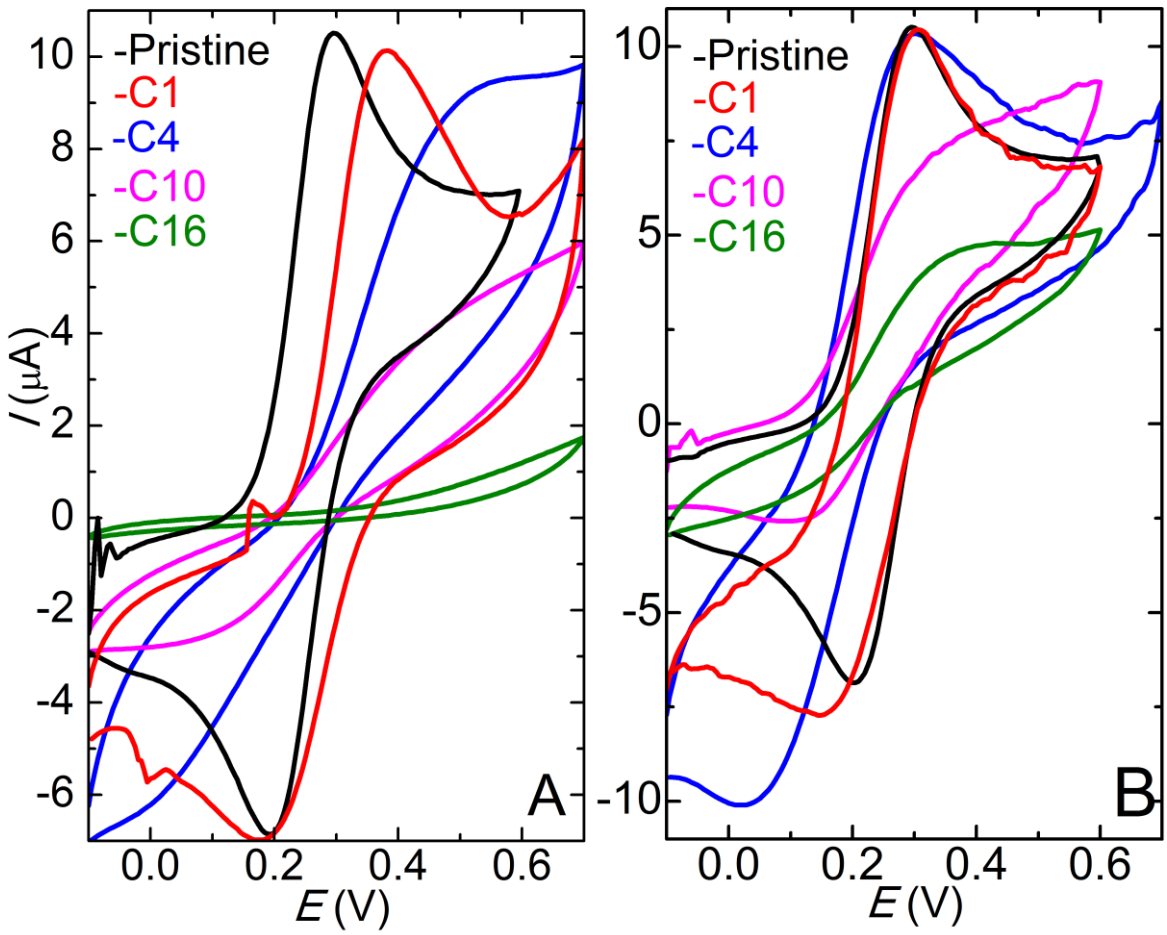

Fig. 5. Cyclic voltammograms of potassium ferrocyanide (c =1 mM) in (A) potassium nitrate (c = 0.1 M) and in (B) potassium nitrate with 50 % methanol (*v*/*v*) at a pristine gold film electrode and at gold film electrodes with grafted ADT-C_xH_n substrates.

Acknowledgement

This work was supported by the GACR under the projects No. P206/12/G151 (ML and HD).

13. Appendix VII - Confirmation of participation

[1] **Libansky M.**, Zima J., Barek J., Dejmkova H., Voltammetric determination of homovanillic acid and vanillylmandelic acid on a disposable electrochemical measuring cell system with integrated carbon composite film electrodes, *Monatshefte Fur Chemie*, 147 (2016) 89-96.
5-year Impact factor: **1.13**; Percentage of participation of Mgr. Milan Libánský ~ **85 %**.

[2] Bergerova M., **Libansky M.**, Dejmkova H., Determination of Urinary Indican on Carbon Film Composite Electrode and Carbon Paste Electrode, *Current Analytical Chemistry*, *Submitted* (2017).
5-year Impact factor: **1.15**; Percentage of participation of Mgr. Milan Libánský ~ **50 %**.

[3] **Libansky M.**, Zima J., Barek J., Reznickova A., Svorcik V., Dejmkova H., Basic Electrochemical Properties of Sputtered Nanostructured Gold Film Electrodes, *Electrochimica acta*, *Submitted* (2017).
5-year Impact factor: **4.72**; Percentage of participation of Mgr. Milan Libánský ~ **75 %**.

[4] Guselnikova O., Postnikov P., Kalachyova Y., **Libansky M.**, Zima J., Kolska Z., Svorcik V., Lyutakov O., Large-scale ultrasensetive, highly reproducible and regenerative smart SERS platform based on PNIPAm grafted gold grating, *ChemNanoMat*, 3 (2016) 135-144.
New journal; Percentage of participation of Mgr. Milan Libánský ~ **25 %**.

[5] Guselnikova O., Postnikov P., Elashnikov R., M. T., Kalachyova Y., **Libansky M.**, Barek J., Kolska Z., Svorcik V., Lyutakov O., Surface modification of Au and Ag plasmonic thin films via diazonium chemistry: evaluation of structure and properties, *Colloids and Surfaces A Physicochemical Engineering Aspects*, *In Press* (2016).
5-year Impact factor: **2.83**; Percentage of participation of Mgr. Milan Libánský ~ **25 %**.

[6] Guselnikova O., Kalachyova Y., Faragova K., **Libansky M.**, Dejmkova H., Svorcik V., Sajdl P., Lyutakov O., Functional SPP-based SERS sensor platform for lipoproteins detection, *Talanta*, *Prepared for submission* (2017).
5-year Impact factor: **3.75**; Percentage of participation of Mgr. Milan Libánský ~ **25 %**.

I declare that the percentage of participation of Mgr. Milan Libánský at the above given papers corresponds to above given numbers.

Prague, 28.02.2017 Prof. RNDr. Jiří Zima, CSc

14. Appendix VIII - List of publications, oral and poster presentations

A) List of journal articles

1. **Libánský M.**, Zima J., Barek J., Dejmkova H., Voltammetric Determination of Arbutin on Carbon Paste Electrode, *Sensing in Electroanalysis 6*, University of Pardubice: Pardubice, 2011, 281-287.
2. **Libánský M.**, Zima J., Barek J., Dejmkova H., Voltammetric Determination of Triclosan Using a System of Disposable Electrochemical Cells with Integrated Carbon Electrode (Voltametrické stanovení triclosanu pomocí systému měrných cel s integrovanou uhlíkovou elektrodou), *Chemicke Listy, 107* (2013) 247-252. (*Original in Czech*)
3. **Libánský M.**, Zima J., Barek J., Dejmkova H., Voltammetric Determination of Triclosan by a System of Specific Duties with Integrated Carbon Electrode **(**Voltametrické stanovení triclosanu pomocí systemu jednorázových měrných cel s integrovanou uhlíkovou elektrodou), *Chemicke Listy, 108* (2014) 243-250. (*Original in Czech*)
4. **Libánský M.**, Zima J., Barek J., Dejmkova H., Construction of an Electrochemical Cell System Based on Carbon Composite Film Electrodes and Its Application for Voltammetric Determination of Triclosan, *Electroanalysis*, 26 (2014) 1920-1927.
5. **Libánský M.**, Zima J., Barek J., Dejmkova H., Voltammetric Determination of Homovanillic Acid and Vanillylmandelic Acid on a Disposable Electrochemical Measuring Cell System with Integrated Carbon Composite Film Electrodes, *Monatshefte fur Chemie*, 147 (2016) 89-96.
6. Guselnikova O., Postnikov P., Elashnikov R., Trusova M., Kalachyova Y., **Libansky M.**, Barek J., Kolska Z., Svorčik V., Lyutakov O., Surface Modification of Au and Ag Plasmonic Thin Films via Diazonium Chemistry: Evaluation of Structure and Properties, *Colloids and Surfaces A: Physicochemical and Engineering Aspects*, 2017 (*In press*).

7. Guselnikova O., Postnikov P., Kalachyova Y., **Libansky M.**, Zima J., Kolska Z., Švorčík V., Lyutakov O., Large-scale Ultrasensetive, Highly Reproducible and Regenerative Smart SERS Platform Based on pNIPAm Grafted Gold Grating, *ChemNanoMat*, 3 (2016) 135-144.
8. **Libánský M.**, Zima J., Barek J., Alena Řezníčková, Václav Švorčík, Dejmková H., Basic Electrochemical Properties of Sputtered Nanostructured Gold Film Electrodes, *Electrochimica Acta*, 2017 (*Submitted*).
9. Bergerová M., **Libánský M.**, Dejmková H., Determination of Urinary Indican on Carbon Film Composite Electrode and Carbon Paste Electrode, *Current Analytical Chemistry*, 2017 (*Submitted*).
10. Guselnikova O., Kalachyova Y., Faragova K., **Libansky M.**, Dejmkova H., Svorcik V., Sajdl P., Lyutakov O., Functional SPP-Based SERS Sensor Platform for Lipoproteine Detection, *Talanta*, 2017 (*Prepared for submission*).

B) List of oral presentations

1. **Libánský M.**, Zima J., Barek J. and Dejmková H.: Determination of Hydroquinone-β-D-glycopyranoside on Carbon Paste Electrode (Stanovení hydrochinon-β-D-glykopyranosidu na uhlíkové pastové elektrodě), *13th Student Scientific Conference* –STU, Bratislava, Slovak Republic (09. 11. 2011).
2. **Libánský M.**, Zima J., Barek J. and Dejmková H.: Voltammetric Determination of Triclosan Using a System of Disposable Electrochemical Cells with Integrated Carbon Electrode (Voltametrické stanovení triclosanu pomocí systému měrných cel s integrovanou uhlíkovou elektrodou), *16th National Competition for the Best Student Scientific Work in the Field of Analytical Chemistry* (The Merck Prize) – Brno, Czech Republic (06. - 07. 02. 2013).
3. **Libánský M.**, Zima J., Barek J. and Dejmková H.: Construction of a Multiple Electrochemical Cell Based on Carbon Film Electrodes, *56th Joint Meeting of the Polish and Hungarian Chemical Societies* – Siedlce, Poland (16. – 20. 09. 2013).
4. **Libánský M.**, Zima J., Barek J., Dejmková H.: New Voltammetric Arrangements for Large Scale Monitoring of Biologically Active Compounds Based on Carbon Composite Film Electrode, *13th The Present State and*

Perspectives of Analytical Chemistry in Practice – Bratislava, Slovak Republic (01. – 03. 06. 2014).

5. **Libánský M.**, Zima J., Barek J., Dejmková H.: Voltammetric Determination of Homovanillic Acid on a Disposable Electrochemical Measuring Cell System with Integrated Carbon Composite Film Electrodes, *XXXV. Modern Electrochemical Methods* – Jetřichovice u Děčína, Czech Republic (18. – 22. 05. 2015).
6. **Libánský M.**, Zima J., Barek J., Dejmková H.: Gold Film and Carbon Composite Film Electrodes for Voltammetric Determination of Oxidizable Organic Compounds, *14th The Present State and Perspectives of Analytical Chemistry in Practice* –Bratislava, Slovak Republic (03. – 06. 05. 2016).

C) List of posters

1. **Libánský M.**, Zima J., Barek J., Dejmková H.: New Voltammetric Arrangements for Inexpensive Monitoring of Biomarkers Based on Carbon Composite Film Electrodes, *Euroanalysis* 2015 – Bordeaux, France (06. – 10. 09. 2015).
2. **Libánský M.**, Zima J., Barek J., Reznickova A., Dejmková H.: Electroanalytical Applications of Grafted Nanostructured Gold Film Electrodes, *6th EuCheMs Chemistry Congress* – Seville, Spain (11. – 15. 2016).

D) List of patents and utility models

1. Czech National Utility Model number 25415. Dejmkova H., **Libansky M.**, Zima J., Barek J.: Electrochemical Measuring Cell and Array of Electrochemical Measuring Cells (*Elektrochemická měřicí cela a soustava elektrochemických měřicích cel)*. 23.05.2013.
2. Czech Patent number 304176. Dejmkova H., **Libansky M.**, Zima J., Barek J.: Electrochemical Measuring Cell and Array of Electrochemical Measuring Cells (*Elektrochemická měřicí cela a soustava elektrochemických měřicích cel)*. 23.11.2013.
3. Czech National Utility Model number 27672. **Libansky M.**, Zima J., Barek J., Dejmkova H.: Array of Working Electrodes and Array of Electrochemical

measuring sensors (*Soustava pracovních elektrod a soustava elektrochemických měřících senzorů)*. 29.12.2014.